



# Effects of model resolution on Arctic land processes



Meike Schickhoff

Hamburg 2024

## Hinweis

Die Berichte zur Erdsystemforschung werden vom Max-Planck-Institut für Meteorologie in Hamburg in unregelmäßiger Abfolge herausgegeben.

Sie enthalten wissenschaftliche und technische Beiträge, inklusive Dissertationen.

Die Beiträge geben nicht notwendigerweise die Auffassung des Instituts wieder.

Die "Berichte zur Erdsystemforschung" führen die vorherigen Reihen "Reports" und "Examensarbeiten" weiter.

## Anschrift / Address

Max-Planck-Institut für Meteorologie  
Bundesstrasse 53  
20146 Hamburg  
Deutschland

Tel./Phone: +49 (0)40 4 11 73 - 0  
Fax: +49 (0)40 4 11 73 - 298

name.surname@mpimet.mpg.de  
www.mpimet.mpg.de

## Notice

*The Reports on Earth System Science are published by the Max Planck Institute for Meteorology in Hamburg. They appear in irregular intervals.*

*They contain scientific and technical contributions, including PhD theses.*

*The Reports do not necessarily reflect the opinion of the Institute.*

*The "Reports on Earth System Science" continue the former "Reports" and "Examensarbeiten" of the Max Planck Institute.*

## Layout

*Bettina Diallo and Norbert P. Noreiks  
Communication*

## Copyright

*Photos below: ©MPI-M  
Photos on the back from left to right:  
Christian Klepp, Jochem Marotzke,  
Christian Klepp, Clotilde Dubois,  
Christian Klepp, Katsumasa Tanaka*



# Effects of model resolution on Arctic land processes



Meike Schickhoff

Hamburg 2024

# Meike Schickhoff

aus Mölln, Deutschland

Max-Planck-Institut für Meteorologie  
The International Max Planck Research School on Earth System Modelling  
(IMPRS-ESM)  
Bundesstrasse 53  
20146 Hamburg

Tag der Disputation: 31. Januar 2024

Folgende Gutachter empfehlen die Annahme der Dissertation:

Prof. Dr. Victor Brovkin

Dr. Mathias Goeckede

Vorsitzender des Promotionsausschusses:

Prof. Dr. Hermann Held

Dekan der MIN-Fakultät:

Prof. Dr.-Ing. Norbert Ritter

Titelgrafik: Foto von Meike Schickhoff, aufgenommen am 2. September 2021 in  
Chersky, Sibirien





dedicated to  
my grandmother Elisabeth (\*1933 - †2013)



## ABSTRACT

---

As computational power increases, the trend in Earth system modelling is moving towards km-scale resolution. Arctic land surface modelling could also benefit from high resolution, however, the effects of land surface model resolution on fluxes and soil state variables in the Arctic have neither been studied regarding the impact of boundary condition resolution nor regarding the impact of climate forcing resolution. Therefore, I compare high (5km) and low (210km) resolution setups of the land surface model JSBACH3 within a case study region in eastern Siberia and investigate effects induced by resolution.

In the first study, I use a high-resolution setup with high-resolution boundary conditions and low-resolution climate forcing to investigate effects induced by model boundary conditions only. Comparing it with a low-resolution setup reveals differences in simulated fluxes and soil state variables between the two setups for the 1980-2009 mean. The differences are mostly small in the summer mean and larger within individual summer months. Soil properties induce larger differences between resolutions than vegetation parameters. I find a statistically significant increase of +20% in the summer mean active layer depth relative to the 210km setup when averaged over the case study area. In August, statistically significant differences amount to +43%. The differences are caused by the discrete treatment of soil thermal processes magnifying the impact of soil parameter heterogeneity of soil organic matter and the Clapp and Hornberger parameter. Differences between setups are further statistically significant for July evaporation and equal +43%.

In the second study, I analyse effects due to forcing resolution only by comparing a high-resolution setup including a 5 year high-resolution forcing and low-resolution boundary conditions to a low-resolution setup. The forcing resolution mainly impacts the hydrology. I find a reduction in evaporation of -21% for the summer mean relative to the 210 km setup and of -27% for July. The difference is statistically significant in July and particularly large in the lowlands which are more water-limited than the domain average simulated in the 210 km setup. In the 5 km setup, the majority of precipitation falls in the highlands and affects only the local water budget within the respective grid cells. In reality, a fraction of the precipitated water in the highlands runs off to the lowlands and feeds evaporation there. This process is, however, not represented in the model due to missing lateral water fluxes connecting grid cells. Thus, the differences between high- and low-resolution setups do not indicate an improved representation of the hydrology due to the high-resolution forcing, but reveal a model

limitation. Lateral water transport between grid cells is presumably an important process to be implemented in land surface models if applied in a high-resolution setup.

This thesis shows that the resolution of model boundary conditions affects soil state variables more than the fluxes, while the forcing resolution impacts the fluxes. Both boundary data resolution and forcing resolution are thus important aspects to consider in high-resolution land surface model simulations.

## ZUSAMMENFASSUNG

---

Mit zunehmender Rechenleistung geht der Trend in der Erdsystemmodellierung hin zu einer Auflösung auf Kilometerskalen. Auch die Modellierung von arktischen Landflächen könnte von einer hohen Auflösung profitieren, jedoch wurden Auflösungseffekte von Landoberflächenmodellen weder bezüglich der Auswirkungen der Auflösung der Randbedingungen noch bezüglich der Auswirkungen der Auflösung der Treiberdaten auf Flüsse und Bodenzustandsvariablen in der Arktis untersucht. Deshalb vergleiche ich hoch (5 km) und niedrig (210 km) aufgelöste Setups des Landoberflächenmodells JSBACH<sub>3</sub> für eine Fallstudienregion in Ostsibirien und untersuche Effekte, die durch die Modellauflösung verursacht werden.

In der ersten Studie verwende ich ein hochaufgelöstes Setup mit hochaufgelösten Randbedingungen und niedrig aufgelöstem Klimaantrieb, um Effekte zu untersuchen, die nur durch die Modellrandbedingungen verursacht werden. Der Vergleich mit dem niedrig aufgelösten Setup zeigt Unterschiede in simulierten Flüssen und Bodenzustandsvariablen zwischen den beiden Setups für das 1980-2009 Mittel. Die Effekte sind im Sommermittel meist gering, aber sie sind größer innerhalb einzelner Sommermonate. Die Bodeneigenschaften haben einen größeren Einfluss auf Unterschiede zwischen den Auflösungen als die Vegetationsparameter. Es ist eine statistisch signifikante Zunahme der Tiefe der aktiven Schicht im Sommermittel relativ zum 210 km Setup vorhanden, die über das Fallstudiengebiet gemittelt +20% beträgt. Im August belaufen sich die statistisch signifikanten Unterschiede auf +43%. Die Unterschiede sind auf die diskrete Behandlung der thermischen Prozesse im Boden zurückzuführen, die die Auswirkungen der Heterogenität der organischen Bodensubstanz und des Clapp- und Hornberger-Parameters verstärken. Die Unterschiede zwischen den Setups sind auch für die Verdunstung im Juli statistisch signifikant und betragen +43%.

In der zweiten Studie vergleiche ich ein hochaufgelöstes Setup einschließlich eines fünfjährigen hoch aufgelösten Klimantriebs und niedrig aufgelösten Randbedingungen mit einem niedrig aufgelösten Setup um die Auswirkungen zu analysieren, die nur auf die Auflösung des Antriebs zurückzuführen sind. Die Auflösung des Klimantriebs wirkt sich hauptsächlich auf die Hydrologie aus. Die Verdunstung zeigt eine Reduktion von 21% im 5 km Setup im Vergleich zum 210 km Setup für das Sommermittel und eine Reduktion von 27% für Juli. Der Unterschied ist im Juli statistisch signifikant und im Tiefland besonders groß, da es wasserbegrenzter ist als der im 210 km Setup simulierte Gebietsdurchschnitt. In der 5 km Simulation fällt der Großteil der Niederschläge im Hochland und wirkt sich auf den

lokalen Wasserhaushalt innerhalb der jeweiligen Gitterzellen aus. In der Realität läuft ein Teil des Niederschlags vom Hochland in das Tiefland ab und speist dort die Verdunstung. Dieser Prozess wird jedoch im Modell aufgrund fehlender lateraler Wasserflüsse zwischen den Gitterzellen nicht abgebildet. Die Unterschiede zwischen hoch- und niedrig aufgelösten Setups deuten also nicht auf eine Verbesserung durch den hochaufgelösten Klimaantrieb, sondern zeigen eine Modellbeschränkung auf. Lateraler Wassertransport zwischen Gridzellen ist vermutlich ein wichtiger Prozess, der in hochaufgelösten Landoberflächenmodellen implementiert werden sollte.

Diese Arbeit zeigt, dass sich die Auflösung der Modellrandbedingungen stärker auf die Variablen im Untergrund auswirkt als auf die Flüsse, während sich die Auflösung des Klimaantriebs auf die Flüsse auswirkt. Sowohl die Auflösung der Randbedingungen als auch die Auflösung der Antriebsfaktoren sind daher wichtige Aspekte, die bei hochaufgelösten Simulationen mit Landoberflächenmodellen zu berücksichtigen sind.

## ACKNOWLEDGMENTS

---

This thesis would not have been possible without the support and help of many people. First and foremost are my supervisors whom I want to thank for their support throughout the last years. I thank Victor for guiding me along my PhD path and for all the motivating and enlightening discussions. I thank Philipp for discussing my many many questions and for the never-ending hypotheses-making of why JSBACH does what it does. I thank Mathias for taking me to Chersky and showing me the real world. I further want to thank my panel chairs Martin and Dirk for the support and outside guidance of my PhD work. Special thanks go to Tobias and Veronika for the very much appreciated technical support throughout my PhD.

Many thanks go to the Land-PhDs Nora, Zoé, Mateo, Constanze, Josie, Pinhsin, Istvan and Jun for all the support, discussions and fun along the way. Same goes for the wider IMPRS community, especially my productive homies Luca, Moritz, Paul, Hernan, Abisha and Co as well as Markus, Zoi and Malena. Special thanks go to Mateo and Nora for being the best office mates, to Zoé for reading so many of my paper drafts and to Istvan, Luca, Céline and Nora for comments on earlier drafts of this thesis. I further want to thank my working group and all 17th floor people for lunches, coffee breaks and inspiring discussions. I want to thank Sylvia, Antje, Connie and Michaela for the organizational support. And I also want to thank the Q-Arctic group for insights on permafrost science from different perspectives and especially Annett and Barbara for helping and contributing to my paper. Last but not least I want to thank my family and friends from the bottom of my heart for all the emotional support throughout the last years.



PRE-PUBLICATIONS RELATED TO THIS  
DISSERTATION

---

APPENDIX A:

**Schickhoff M.**, de Vrese P., Bartsch A., Widhalm B., and Brovkin V. "Effects of land surface model resolution on fluxes and soil state in the Arctic". Manuscript in revision in: *Environmental Research Letters*.

APPENDIX B:

**Schickhoff M.**, de Vrese P., and Brovkin V. "High-resolution forcing strongly changes evaporation in land surface model applied to Arctic condition". Manuscript in preparation.



## CONTENTS

---

### Unifying Essay

1	Introduction	3
1.1	Land processes in the Arctic	3
1.2	Land surface and subsurface heterogeneity	5
1.3	Model resolution	6
1.4	Open questions	9
2	Effects of model boundary data resolution	13
2.1	Resolution effects of vegetation and soil parameters	14
2.2	Effects on active layer depth	15
2.3	Effects on evaporation	18
2.4	Discussion	20
3	Effects of climate forcing resolution	23
3.1	Resolution effects	24
3.2	Highlands and lowlands	25
3.3	Evaporation and transpiration in JSBACH	27
3.4	Discussion	27
4	Conclusion	31
4.1	Discussion and implications	32

### Appendices

A	Effects of land surface model resolution on fluxes and soil state in the Arctic	39
A.1	Introduction	43
A.2	Methods	44
A.3	Results	45
A.4	Discussion	53
A.5	Conclusion	55
A.6	Supplementary material	56
B	High-resolution forcing strongly changes evaporation in land surface model applied to Arctic condition	67
B.1	Introduction	71
B.2	Data and Methods	72
B.3	Results	74
B.4	Discussion	79
B.5	Conclusion	81

	Bibliography	83
--	--------------	----

## LIST OF FIGURES

---

- Figure 2.1 1980-2009 August mean active layer depth and July mean evaporation in 210 km (up) and 5 km (down) resolution. White rectangles represent water bodies which are not modelled. 16
- Figure 2.2 Annual cycle of active layer depth averaged spatially and over the 1980-2009 period. Red marker indicates days with statistically significant differences between resolutions. 18
- Figure 3.1 Boxplots show resolution effects of precipitation (upper left), air temperature at lowest atmospheric layer (upper right), evaporation (lower left) and transpiration (lower right). Resolution effects are calculated as the difference of simulations in 5 km relative to 210 km setups (Equ. 3.1) for JJA for every grid cell on the 5 km grid. Grid cells in the 5 km setup are differentiated in highland (elevation  $\geq 300$  m a.s.l.) and lowland locations. Lowlands encompass the vast majority of the case study area. Resolution effects for temperature and precipitation balance out over the case study area as they are input parameters. 26
- Figure 3.2 The boxplots show the dependence of evaporation on precipitation for JJA in the 5 km setup. 28

## LIST OF TABLES

---

Table 2.1	Model setups for 5 km and 210 km simulations. 14
Table 2.2	$rRE_X^{\text{control}}$ signifies the resolution effects between the two control simulations in 5 km and in 210 km resolution for the respective variables. They are calculated as the relative differences of the 5 km simulation relative to the 210 km simulation of 1980-2009 mean case study area averages [%] (Equ. 2.1). Bold font indicates statistically significant differences between resolutions. Soil temperature difference refers to temperature in 19 cm depth [°C] (Equ. 2.1a). Transp. refers to transpiration, ALD to active layer depth and GPP to gross primary productivity. 14
Table 2.3	$\Delta rRE_X$ signifies the difference between resolution effects of simulations with uniform parameters and resolution effects of the control simulations for the respective variables [%] (Equ. 2.2). Uniform parameters are represented in the lines and output variables in the columns. The 1980-2009 summer mean and July mean are shown (for June and August see ch. A.6.). Soil temperature difference refers to temperature in 19 cm depth [°C]. Transp. refers to transpiration, ALD to active layer depth and GPP to gross primary productivity. Veg. param. refers to vegetation parameters including the root depths and soil param. refers to soil parameters. 15
Table 3.1	Model setups for 5 km and 210 km simulations. 24

Table 3.2  $rRE_x^{\text{control}}$  signifies the resolution effects between the two control simulations in 5 km and in 210 km resolution for the respective variables in this table. They are calculated as the relative differences between the 5 km simulation and the 210 km simulation of summer mean values averaged over the case study area [%] (Equ. 2.1). Soil temperature difference refers to the temperature in 19cm depth [°C]. GPP refers to gross primary productivity, ALD to active layer depth, LHF to latent heat flux and SHF refers to sensible heat flux. 25

## UNIFYING ESSAY



## INTRODUCTION

---

The ongoing increase in computational power creates new possibilities for the modelling of land processes in the Arctic. While traditional land surface models operate on horizontal scales of 100-300 km, higher resolutions on km-scale are now feasible. This is especially advantageous for modelling permafrost areas which are characterized by an enormous surface and subsurface heterogeneity (Torre Jorgenson et al., 2013; van Cleve et al., 1983; Viereck, 1992). However, the impact of model resolution on the northern permafrost areas was never systematically investigated. This dissertation deals with the effects of spatial resolution on fluxes and soil state variables in the Arctic. The first study approaches this topic from the angle of boundary data resolution, i.e. resolution of elevation, vegetation and soil parameters, while the second study analyses effects of climate forcing resolution.

In the following introduction, I first set the scene and present the background to this work. I start with explaining Arctic land processes which are relevant for the following chapters. I further shed light on heterogeneity in the northern permafrost areas and on high-resolution Earth system and land surface models. Finally, I introduce the research questions before I summarize the two studies in chapter two and three. In chapter four, I conclude my findings.

### 1.1 LAND PROCESSES IN THE ARCTIC

The Arctic region contains tremendous amounts of frozen soil carbon. The Arctic terrestrial permafrost carbon pool is estimated to contain 1100-1700 Gt C which is about twice the size of the atmospheric carbon pool (Hugelius et al., 2013a; Hugelius et al., 2014; Lindgren et al., 2018; Tarnocai et al., 2009; Zimov et al., 2006). The soil carbon is at increasing risk of thawing since the Arctic warms at least two times faster than the global mean average (Biskaborn et al., 2019; IPCC, 2013; Meredith et al., 2019; Rantanen et al., 2022; Serreze & Barry, 2011). Permafrost is defined as ground with below-zero temperatures for at least two consecutive years (Guo & Wang, 2017). While frozen conditions prevent soil decomposition, thawing induces microbial activity and the associated release of greenhouse gases. The resulting carbon fluxes increase with a warming Arctic and thereby induce a rise in global temperatures - a process called the permafrost carbon feedback (Kleinen & Brovkin, 2018; Koven et al., 2015; Natali et al., 2021; Schuur et al., 2015; Turetsky et al., 2019).

*Permafrost carbon*

In summer, the sun warms the Earth's surface and a heat flux is generated which thaws the upper part of the soil. This part is termed the active layer. It is usually quantified by measuring its depth within the soil - the active layer depth - which increases with climate change (Dobiński, 2020; Smith et al., 2022b).

*Soil hydrology*

The release of carbon from the active layer depends on the local hydrological conditions. Hydrology thus plays a key role in the carbon balance of the northern high latitudes. The hydrological dynamics are also especially complex as snow and soil ice affect the water fluxes (Bring et al., 2016; Li et al., 2023). The soil is characterized by recurring periods of freezing and thawing. Soil ice is impeding the vertical percolation of water through the soil and can act as an impermeable layer. Soil ice thereby affects infiltration rates and lateral water movements within the soil (Mackay, 1983; Walvoord & Kurylyk, 2016). Moreover, ice influences the thermophysical soil properties. For example, it increases the soil thermal conductivity in comparison to liquid water. And phase changes within the soil affect the soil temperatures. Energy is required to melt soil ice in spring which slows down the temperature increase. In fall, when liquid water is freezing, latent heat is released and slows down the temperature decrease. These characteristic periods of soil temperatures remaining at 0°C due to latent heat absorption or release, is termed the zero curtain effect (Romanovsky & Osterkamp, 2000).

Liquid water at temperatures below 0°C can occur in permafrost soils and is known as supercooled water. It exists due to salts or other solutes inducing a freezing point depression or due to adhesion forces binding the water closely to soil particles. In models, the amount of supercooled water in the soil is estimated by a formulation using the Clapp and Hornberger parameter (Ekici et al., 2014; Niu & Yang, 2006). This parameter characterizes soil hydraulic properties and is empirically approximated by use of suction wetness data. Its values increase from coarse to fine soils with higher values translating into higher supercooled water amounts (Clapp & Hornberger, 1978).

*Soil properties*

Other soil parameters important in the context of this thesis are soil organic matter and soil porosity. The soil organic matter fraction describes the amount of organic material in the soil relative to the amount of mineral soil particles. Organic material comprises dead animal and plant remains at different phases of decomposition. Soil organic matter exhibits different characteristics than mineral soil particles which affects overall soil properties. For example, the heat conductivity of the mixed mineral and organic soil is much smaller than for pure mineral soils (Lal, 2009; Lawrence & Slater, 2008; Lehmann & Kleber, 2015).

Soil porosity describes the amount of pore space within the soil. It also affects the heat conductivity, because the soil pores, which are filled with air, water and ice, comprise different heat conductivities than the soil particles. Organic material comprises a much larger pore volume than mineral soils. The soil porosity of organic soils is thus greater than the porosity of mineral soils (Lawrence & Slater, 2008; Tong et al., 2016). The soil porosity of mineral soils depends on the soil texture, likewise to other mineral soil properties.

The surface hydrology is closely intertwined with the soil hydrology. The water budget at the surface is described by  $\Delta_{\text{soil}} = P - E - T - D - R$ , where  $\Delta_{\text{soil}}$  denotes the change in the soil moisture and ice content. P stands for precipitation, E for evaporation, T for transpiration, D for both drainage and subsurface runoff and R for surface runoff. The partitioning of precipitated water in infiltration and runoff depends not only on the local slope, but also on the soil hydrological conditions in which ice plays a significant role as explained above (Bring et al., 2016; Li et al., 2023). The heat release associated with evapotranspiration constitutes the latent heat flux and thus evapotranspiration affects the ratio of latent to sensible heat fluxes. Thereby the local hydrology also influences near-surface temperatures.

*Surface hydrology*

As the local hydrology impacts transpiration, it also affects the vegetation cover. Vegetation in the Arctic can be broadly divided into the tundra in the North and the taiga further south. The tundra is characterized by being a treeless landscape composed of grasses, mosses, lichens and dwarf shrubs (Heijmans et al., 2022). Taiga signifies the large boreal forests. The taiga tundra ecotone denotes the boundary between them and exhibits a mix of trees, grasses and shrubs (Montesano et al., 2020).

*Vegetation*

## 1.2 LAND SURFACE AND SUBSURFACE HETEROGENEITY

Arctic land areas exhibit an enormous heterogeneity in surface and subsurface characteristics. Vegetation, topography, hydrological conditions, surface materials and soil properties differ substantially across space (Torre Jorgenson et al., 2013; van Cleve et al., 1983; Viereck, 1992). Permafrost soils belong to Earth's most heterogeneous soils (Siewert et al., 2021). Also carbon fluxes exhibit a large spatial variability (Juutinen et al., 2022; Kou et al., 2022). Carbon fluxes in tundra environments even show substantially larger variability across landscape types than interannual variability (Treat et al., 2018). Surface and subsurface heterogeneity plays out at a wide variety of scales. Differentiation between large-scale biomes such as boreal forests and tundra takes place on very coarse scales. Another example of large-

*Heterogeneity in the Arctic*

scale differences would be the distinction between large mountain ranges and huge lowlands such as the Ural mountains and the West Siberian Plain. In contrast, heterogeneity also acts on very small scales. Cryostructures in the soil can introduce heterogeneity on the cm-scale (Ping et al., 2015). Various generations of ice-wedges induce variability on scales of meters to tens of meters (Lara et al., 2020; Siewert et al., 2021). Thermokarst lakes and pingos are examples of heterogeneity on variable scales between tens to hundreds of meters (Gurney, 1998; Jones et al., 2011). And geomorphic disturbances and catenary shifts cause variability on landscape scales of hundreds of meters (Siewert et al., 2021).

*Heterogeneity in the  
case study area*

In the following, I want to focus on surface and subsurface characteristics on scales that can be resolved in a horizontal model resolution of 5 km, but not in a resolution of 210 km. I will further concentrate on heterogeneities which occur within the case study area that I use in this thesis. The case study area is located around Chersky in eastern Siberia within the continuous permafrost zone. The area stretches from 158.4° to 162°E and from 67.5° to 69°N. The largest part is occupied by lowlands, i.e. areas that are located below 300 m a.s.l. (Jones et al., 2022; Paltan et al., 2015). The lowlands have an average elevation of 50 m. In the mid-south, a small mountain range constitutes highlands above 300 m a.s.l. with an average elevation of 454 m (Amante & Eakins, 2009). Vegetation differs across the area. In the very north, the southern tip of the Kolyma-Indighirka lowlands is situated which comprises wet tundra vegetation (Veremeeva & Gubin, 2009). This is represented by grasses in the model. The highlands in the south also exhibit grasses. Anywhere else, boreal forests with shrubs and trees dominate (European Commission Joint Research Centre, 2003). The soil shows heterogeneity within the area in terms of soil texture, soil organic matter fraction and soil depth. The soil texture varies between silt loam, loam, clay, clay loam, sandy loam and loamy sand whereby the first three types dominate the area (FAO/IIASA/ISRIC/ISS-CAS/JRC, 2009). The soil organic matter fraction also shows variability. It is especially low in the highlands with on average 17% of organic material within the top 30 cm of the soil column, while the average amounts to 49% for the rest of the area (Hugelius et al., 2013a; Hugelius et al., 2013b). Lastly, soil depth until bedrock varies significantly. Soils in the highlands are often only 10 cm deep while they extend up to 32 m in the lowlands (Hengl et al., 2017; Shangguan et al., 2017).

### 1.3 MODEL RESOLUTION

*Earth system model  
resolution*

Supercomputer power increased tremendously over time. Alone from

the 1970s to the 2000s, it grew by a factor of a million (Solomon et al., 2007). The growth in computational power supported the improvement of climate model simulations along several lines. First, the models became more complex as more and more processes and Earth system components were included. Second, the simulation length increased. Third, the number of simulations grew. And fourth, the spatial resolution significantly improved (Edwards, 2011; Solomon et al., 2007). While around 1990 grid spacings of 500km were common, recently the trend emerged to run coupled Earth system models on km-scale (Hohenegger et al., 2020). This high resolution allows the explicit representation of deep convection and the models are thus called storm-resolving models (Sato et al., 2008). They show important improvements regarding processes relevant for land climate interactions compared to lower resolution models. The advantages include a more realistic diurnal cycle of precipitation (Hohenegger et al., 2008), a better representation of orographic and convective precipitation and an improved occurrence of precipitation extremes (Hohenegger et al., 2023; Prein et al., 2015). Temperatures in mountainous regions are more realistically simulated as well as wind extremes (Iles et al., 2020; Prein et al., 2013). An improved representation of clouds in high-resolution models leads to more realistic net shortwave radiation (Hohenegger et al., 2020). The partitioning between rain and snow as well as snow melt are better represented which is important especially for the Arctic (Liu et al., 2017; Rasmussen et al., 2014; Wang et al., 2018). These km-scale Earth system model simulations have however one big disadvantage regarding the study of land processes: Variables such as soil carbon, soil ice and soil moisture require long spin-ups of 50-80 years in order to be in equilibrium. Simulating these time scales in horizontal resolutions of kilometers with global Earth system models is currently not feasible due to limited computational resources.

One possibility to make use of the advantages of high-resolution simulations for the study of land processes is to apply the simulated atmospheric variables as high-resolution climate forcing for land-surface-model-only simulations. If the high-resolution forcing is used as a cyclic forcing, even a long spin-up can be conducted. After all, the quality of land-surface-model-only simulations does not only depend on the model and the boundary conditions used, but also on the realism of the climate forcing (Balsamo et al., 2015). The spatial distribution and intensity of precipitation events impacts all water fluxes and thereby also carbon fluxes such as gross primary productivity. The latter is also influenced by the distribution of clouds impacting photosynthesis. Wind speed can affect evapotranspiration due to the turbulent exchange of dry and moist air. Temperature is crucial in nearly all land processes in the Arctic as it is an energy-limited re-

*High-resolution  
forcing*

gion. Previous findings using a downscaled high-resolution forcing for Oklahoma show indeed that simulated surface and root-zone soil moisture are closer to observations than with a low-resolution forcing (Rouf et al., 2021).

*High-resolution land models*

Not only did the climate forcing resolution recently increase, there also have been advances using high-resolution land surface models, usually on regional scales (Chen et al., 2014; Cheng et al., 2023; Rasmussen et al., 2014; Singh et al., 2015). Most modelling studies targeting Arctic terrestrial processes however employ traditional low-resolution models (Burke et al., 2020; de Vrese & Brovkin, 2021; Kleinen & Brovkin, 2018; Koven et al., 2013; McGuire et al., 2018). Previous findings show that resolution is important regarding the representation of land heterogeneity, especially in the Arctic. For example, estimates of methane emissions in the Arctic may be biased in low-resolution wetland models due to a coarse representation of interactions between soil moisture and soil carbon (Albuhaisi et al., 2023). The uncertainty in carbon flux estimates from tundra landscapes also increases with decreasing biogeochemical model resolution due to a reduced representation of tundra heterogeneity (Lara et al., 2020). Especially the coarse representation of land cover may lead to substantial underestimation of methane fluxes due to an imprecise account of the wetland fraction as shown for northeastern European Russia with a process-based biogeochemical model (Treat et al., 2018). Moreover, also the hydrology is affected by resolution. Compared to observations, soil moisture, terrestrial water storage and snow water equivalent significantly improved with increased resolution of soil and topographic model boundary data in a land surface model applied to the southwestern U.S. (Singh et al., 2015). A statistical approach shows further that active layer depth on  $0.05^\circ$  scale may vary up to 150cm and soil temperatures up to  $2^\circ\text{C}$  within one  $0.5^\circ$  grid cell (Beer, 2016).

*Tiling schemes*

A common way to represent small-scale heterogeneity in low-resolution land surface models is to use tiling schemes. Most commonly, tiling schemes represent sub-grid heterogeneity in vegetation by defining different vegetation types and calculating their respective cover fractions of the grid box area. Some vegetation-dependent processes are then calculated per tile (Blyth et al., 2021; Fisher & Koven, 2020; Hartley et al., 2017). Additional processes can be included in tiling schemes, for example lakes and wetlands (Specht et al., 2022). For permafrost regions, tiling schemes representing microtopography in ice-rich landscapes were introduced (Aas et al., 2019; Cai et al., 2020; Nitzbon et al., 2020a). In contrast to tiling schemes, high-resolution land surface models represent heterogeneity on km grid-scales explicitly. This is an advantage, since most land surface models do not incorporate sophisticated tiling schemes covering many different pro-

cesses. Thus, heterogeneity in boundary conditions is mostly better represented in high-resolution models than in low-resolution models with tiling schemes. Particularly soil parameter heterogeneity is not often represented in tiling schemes. In JSBACH3, the model which I use for this thesis, a tiling scheme is implemented for vegetation but not for soil properties or elevation.

High-resolution land surface models further offer advantages over tiling in combination with a high-resolution forcing or in high-resolution coupled simulations. Particularly precipitation shows a high spatial variability in high resolution which is not trivial to allocate to the different tiles in a low-resolution land surface model. Thus, in order to advance land surface model simulations by an improved forcing, it is favourable to use high-resolution setups in combination with high-resolution forcings.

However, high-resolution land models do not make tiling schemes obsolete. Even on km-scale resolutions, there is still a large amount of sub-grid heterogeneity on small scales which requires representation.

#### 1.4 OPEN QUESTIONS

In the previous subchapters, I shed light on the reasons why the northern permafrost areas are a very unique and significant region of the Earth. The soils hold large amounts of frozen carbon which is at great risk of thawing with ongoing warming. At the same time, the Arctic is especially affected by climate change as it warms much faster than the global mean. In order to make precise projections of the future Arctic hydrology and its carbon fluxes with ongoing climate change, increased land surface model resolution may be advantageous to better capture the heterogeneity of local hydrological and soil conditions. While traditional land surface models run on scales of 100-300 km, simulations on km-scale currently move into focus and may offer benefits. Unlike atmospheric models which can explicitly resolve deep convection on km-scale and thereby reduce the amount of uncertain parameterizations, parameterizations for the land surface cannot be reduced on km-scale. The model code thus does not change between low and km-scale resolutions. However, both the model boundary data and the climate forcing are significantly better resolved on km-scale and may impact the outcome. I thus investigate the resolution of land-surface-model-only simulations out of those two perspectives.

In the first study I focus on the impact of boundary data resolution which may indeed play an important role. Previous findings show that high-resolution topographic and soil boundary data improve the modelled hydrology in a land surface model for southwestern U.S. (Singh et al., 2015). I have illustrated above that Arctic land areas are characterized by an especially large heterogeneity of surface and

*First study*

subsurface characteristics. For example, not only vegetation, but also mineral soil textures and soil organic matter fractions vary significantly within the case study area I am focusing on in this thesis. Thus, increasing the model resolution may be particularly advantageous for modelling Arctic land areas. Previous studies reveal that increasing the resolution indeed improves the representation of land heterogeneity regarding simulated carbon fluxes in regional biogeochemical models (Albuhaisi et al., 2023; Lara et al., 2020; Treat et al., 2018). Investigating the impacts of resolution is thus important in order to make educated decisions concerning future modelling activities targeting Arctic hydrology and carbon budgets. However, the effects of model boundary data resolution on Arctic land areas were never systematically studied with a land surface model, even though computational power continuously increases and makes pan-Arctic land surface model resolutions on km-scale feasible. Therefore, I address this gap with the research question of the first study:

*1<sup>st</sup> research question*

WHAT ARE THE EFFECTS OF HIGH-RESOLUTION BOUNDARY CONDITIONS ON SIMULATING ARCTIC TERRESTRIAL PROCESSES?

To answer this question, I compare simulations of the land surface model JSBACH3 in a high-resolution setup on 5 km-scale with a setup in a traditional low resolution of 210km for a case study area in eastern Siberia. The 5 km setup includes high-resolution boundary data for elevation, vegetation and soil parameters and a low-resolution climate forcing in order to investigate effects by boundary conditions only. I quantify differences in fluxes and soil state variables between the setups and explain the processes inducing the differences.

*Second study*

While the first study deals with the effects of model boundary data in a high-resolution model, the second study addresses the role of forcing resolution. As Earth system models are increasingly run on km-scale (Hohenegger et al., 2023; Hohenegger et al., 2020; Satoh et al., 2008; Stevens et al., 2020), their output can be used as a (cyclic) climate forcing for land surface models. The high-resolution forcing availability thereby significantly improved, since earlier only downscaled data, often with biases especially in the spatial distribution of precipitation, were obtainable or reanalysis data such as ERA5 on scales of 30km. Previous studies analysing the effects of forcing resolution on land surface processes use these options as climate forcing (Albergel et al., 2018; Rouf et al., 2021). The now available Earth system model output on km-scale promises improvements as especially convective and orographic precipitation as well as precipitation extremes are more realistically represented. The spatial distribution of precipitation significantly impacts the local hydrology and thereby also soil state and carbon fluxes. Temperatures in mountainous regions are also better resolved and temperature is a crucial driver of Arctic land processes

since the Arctic is an energy-limited region. Both temperature and precipitation depend on the orography and the Arctic is shaped by alternating lowlands and highlands. A high-resolution forcing thus seems advantageous for Arctic land surface modelling. The impact and potential limitations of a km-scale high-resolution forcing on Arctic land processes were never systematically analyzed. This is however crucial to effectively direct future modelling activities for the Arctic, since the trend goes to high-resolution simulations. The second research question thus reads:

WHAT ARE THE EFFECTS OF A HIGH-RESOLUTION CLIMATE FORCING ON SIMULATING ARCTIC TERRESTRIAL PROCESSES?

*2<sup>nd</sup> research question*

To address this question, I use a similar model setup as in the first study. I use the same land surface model JSBACH3 for the same case study area. However, now model boundary conditions are in 210km resolution for both setups, while the forcing is resolved once in 5km and once in 210km which enables analysis of forcing resolution effects only. I compare the two setups and quantify and explain differences due to forcing resolution.



The Arctic is characterized by tremendous surface and subsurface heterogeneity on different scales. To better capture some of these heterogeneities, land surface modelling in high spatial resolution seems favourable. However, the effects of model boundary data resolution on Arctic fluxes and soil state variables were never systematically studied. Therefore, I address this topic with my first study.

*Introduction*

I confine the spatial simulation extent to the case study area around Chersky in eastern Siberia (ch. 1.2) and use the land surface model JSBACH<sub>3</sub> in two different resolution setups (Table 2.1). In the first setup, I use a horizontal resolution of  $0.045^\circ$  which corresponds to  $5 \times 1.9$  km in the case study area. For this setup, I use high-resolution boundary data for elevation, vegetation and soil. The climate forcing is resolved in  $1.88^\circ$  resp.  $210 \times 78$  km in the case study area. In the second setup both boundary data and climate forcing are in low-resolution of 210 km. Both setups are land-surface-model-only setups without feedbacks to the atmosphere. I run the model for a spin-up of 80 years and an analysis period of 30 years. After running the simulations, I compare the outputs of both setups and calculate resolution effects as the differences of the 5 km simulation relative to the 210 km simulation of 30 year mean case study area averages. The relative resolution effects of variable X ( $rRE_X$ ) are defined as

*Methods*

$$rRE_X = \frac{(X_{5km} - X_{210km}) \cdot 100}{|X_{210km}|} \quad (2.1)$$

The relative differences facilitate comparisons between different variables. Resolution effects in soil temperature (ST) are calculated as absolute resolution effects  $aRE_{ST}$  with  $aRE_{ST} = ST_{5km} - ST_{210km}$  (2.1a). In addition to these control simulations (with resolution effects  $rRE_X^{control}$ ), I conduct idealized simulations in which I set one or several parameters (to assess synergetic effects) to spatially uniform. I calculate the case study area average for the respective input parameter and this value is employed to force every grid cell in the simulation. This enables estimating the impact of the individual or sets of parameters. Resolution effects of these idealized simulations  $rRE_X^{uniform}$  are calculated and deducted from the resolution effects of the control simulations:

$$\Delta rRE_X = rRE_X^{control} - rRE_X^{uniform} \quad (2.2)$$

Model setup	Model resolution [km]	Boundary conditions [km]	Climate forcing [km]
5 km setup	5	5	210
210 km setup	210	210	210

Table 2.1: Model setups for 5 km and 210 km simulations.

## 2.1 RESOLUTION EFFECTS OF VEGETATION AND SOIL PARAMETERS

Summer mean resolution effects are largest for active layer depth with  $rRE_{ALD}$  of 20%, whereby the differences between resolution setups are statistically significant (Table A.1). Soil temperature at 19 cm depth also shows statistical significant differences  $\alpha RE_{ST}$  of  $0.34^{\circ}C$ . Resolution effects of drainage, evaporation, GPP and transpiration are small in the summer mean due to smaller differences and high interannual variability in the fluxes. Most resolution effects are larger within individual months than in the summer mean. In July, evaporation, active layer depth and soil temperature show statistical significant differences. They are largest in evaporation with  $rRE_{Evap}$  of 43%. In August, active layer depth and soil temperature show statistical significant differences with  $rRE_{ALD}$  of 43% in active layer depth and  $\alpha RE_{ST}$  of  $0.5^{\circ}C$  in soil temperature.

	ALD [%]	Drainage [%]	Evaporation [%]
JJA $rRE_X^{control}$	20	0.8	5.5
June $rRE_X^{control}$	1.7	12	-3.8
July $rRE_X^{control}$	12	-7.1	43
August $rRE_X^{control}$	43	7.4	13
	GPP [%]	Soil temp. [ $^{\circ}C$ ]	Transp. [%]
JJA $rRE_X^{control}$	4.8	<b>0.34</b>	3.3
June $rRE_X^{control}$	-8.0	0.3	22
July $rRE_X^{control}$	13	<b>0.2</b>	21
August $rRE_X^{control}$	1.4	<b>0.5</b>	-7.6

Table 2.2:  $rRE_X^{control}$  signifies the resolution effects between the two control simulations in 5 km and in 210 km resolution for the respective variables. They are calculated as the relative differences of the 5 km simulation relative to the 210 km simulation of 1980-2009 mean case study area averages [%] (Equ. 2.1). Bold font indicates statistically significant differences between resolutions. Soil temperature difference refers to temperature in 19 cm depth [ $^{\circ}C$ ] (Equ. 2.1a). Transp. refers to transpiration, ALD to active layer depth and GPP to gross primary productivity.

	ALD [%]	Drainage [%]	Evaporation [%]
JJA $\Delta rRE_{\chi}$ veg. param.	2.3	3.2	-0.5
JJA $\Delta rRE_{\chi}$ soil param.	20	-2.3	6.4
July $\Delta rRE_{\chi}$ veg. param.	2.2	0.9	6.1
July $\Delta rRE_{\chi}$ soil param.	12	-8.1	42
	GPP [%]	Soil temp. [°C]	Transp. [%]
JJA $\Delta rRE_{\chi}$ veg. param.	-1.6	0.03	-3.4
JJA $\Delta rRE_{\chi}$ soil param.	7	0.31	7.2
July $\Delta rRE_{\chi}$ veg. param.	-1.5	0.03	-3.1
July $\Delta rRE_{\chi}$ soil param.	15	0.19	24

Table 2.3:  $\Delta rRE_{\chi}$  signifies the difference between resolution effects of simulations with uniform parameters and resolution effects of the control simulations for the respective variables [%] (Equ. 2.2). Uniform parameters are represented in the lines and output variables in the columns. The 1980-2009 summer mean and July mean are shown (for June and August see ch. A.6.). Soil temperature difference refers to temperature in 19 cm depth [°C]. Transp. refers to transpiration, ALD to active layer depth and GPP to gross primary productivity. Veg. param. refers to vegetation parameters including the root depths and soil param. refers to soil parameters.

Model simulations with spatially uniform vegetation and root depths exhibit small differences  $\Delta rRE$  for both the summer mean and July (Table A.2). Much larger differences  $\Delta rRE$  are obtained by simulations with uniform soil parameters for both time periods. This reveals that soil parameter heterogeneity has a larger effect on differences between resolutions than vegetation properties. This also applies to June and August (appendix A). In the following, I focus on the processes inducing resolution effects in active layer depth and evaporation, since they both show large and statistically significant resolution effects of 43% in August and July respectively. Processes inducing soil temperature resolution effects are similar to active layer depth processes.

*Importance of  
vegetation and soil*

## 2.2 EFFECTS ON ACTIVE LAYER DEPTH

Active layer depth shows large and statistically significant differences between resolutions. Simulations with individual parameters set to spatially uniform show the largest differences  $\Delta rRE_{ALD}$  for the soil parameters soil organic matter (19% in August) and the Clapp and Hornberger parameter (15% in August). Simulations with both parameters set to uniform simultaneously results in difference  $\Delta rRE_{ALD}$  of 40% in August. This shows that soil organic matter and the Clapp

and Hornberger parameter induce a large part of active layer depth resolution effects. Thus, I explain their mechanisms in the following.

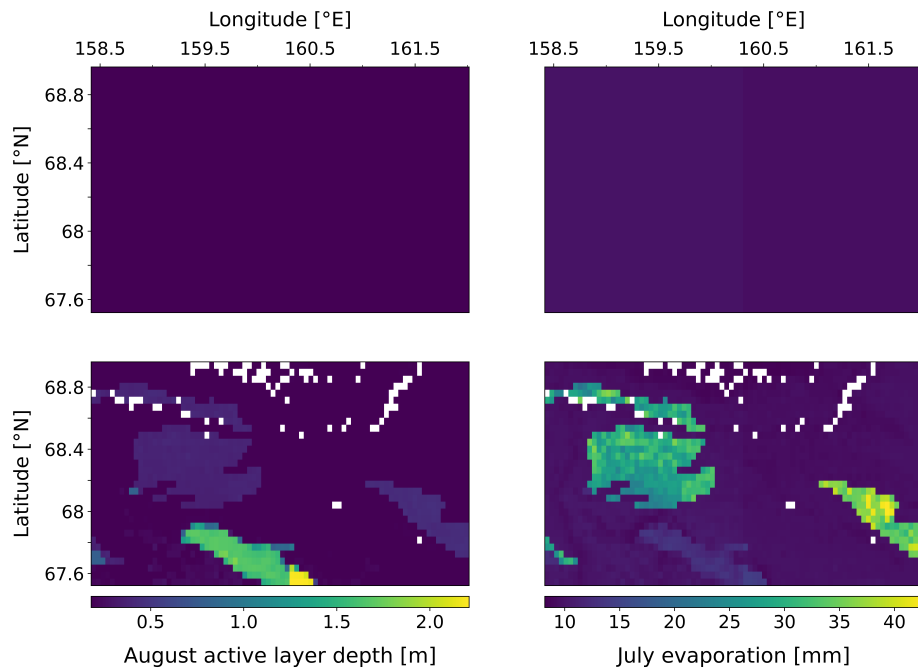


Figure 2.1: 1980-2009 August mean active layer depth and July mean evaporation in 210 km (up) and 5 km (down) resolution. White rectangles represent water bodies which are not modelled.

#### *Soil organic matter*

Soil organic matter is heterogeneously distributed across the case study area. The mountain range in the south is characterized by especially low soil organic matter amounts and shows by far the deepest active layer depths (Fig. A.1). Otherwise, soil organic matter is more homogeneously spread. Soil organic matter affects many soil properties. In this context, its impact on the soil heat conductivity, the soil porosity, soil moisture and soil ice is crucial. The heat conductivity of organic soils is usually smaller than of mineral soils which is due to several effects. The organic soil particles themselves have a smaller heat conductivity than mineral particles such as sand, silt or clay. Moreover, organic soils are characterized by a much larger porosity than mineral soils. In dry soils, the many soil pores are filled with air which exhibits an especially low heat conductivity. Thus, the dry soil heat conductivity is smaller for organic soils than for mineral soils. The saturated soil heat conductivity also depends on the organic and mineral fractions of the soil as well as on the relative water and ice contents of the soil. It is usually much larger than the dry soil heat conductivity, because water and ice are better heat conductors than air. Furthermore, soil organic matter also affects the soil saturation degree of the soil. The absolute soil moisture is often large for organic

soils, because the porosity is large. The soils provide much space that can be filled with water. However, in the model, the soil saturation degree is usually larger for mineral soils, since the smaller pore space is more quickly filled up with water and ice than the large pore space of organic soils. The soil saturation degree  $sat$  is calculated as

$$sat = \frac{water_{soil} + ice_{soil}}{d_{soil} \cdot porosity} \quad (2.3)$$

$water_{soil}$  denotes the soil layer water content,  $ice_{soil}$  the soil layer ice content,  $d_{soil}$  the soil layer depth and  $porosity$  the volumetric porosity of the mixed mineral and organic soil. The smaller porosity in mineral soils relative to organic soils decreases the denominator and thereby increases the saturation degree for mineral soils. A higher saturation degree increases the total heat conductivity  $\lambda_{tot}$  which is calculated by  $\lambda_{tot} = \lambda_{sat} \cdot Ke + \lambda_{dry} \cdot (1 - Ke)$  with the saturated heat conductivity  $\lambda_{sat}$ , the dry heat conductivity  $\lambda_{dry}$  and the Kersten number  $Ke$  which depends on the the decadic logarithm of the saturation degree. A higher saturation degree increases the Kersten number and thereby increases the total heat conductivity, since the saturated heat conductivity is much larger than the dry heat conductivity.

Due to the reasons explained above, the total heat conductivity of soils with small organic matter amounts is larger than for soils with high organic matter amounts. And a greater soil heat conductivity leads to deeper active layer depths. The top soil layer is thereby crucial since it determines the amount of energy getting transferred from the surface to the soil. The average active layer depth of soils with a soil organic matter fraction larger than 18% amounts to 22 cm with a maximum of 81 cm. In contrast, soils with soil organic matter fractions smaller than 14% show a mean active layer depth of 158 cm, with a minimum of 80 cm and a maximum of 221 cm.

Active layer depths are slightly deeper than average in areas which hold high Clapp and Hornberger parameter values (Fig. A.1). This parameter determines the amount of supercooled water in the soil, with high parameter values equating to a large supercooled water amount. With more supercooled water in the soil, less soil ice needs to be melted in spring. Thus, more of the available energy can go directly into temperature increase rather than phase change which leads to deeper active layer depths. Additionally, these areas hold high soil moisture amounts in the top soil layer. A high soil moisture increases the numerator of equation 2.3 and thereby also the saturation degree and the total soil heat conductivity which increases the active layer depth. Both processes together induce the larger than average active layer depths in areas with high Clapp and Hornberger parameter

*Clapp and  
Hornberger  
parameter*

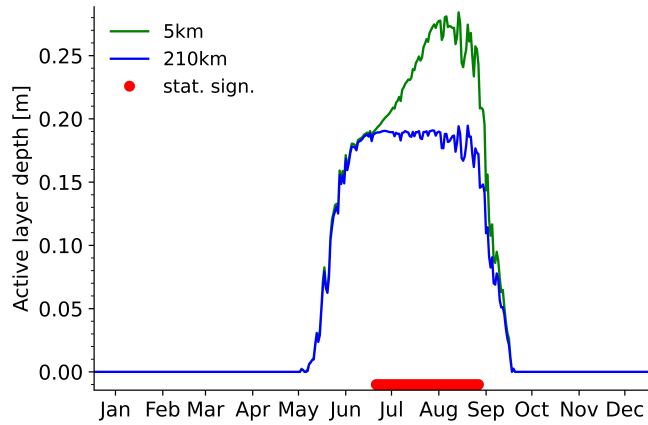


Figure 2.2: Annual cycle of active layer depth averaged spatially and over the 1980-2009 period. Red marker indicates days with statistically significant differences between resolutions.

values.

#### *Thaw dynamics*

The spatially averaged 5 km and 210 km setups show different thaw dynamics in the active layer depth annual cycle (Fig. A.2). The 210 km setup stops thawing at 19 cm soil depth, which marks the depth of the second soil layer. The second soil layer is already much thicker than the top soil layer and thus contains much more soil ice. In the 210 km setup, all the available energy goes into phase change and creates a zero curtain effect extending over the whole summer, since there is not enough energy to thaw through all the soil ice. In contrast, in the 5 km setup, more energy is available on average and thus the soil thaws deeper than the second soil layer. The surplus of energy is due to the increased heat conductivities in areas with low soil organic matter fractions or high Clapp and Hornberger parameter values.

#### *Nonlinear vertical discretization*

The main reason for the different thaw dynamics is the discrete treatment of soil thermal processes. Each soil layer is represented by only one temperature, one soil ice content etc. This makes thawing of a soil layer binary and not gradual. In addition, the soil in the model shows a nonlinear vertical discretization. Deeper soil layers are thicker than soil layers located closer to the surface. Thicker soil layers contain more soil ice than thinner layers. Thus, they need more energy to thaw and maintain a longer zero curtain effect. These effects introduce nonlinearity into the thawing process, since the soils do not thaw gradually but discrete.

### 2.3 EFFECTS ON EVAPORATION

#### *Evaporation partition*

Evaporation shows large and statistically significant resolution effects

in July (+43%). Total evaporation is constituted of snow, skin and soil evaporation. Snow evaporation is negligible in summer. Skin evaporation refers to evaporation from wet surfaces on soil and vegetation. It makes up the largest share of total evaporation, but does not induce resolution effects since it equates to 8.9 mm in both resolution setups in July. Skin evaporation is computed by multiplying the wet skin fraction with potential evaporation. The wet skin fraction depends upon precipitation, the leaf area index and the maximum vegetated fraction of the grid box. The dependence on vegetation parameters does not cause resolution effects, because they do not differ greatly across the case study area. The potential evaporation depends on the vapour pressure deficit, temperature and wind speed. All climate forcing variables are resolved in 210km in both resolution setups and do not induce resolution effects in skin evaporation. In contrast, soil evaporation causes resolution effects. It amounts to 4.8 mm in the 5 km setup and to 0.7 mm in the 210 km setup in July. Soil evaporation draws water from the top soil layer. It depends upon potential evaporation, which does not induce resolution effects, and on the relative humidity  $h$  at the surface.

$$h = 0.5 \cdot \left(1 - \cos\left(\pi \cdot \frac{\theta}{\theta_{cap}}\right)\right) \quad (2.4)$$

$\theta$  describes the top layer soil moisture and  $\theta_{cap}$  the top layer soil field capacity. Soil evaporation is thereby nonlinearly dependent on the top layer soil moisture. This nonlinearity induces the resolution effects.

Large top layer soil moisture is found in areas which hold high values of the Clapp and Hornberger parameter and thus also high amounts of supercooled water. Supercooled water is available for diffusion processes in the soil as soon as its temperature crosses 0°C. It is thus more readily available than soil ice which needs to get melted first. The water diffuses from the moist thawing front upwards to the relatively drier top soil layer and increase the absolute soil moisture there. Moreover, the Clapp and Hornberger parameter enters the equation for soil diffusion processes and leads to increasing diffusion with increasing parameter values. The Clapp and Hornberger parameter is thus the main actor for evaporation resolution effects.  $\Delta rRE_{evap}$  equals 42% in simulations with uniform Clapp and Hornberger parameter and less than 6.5% in all other simulations with uniform parameters. The areas with large evaporation fluxes in figure A.1 hold clay soils which are characterized by high Clapp and Hornberger parameter values.

*Clapp and  
Hornberger  
parameter*

## 2.4 DISCUSSION

*Importance of  
vegetation and soil*

When comparing 5 km and 210 km setups I show that soil parameters induce stronger resolution effects than vegetation characteristics. This is in line with previous findings that show a higher sensitivity of modelled energy and water fluxes to soil properties than to vegetation (Li et al., 2018). I hypothesize that vegetation could play a larger role in coupled simulations than in the here conducted land-surface-only simulations. In coupled atmosphere and land simulations, feedbacks of vegetation with climate occur and could induce resolution effects. The roughness length differs between trees and grasses which affects the boundary layer turbulence and thereby the land surface temperature. Also the albedo in winter differs greatly between trees and grasses and influences the surface temperatures. Tree crowns stick out of the snow blanket, while grasses are completely snow-covered. In contrast to coupled simulations, in land-surface-model-only simulations the surface temperature depends largely on the climate forcing and is not much affected by land processes.

*Soil parameters*

Soil organic matter and the Clapp and Hornberger parameter induce large parts of the resolution effects by impacting soil moisture. Also previous findings show changes in simulated soil moisture with higher model resolution (Ji et al., 2017; Singh et al., 2015). The sensitivity of high-resolution simulations to soil heterogeneity implies the need for high-quality soil input parameters. This poses problems, since soil parameters in the Arctic come with high uncertainties. Due to scarce observations, parameters are often estimated by approximation from remotely sensed land cover or by use of traditional generalized soil maps. Especially soil carbon shows large uncertainties in boreal and Arctic regions (Hugelius et al., 2014; Tifafi et al., 2018).

*Nonlinear vertical  
discretization*

I show that the resolution effects are attributable to model nonlinearities. The discrete treatment of soil thermal processes induces nonlinear behaviour in soil thawing processes. I hypothesize that with a much higher vertical soil resolution, the resolution effects in active layer depth would decrease, because the soil could thaw more gradually. A higher vertical soil resolution for the upper soil column covering the active layer is presumably favourable for Arctic land surface models in order to enable more gradual thawing and reduce biases due to discrete thawing. In between eight Arctic land surface models taken for an inter-comparison, the amount of soil layers ranges between 3 and 30 with an average of 14 for a soil depth ranging from 2 to 47m (Andresen et al., 2020). In this study I applied 18 soil layers including 11 layers within the upper three meters, which is more than average, but likely not enough. Much finer soil resolutions are

favourable.

As explained in the introduction (Ch. 1.2), heterogeneity in the Arctic acts on very different scales. On a 5 km scale, I capture much more heterogeneity especially in soil parameters than in 210 km resolution. However, there is still a great amount of sub-grid heterogeneity in 5 km resolution that the model does not capture. Resolution effects could increase with even higher resolution. However, testing this is beyond the scope of this thesis. In order to employ JSBACH<sub>3</sub> on scales of meters to hundreds of meters, many processes may need representation which are currently not accounted for. An easier way forward would be to represent additional sub-grid processes on tiles such as microtopography in ice-rich landscapes (Aas et al., 2019; Nitzbon et al., 2020a).

*Heterogeneity*

In this study I show that there are resolution effects on fluxes and soil state variables with soil state variables being more impacted than fluxes. Thus, resolution of boundary conditions does matter, especially for variables influenced by model nonlinearities.

*Chapter conclusion*



High-resolution climate forcing data on km-scale offers several advantages for the simulation of Arctic land surface processes. The Arctic is characterized by alternating highlands and lowlands as well as the proximity to the Arctic ocean. On km-scale resolution, orographic precipitation and temperatures in mountainous regions are better resolved. Also convective precipitation and precipitation extremes are more realistically represented as well as wind speed extremes which occur more often at ocean coasts than inland. The recently available global km-scale Earth system model simulations cover only short time scales, but can be used as a cyclic climate forcing for land-surface-model-only simulations. However, the impact of a high-resolution climate forcing on terrestrial processes in the northern permafrost areas as well as potential limitations were never systematically studied. Therefore, I focus my second study on this topic.

*Introduction*

For better comparison, the simulation spatial extent is restricted to the same case study area as in the first study (Ch. 1.2). I conduct simulations with the land surface model JSBACH<sub>3</sub> for two resolution setups (Table B.1). The first setup runs on 5 km resolution and includes climate forcing data on 5 km-scale. The model boundary conditions are resolved in 210 km to enable investigation of forcing effects only. The second setup operates on 210 km resolution including 210 km forcing data and boundary conditions. The temporal extent of the forcing data amounts to five years. It is used as cyclic forcing for a spin-up of 80 years plus an analysis period of five years. An analysis period of 30 years would not be meaningful due to the same recurring forcing values inducing very similar output. Tests for statistical significance were not conducted against the interannual variability due to the availability of only five years, but against the variability within individual months (Ch. B.2). To compare the output of the two setups, relative resolution effects of variable  $X$   $rRE_X$  are calculated analogously to 2.1. For statistical distributions, absolute units instead of relative units are used and resolution effects  $aRE_X$  are computed as:

*Methods*

$$aRE_X = X_{5km} - X_{210km} \quad (3.1)$$

In addition to these control simulations, I use idealized simulations to estimate the impact of individual forcing variables. They are conducted analogously as in the first study and resolution effects

$rRE_X^{\text{uniform}}$  are calculated and subsequently differences  $\Delta rRE_X$  to the control simulations are computed. I differentiate the case study area within the 5 km setup into highlands and lowlands to enable a detailed analysis of processes inducing resolution effects. Lowlands are defined as areas which are located below 300 m a.s.l. and highlands as areas of higher altitude (Jones et al., 2022; Paltan et al., 2015). Highlands include 7% of grid cells in the 5 km setup.

Model setup	Model resolution [km]	Boundary conditions [km]	Climate forcing [km]
5 km setup	5	210	5
210 km setup	210	210	210 (upscaled from 5)

Table 3.1: Model setups for 5 km and 210 km simulations.

### 3.1 RESOLUTION EFFECTS

Evaporation shows large resolution effects  $rRE_{\text{evap}}$  of -21% (-8mm) in the summer mean (Table B.2). Drainage resolution effects  $rRE_{\text{drain}}$  amount to 9%. And latent heat flux, which corresponds to the heat transported in evapotranspiration, exhibits resolution effects  $rRE_{\text{LHF}}$  of -7%. The other variables displayed in table B.2 show small to negligible resolution effects. Thus, resolution impacts mainly the modelled surface and subsurface hydrology.

#### *Role of precipitation*

Simulations with uniform precipitation show differences to the control simulations  $\Delta rRE_{\text{evap}}$  of -22% for evaporation. In contrast,  $\Delta rRE_{\text{evap}}$  amounts to  $\pm 1\%$  for other forcing variables set uniform. Precipitation is therefore the main driver of evaporation resolution effects. Simulations with uniform precipitation also exhibit larger differences  $\Delta rRE_{\text{drain}}$  for drainage of 8% than simulations with other uniform forcing variables. The spatial distribution of precipitation in connection with orography induces the resolution effects in evaporation and drainage (see below).

#### *June, July and August*

Evaporation resolution effects are largest and statistically significant in July (-27%, -4.8 mm) and smaller in June (-20%, -1.0 mm) and August (-15%, -2.3 mm). Evaporation fluxes are also largest in July due to warm temperatures (12°C) and much precipitation (79 mm). August evaporation is limited by temperature (9°C) and June evaporation by precipitation (21 mm). Thus, precipitation and temperature both affect evaporation, but, as shown above, precipitation is playing a greater role for the resolution effects. I will elaborate on this in the following subchapter by differentiating between highlands and lowlands in the 5 km setup to enable a more detailed analysis of causes for the large

resolution effects in evaporation.

	ALD [%]	Drainage [%]	Evaporation [%]
JJA $rRE_X^{\text{control}}$	-0.4	8.9	-21
	GPP [%]	LHF [%]	Runoff [%]
JJA $rRE_X^{\text{control}}$	-3.7	-7.3	5.4
	SHF [%]	Soil temp. [°C]	Transpiration [%]
JJA $rRE_X^{\text{control}}$	3.4	-0.05	-1.1

Table 3.2:  $rRE_X^{\text{control}}$  signifies the resolution effects between the two control simulations in 5 km and in 210 km resolution for the respective variables in this table. They are calculated as the relative differences between the 5 km simulation and the 210 km simulation of summer mean values averaged over the case study area [%] (Equ. 2.1). Soil temperature difference refers to the temperature in 19cm depth [°C]. GPP refers to gross primary productivity, ALD to active layer depth, LHF to latent heat flux and SHF refers to sensible heat flux.

### 3.2 HIGHLANDS AND LOWLANDS

Precipitation is substantially differently distributed between highlands and lowlands (Fig. B.2; note that precipitation resolution effects as well as temperature resolution effects balance out over the case study area as both variables are input parameters). Due to orographic precipitation processes, the precipitation flux amounts on average to 245 mm in the highlands and to 175 mm in the lowlands (note that the highlands encompass a much smaller area than the lowlands). This difference is evident in figure B.2 which shows large positive resolution effects in the highlands and slightly negative effects in the lowlands for precipitation. Temperature shows the opposite distribution with large and negative effects in the highlands and slightly positive effects in the lowlands. This is due to temperatures decreasing with altitude.

*Precipitation and temperature*

Evaporation resolution effects are large and negative in the lowlands with a median of -9 mm and small and slightly negative in the highlands with a median of -1 mm. The distribution between highlands and lowlands shows similarities to the precipitation distribution. High precipitation fluxes in the highlands can feed higher evaporation fluxes of 35 mm in the highlands, while smaller precipitation fluxes in the lowlands limit evaporation there to 29 mm. Evaporation resolution effects are not positive in the highlands due to colder temperatures in the highlands relative to the 210 km setup which limit the available energy and thereby evaporation fluxes. In the lowlands, temperatures are warmer, but evaporation is limited by the water-availability. In the

*Evaporation*

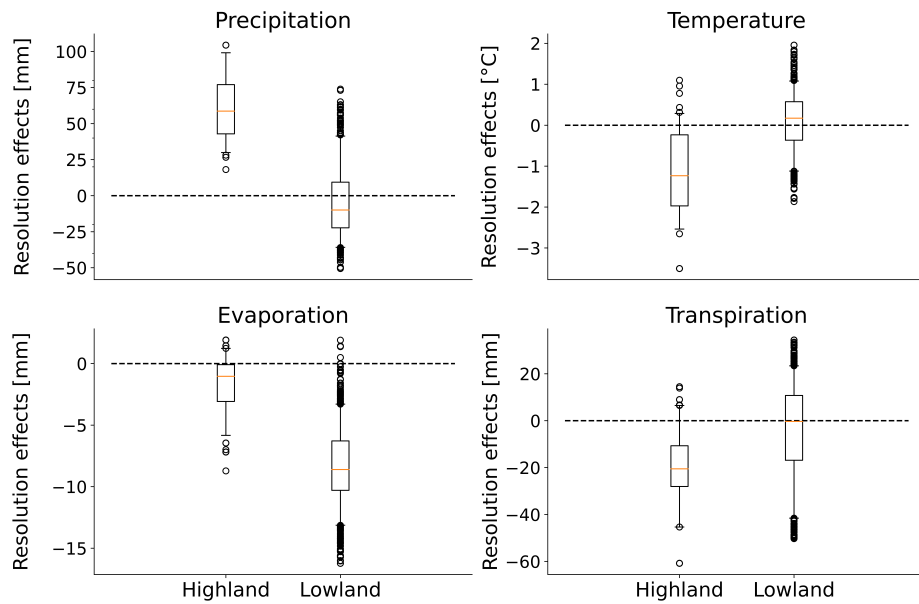


Figure 3.1: Boxplots show resolution effects of precipitation (upper left), air temperature at lowest atmospheric layer (upper right), evaporation (lower left) and transpiration (lower right). Resolution effects are calculated as the difference of simulations in 5 km relative to 210 km setups (Equ. 3.1) for JJA for every grid cell on the 5 km grid. Grid cells in the 5 km setup are differentiated in highland (elevation  $\geq 300$  m a.s.l.) and lowland locations. Lowlands encompass the vast majority of the case study area. Resolution effects for temperature and precipitation balance out over the case study area as they are input parameters.

5 km setup, the lowlands are more water-limited compared to the 210 km setup. Since lowlands entail a much larger area than the highlands, overall resolution effects in evaporation are large and negative like in the lowlands, meaning evaporation fluxes are smaller in the 5 km setup than in the 210 km setup.

#### *Transpiration*

In contrast to evaporation, transpiration fluxes are larger in the lowlands (84 mm) than in the highlands (63 mm). Figure B.2 shows similar distributions for transpiration as for temperature. Transpiration thus does not show the same precipitation-dependency as evaporation, but depends more on temperature. Colder temperatures in the highlands relative to the 210 km setup limit transpiration fluxes there and cause large and negative highland resolution effects (-21 mm). In contrast, resolution effects are negligible in the lowlands (-0.3 mm). For transpiration, less precipitation in the lowlands relative to the 210 km setup is balanced by warmer temperatures. Due to the much larger lowland area than highland area within the case study region, overall resolu-

tion effects in transpiration are small (-1 mm, -1%).

The resolution effects in drainage are also associated with the spatial distribution of precipitation. High precipitation fluxes in the highlands cause very high drainage fluxes in the highlands. In the lowlands, drainage fluxes are smaller due to less precipitation, but still slightly larger than in the 210km setup to balance the small lowland evaporation fluxes in terms of the terrestrial water balance.

*Drainage*

### 3.3 EVAPORATION AND TRANSPIRATION IN JSBACH

Evaporation fluxes are differentiated into snow evaporation (negligible in summer), soil evaporation and skin evaporation in JSBACH. Skin evaporation occurs from the skin reservoir which is the very thin film of water on top of vegetation and bare ground. It contributes the largest portion to total evaporation, namely 84% in 5 km and 88% in 210 km. Soil evaporation equals 15% of total evaporation in 5 km and 11% in 210 km setups. It feeds from water within the top soil layer which comprises the upper 6.5 cm of the soil. Both skin and soil evaporation depend on small water reservoirs which quickly dry out. Thus, it requires regular precipitation to maintain high evaporation fluxes. However, at very high precipitation amounts as in the highlands, evaporation fluxes are leveling off and are not increasing further, because they are restricted by temperature and vapour pressure deficit. Evaporation thus shows a nonlinear dependence on precipitation (Fig. B.4). Moreover, the skin reservoir and the top soil layer provide a limited storage capacity for water due to their small reservoirs. Thus, they cannot accumulate much water in heavy precipitation events which contributes to the nonlinear dependence on precipitation (Fig. B.4).

*Evaporation*

In contrast, transpiration draws water from the entire thawed part of the rootzone, which amounts to 29 cm in depth over the JJA average. The water reservoir is thus much larger for transpiration than for evaporation. Transpiration is thereby not as dependent on regular precipitation. Since also the water storage capacity of the rootzone is larger, more precipitated water during heavy precipitation events can be stored for later use. Due to these reasons, transpiration is not as sensitive to precipitation as evaporation. A higher dependence on temperature is present, since the Arctic is an energy-limited region.

*Transpiration*

### 3.4 DISCUSSION

I compare simulations with high and low resolution forcing and reveal large resolution effects in evaporation which are statistically significant

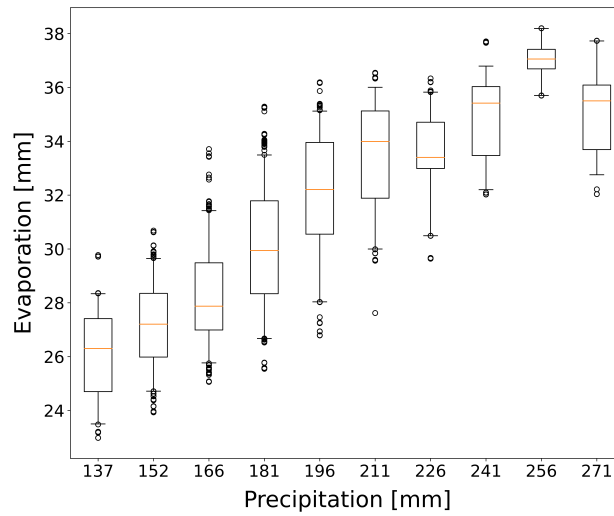


Figure 3.2: The boxplots show the dependence of evaporation on precipitation for JJA in the 5 km setup.

in July. Drainage and latent heat flux exhibit smaller resolution effects. Thus, the surface and subsurface hydrology is mainly affected by forcing resolution. This corresponds to previous findings which show a higher sensitivity of hydrological variables to forcing resolution than vegetation variables (Albergel et al., 2018).

#### *Highlands and lowlands*

Resolution effects in evaporation are larger and more negative in the lowlands than in the highlands, i.e. evaporation fluxes are smaller in the lowlands than in the highlands. This is due to precipitation fluxes being larger in the highlands than in the lowlands. In reality, precipitation fluxes are indeed usually larger in the highlands, but a fraction of the water is usually transported by surface and subsurface runoff to the lowlands. The lowlands are usually characterized by wetter soils than the highlands and (seasonally) ponding water which feeds high evaporation fluxes. Evaporation fluxes in the highlands are usually relatively smaller, since colder temperatures and the vapour pressure deficit limit the fluxes. Slopes in the highlands further impede ponding water and thereby decrease evaporation fluxes. The resolution effects in evaporation thus do not constitute an improved result due to the high-resolution forcing. They rather reveal that the precipitated water in the highlands does not get transported to the lowlands in the model which results in smaller evaporation fluxes in the lowlands than in the highlands.

In the highlands, the precipitated water which exceeds the water storage capacity of the soil and the atmospheric moisture demand goes directly into river discharge in the model. Neither surface nor subsurface runoff connects highlands with lowlands in the model and

the subsurface runoff is treated independently of the local slope. In reality, due to permafrost building an impermeable layer in the ground, subsurface runoff occurs mostly close to the surface and is following similar slopes as surface runoff connecting highlands with lowlands. A fraction of the simulated drainage water in the highlands would in reality move via (subsurface) runoff from highlands to lowlands. In the case study area, the water pathway from the highlands to the ocean leads from the highlands through the lowlands to the Kolyma river and then to the ocean. Hence, the water should run from highlands to lowlands.

The resolution effects found in this study reveal shortcomings of the model employed and indicate that the implementation of lateral water transport between grid cells is a crucial prerequisite for land surface models if applied in high-resolution. This is in line with findings by the hydrological community who emphasize the importance of inclusion of lateral water fluxes in high-resolution land surface models (Clark et al., 2015; Ji et al., 2017; Maxwell & Condon, 2016).

Lateral water transport between grid cells is not commonly represented in land surface models. Often, models incorporate a river routing scheme to collect water from runoff and drainage and transport it to the sea in order to compute the freshwater flux into the ocean (Hagemann et al., 2020; Riddick et al., 2018). This however does not include transporting water between different land areas. Other approaches represent lateral water fluxes on sub-grid scales in low-resolution land surface models (Clark et al., 2015; Fan et al., 2019; Nitzbon et al., 2020b; Smith et al., 2022a). This improves the evapotranspiration estimates along altitude gradients (Rouholahnejad Freund & Kirchner, 2017; Swenson et al., 2019). These water fluxes are however connections within one grid cell and not between different grid cells. Regarding high-resolution models, this study points out the necessity to include lateral water transport between grid cells.

*Lateral water transport*

In study 1, the active layer depth shows the largest resolution effects while in this study evaporation does. The resolution of boundary conditions and especially of soil parameters thus affects active layer depth as subsurface and soil state variable more than the fluxes, while the forcing resolution impacts evaporation as water flux and surface variable most. The forcing resolution does not induce resolution effects in active layer depth, because the total top soil layer heat conductivities in the 5 km setup show a very localized distribution and only range from 1.27 to 1.35 W/m/K in the summer mean. In contrast, soil parameters induce a distribution with a wide spread, ranging from 1.02 to 2.40 W/m/K. The very different soil heat conductivities in study 1 get nonlinearly translated into very different active layer depths by the discrete treatment of soil thermal processes. In this second study there

*Comparison with study 1*

are negligible resolution effects in active layer depth, since forcing variables in the 5 km setup cause a very localized distribution of soil heat conductivities with similar values as in the 210 km setup.

*Chapter conclusion*

In this study I show that there are large resolution effects in evaporation and smaller effects in drainage. Forcing resolution thus does matter and affects the water fluxes.

## CONCLUSION

---

In the previous chapters, I analysed effects on fluxes and soil state variables induced by high-resolution boundary conditions and by a high-resolution forcing. In the following, I want to first answer my research questions in order to sum up my results and then dive into the discussion and implications of my work. The first research question reads:

WHAT ARE THE EFFECTS OF HIGH-RESOLUTION BOUNDARY CONDITIONS ON SIMULATING ARCTIC TERRESTRIAL PROCESSES?

*1<sup>st</sup> research question*

In this study I compare a high-resolution setup on 5 km scale with high-resolution boundary conditions and low-resolution forcing to a low-resolution setup on 210 km scale. I show that there are resolution effects on fluxes and soil state variables, i.e. differences in high- relative to low-resolution simulations. The effects are mostly small in the summer mean, but greater within individual summer months. I reveal that soil parameters induce major shares of the resolution effects and that vegetation parameters are less important regarding resolution. Active layer depth shows large and statistically significant resolution effects of +20% in the summer mean and +43% in August. The effects are caused by the heterogeneous distributions of soil organic matter and the Clapp and Hornberger parameter and are nonlinearly amplified by the discrete treatment of soil thermal processes. Evaporation exhibits statistically significant resolution effects of +43% in July.

The second research question reads:

WHAT ARE THE EFFECTS OF A HIGH-RESOLUTION CLIMATE FORCING ON SIMULATING ARCTIC TERRESTRIAL PROCESSES?

*2<sup>nd</sup> research question*

By comparing a high-resolution setup on 5 km scale with high-resolution forcing and low-resolution boundary conditions to a low-resolution setup on 210 km scale, I reveal that forcing resolution impacts the hydrology. I find resolution effects of -21% in evaporation in the summer mean. In July, the effects amount to -27% and are statistically significant. In the high-resolution setup, the lowlands show particularly large and negative resolution effects, meaning evaporation fluxes are smaller compared to the low-resolution setup. The smaller fluxes are due to the lowlands being water-limited in the 5 km setup as precipitation falls mainly in the highlands and water is not transported laterally from the highlands to the lowlands in the model, the latter in contrast to reality. The resolution effects thus do

not represent an improvement in the simulated hydrology due to the high-resolution forcing, but rather indicate shortcomings of the model employed. The results suggest that the implementation of lateral water transport between grid cells is a crucial requirement for land surface models applied in high-resolution.

#### 4.1 DISCUSSION AND IMPLICATIONS

##### *Parameterizations in high resolution*

The general paradigm is that high-resolution must be better than low-resolution since boundary conditions and forcing data are better resolved. This is, however, not true if assumptions made for 200 km scale simply do not work on km-scale. On scales of 200 km, it is a logical assumption that every grid cell has access to a big river transporting water to the ocean, so the hydrology of one grid cell would not necessarily influence the hydrology of adjacent grid cells. My results indicate that this assumption does not hold on scales of 5 km. Lateral water fluxes connecting grid cells with each other are presumably required for km-scale resolutions. Another improvement for high-resolution models would be making subsurface runoff topography-dependent, since also the subsurface includes topographic gradients redirecting water between grid cells.

Other assumptions that could cause difficulties on km-scale, but are not examined in this thesis, include the transmission of fires. For example, Siberian wild fires could easily expand over an area larger than one 5x1.9 km grid cell (Mccarty et al., 2021). However, fire transmission between grid cells is not implemented in most land surface models. The assumption that most fires are smaller than the grid box area is valid for 210 km setups, but likely not for 5 km setups. High-resolution models could potentially also require parameterizations for fire transmission between grid cells. Thus, in contrast to atmosphere and ocean models which need less parameterizations in high resolution, land models may need more parameterizations.

##### *Computational costs*

Another important aspect of high-resolution simulations compared to low-resolution simulations are the computational costs. A doubling of the resolution of JSBACH3 in a land-surface-model-only setup quadruples the costs since one grid cell is split into four smaller grid cells. Plus there are additional 10-20% extra costs due to writing of longer restart files. If, for example, lateral water transport in JSBACH3 gets implemented, computational costs would additionally increase significantly due to increased computational complexity. Moreover, ensemble simulations or simulations of long time scales are not feasible in high resolution within the foreseeable future. The costs are thus a crucial factor concerning the choice of resolution for future land

surface models.

The first study suggests that a higher vertical soil resolution is favourable since it makes soil thawing less discrete and more gradual. This applies for the upper soil layers which are located within the active layer. A higher vertical soil resolution would improve both resolution setups, since it is independent of the horizontal resolution. However, it would also add computational costs, especially since the time stepping would also have to be increased to adjust it to the vertical resolution.

*Vertical soil resolution*

Limitations to both studies are the use of only one land surface model and the coverage of only a small area. Different land surface models may represent details of processes such as the calculation of soil heat conductivity differently (Dai et al., 2019). Thus, resolution effects may vary among different land surface models. Some implications of this work however apply to many land surface models. Lateral water transport is not commonly represented in land surface models and most models would improve from an increased vertical soil resolution. Also the uncertainty of soil parameters in the Arctic concerns all modelling communities using them as input.

*Limitations*

The confinement to a small area restricts the direct transfer of results to pan-Arctic scale. The exact numbers I presented for the resolution effects would certainly change for a different region. Most processes would however occur similarly. For example, very small soil organic matter amounts will also in other areas induce an especially large soil heat conductivity and deep active layers. However, especially large soil organic matter amounts do not occur within the case study region. They could increase the soil hydraulic conductivity tremendously and thereby induce additional resolution effects.

The availability of only five years of high-resolution forcing data poses a limitation to my second study. The interannual variability in fluxes and soil state variables is represented to a quite limited extent. Only having five years of data also inhibits the applicability of tests for statistical significance against the interannual variability.

I did not conduct a model evaluation, so I cannot deduce from my results if high- or low-resolution simulations are better compared to observations. However, I also did not target a model evaluation. Instead, I use idealized simulations with the aim of investigating model processes which induce differences between simulations of the two model setups. The knowledge about which processes induce resolution effects, and how and why, may support the planning of future high-resolution simulations, especially also in regard of model limitations. Moreover, the conduction of an evaluation would not have been straightforward, since alone the two different forcings used in study 1 and 2 are very different in regard of yearly mean precipitation (219

mm and 416 mm) and yearly mean temperature ( $-11.9^{\circ}\text{C}$  and  $-8.3^{\circ}\text{C}$ ) and thus induce different fluxes. Furthermore, observations are scarce in the Arctic and for many variables only point-scale observations are available for comparison.

Other limitations to my work include the absence of some processes in the model such as fire, dynamic vegetation, a full carbon budget and nutrient availabilities. These processes could possibly also be affected by resolution. I especially expect resolution effects to occur for fire-related processes due to fire not being transferred between grid cells as discussed above.

I further did not conduct simulations with coupled atmosphere and land model components, since long spin-ups in such high resolution with a coupled model are currently computationally not feasible. It would however be interesting to study the effects of resolution on land-atmosphere interactions. For example, the resolution effects in evaporation that I investigated in the first study might decrease in a coupled setup, since humidity then reacts to evapotranspiration. In simulations with a prescribed climate forcing, the humidity at lowest atmospheric level may stay small even with high evapotranspiration rates. In a coupled setup, the humidity would react to high evapotranspiration fluxes and increase and evapotranspiration would in turn decrease.

#### *Outlook*

The next logical step in the line of my work is to investigate resolution effects comparing a high-resolution setup including both high-resolution boundary conditions and high-resolution forcing with a low-resolution setup. I hypothesize that in this setup active layer depth resolution effects could decrease slightly. The active layer is mostly affected by soil parameters and not by the climate forcing. However, the deepest active layer depths are located in the highlands which also show the coldest temperatures. Therefore, active layer depths might decrease slightly in the highlands and resolution effects may thus also decrease slightly. Evaporation resolution effects on the other hand might decrease more. The effects investigated in study 2 are large and negative in the lowlands. And the effects analysed in study 1 are positive in areas with high Clapp and Hornberger parameter values. Since these areas are located within the lowlands, total evaporation resolution effects may decrease.

A bigger step into the future of this work could possibly include the development of a pan-Arctic land surface model on km-scale. I already discussed some of the disadvantages of high-resolution models such as the computational costs and missing process representations. Provided that lateral water transport between grid cells is implemented and the computational resources are available, km-scale land surface models could provide benefits over low-resolution models. For example, in the first study I show that the heterogeneity of soil parameters

in high-resolution impacts the top soil heat conductivity and active layer depth. Small variations in soil temperatures can potentially have large impacts if e.g. thermokarst processes were implemented in the model. In the second study I show that the water fluxes react sensitive to the spatial distributions of temperature and precipitation in high resolution. Evapotranspiration estimates may thus improve particularly in mountaineous regions which may also improve the latent heat flux. Depending on the application and target, high-resolution simulations could thus add value and complement low-resolution modelling strategies.

Currently, the trend in Earth system modelling goes to high resolution, but the effects of land surface model resolution on Arctic terrestrial processes were never systematically studied before. In this thesis I show that land surface model resolution does affect simulated fluxes and soil state variables in the Arctic. By combining both studies I reveal that the resolution of model boundary conditions influences soil state variables more than it impacts fluxes, while the forcing resolution affects the fluxes. I thus conclude that boundary data resolution and climate forcing resolution are both important factors to account for when planning future high-resolution modelling activities.

*Conclusion*



## APPENDICES





## EFFECTS OF LAND SURFACE MODEL RESOLUTION ON FLUXES AND SOIL STATE IN THE ARCTIC

---

The work in this appendix is a manuscript in revision:

**Schickhoff M.**, de Vrese P., Bartsch A., Widhalm B., and Brovkin V.  
"Effects of land surface model resolution on fluxes and soil state in the  
Arctic". Manuscript in revision in: *Environmental Research Letters*.

### AUTHOR CONTRIBUTIONS

MS, PdV and VB designed the study. MS adapted the model to higher resolution, conducted the simulations and carried out the analysis. AB and BW processed the vegetation input data. MS, PdV, VB and AB contributed to the writing.



# Effects of land surface model resolution on fluxes and soil state in the Arctic

**Meike Schickhoff<sup>1</sup>, Philipp de Vrese<sup>1</sup>, Annett Bartsch<sup>2</sup>,  
Barbara Widhalm<sup>2</sup> and Victor Brovkin<sup>1,3</sup>**

<sup>1</sup> Max Planck Institute for Meteorology, Bundesstrasse 53, 20146 Hamburg, Germany

<sup>2</sup> b.geos, Industriestrasse 1, 2100 Korneuburg, Austria

<sup>3</sup> Center for Earth System Research and Sustainability, University of Hamburg, Bundesstrasse 55, 20146 Hamburg, Germany

## ABSTRACT

The northern high-latitudes are characterized by a rich landscape heterogeneity on different scales. However, the effect of horizontal land surface model resolution on fluxes and soil state variables in the Arctic has never been systematically studied. Here, we compare 210km and 5km setups of the land surface model JSBACH<sub>3</sub> for a case study in eastern Siberia to investigate whether and why resolution matters in simulating the interactions of soil physics, hydrology and vegetation. We show for the first time that there are model resolution effects on fluxes and soil state variables. Most effects are small in the summer mean, but larger within individual months. Heterogeneous soil properties induce large parts of the resolution effects while vegetation characteristics play a minor role. Active layer depth shows large and statistically significant differences of 20% between resolutions in the summer mean and 43% for August. The differences are due to the discrete treatment of soil thermal processes amplifying the impact of the heterogeneous distribution of soil organic matter content and of the Clapp and Hornberger parameter. Evaporation resolution effects amount to 43% in July and are statistically significant.

## A.1 INTRODUCTION

Earth system modelling is moving towards km-scale resolution (Hohenegger et al., 2023; Korn et al., 2022; Satoh et al., 2014). High spatial resolution also seems advantageous for Arctic land surface modelling, since the northern high-latitudes are characterized by a rich surface and subsurface heterogeneity. Topography, climate, surface materials, vegetation, hydrological conditions, and soil properties vary significantly over space (van Cleve et al., 1983; Viereck, 1992). Soil organic carbon in tundra environments shows high enough variation coefficients to belong to Earth's most varied soils (Siewert et al., 2021). And greenhouse gas fluxes vary more among Arctic land cover types than from year to year (Treat et al., 2018). The spatial scale of the heterogeneous characteristics is well below the traditional Earth system model resolutions of 100-300km. On these traditional scales, big mountain ranges and large river deltas can be resolved and large-scale biomes like tundra or taiga can be differentiated in models. On medium scales of 1-10km, smaller mountains, local forests and burned areas can be resolved. And differentiation between upland and lowland areas as well as between yedoma soils and younger sediments can be included. On even finer scales of 1-100m, polygonal tundra land forms, small lakes, ponds, thermokarst features and pingos could be integrated. Coarse resolution models thus cannot resolve many small-scale soil and vegetation properties and processes. For example, the uncertainty in simulations of regional carbon dynamics increases with coarser resolution and worse representation of tundra heterogeneity (Lara et al., 2020). Neglecting peatland heterogeneity can significantly bias modelled regional methane fluxes (Kou et al., 2022). The methane emissions may get over- or underestimated in low-resolution biogeochemical models due to a rough representation of small-scale interactions between input parameters (Albuhaisi et al., 2023).

This suggests that high-resolution land surface models are favourable for accurately simulating Arctic hydrology and carbon dynamics. However, the impact of spatial resolution on terrestrial processes in the Arctic has never been systematically studied, even though this is of crucial importance for confident choices regarding the future development of pan-Arctic high-resolution land surface models. Therefore, we test whether resolution matters and which processes make the model outcome resolution dependent. We develop a high-resolution version of the land surface model JSBACH<sub>3</sub> on the scale of 5 km for a case study in the Chersky region in eastern Siberia. We compare the results with the output of the same model in a traditional Earth system model resolution of 210km and thereby investigate whether resolution plays a role in simulating the interactions of hydrology, vegetation and climate in the Arctic. We also quantify which model

parameters and processes exert control on the differences between fine and coarse resolutions.

## A.2 METHODS

### A.2.1 CASE STUDY AREA

The case study area is situated in eastern Siberia within the continuous permafrost zone and extends from 158.4°-162°E and 67.5°-69°N. In the very north of the area, the southern tip of the Kolyma Indighirka lowlands is situated. These lowlands are characterized by many thermokarst lakes and tundra vegetation (Veremeeva & Gubin, 2009). South of them shrubs and trees are dominant (European Commission Joint Research Centre, 2003). Clay, loam and silt loam soils are prevalent and sandy loam soils occur in the east (FAO/IIASA/ISRIC/ISS-CAS/JRC, 2009). The mid-south is dominated by a mountain range which comprises tundra vegetation and low soil organic matter content (SOM). Otherwise, SOM is relatively evenly distributed over the case study area (Hugelius et al., 2013a; Hugelius et al., 2013b).

### A.2.2 EXPERIMENTAL SETUP

The land surface model JSBACH3 is the land component of the global Earth System Model MPI-ESM (Giorgetta et al., 2013). We use the model version 3.2 (Reick et al., 2021) including permafrost soil physics and a SOM scheme ranging from the surface to three meters depth (de Vrese et al., 2021). The soil is vertically resolved into 18 layers with differing thickness up to a maximum depth of 40m including bedrock. 11 layers are located within the first three meters. We run the model in two different horizontal resolutions, in 1.88° which corresponds to 210x77km in the case study area, and in 0.045° which corresponds to ca. 5x2km. The temporal resolution is 30 minutes. We use a standalone setup, thus we do not include feedbacks to the atmosphere. The model is forced with meteorological data from the Global Soil Wetness Project Phase 3 (Dirmeyer et al., 2006). We use 1.88° forcing resolution for both horizontal resolution setups to investigate solely model effects, and not forcing effects. The spin-ups span over the historical period from 1901 to 1979 and the analysis period encompasses 1980-2009.

We compute resolution effects of variable  $X$  as

$$RE_X = \frac{(X_{5\text{km}} - X_{210\text{km}}) \cdot 100}{|X_{210\text{km}}|} \quad (\text{A.1})$$

This gives differences in percent to allow comparing resolution effects between different variables. Resolution effects of the control simulations  $RE_X^{\text{control}}$  denote the difference between the 210km simulation and the 5km simulation, in which all input parameters are present in 5km resolution. Additionally, we use a set of idealized simulations to investigate the importance of individual parameters or sets of parameters (to test synergetic effects). In these simulations, the parameters are individually set to spatially uniform in both resolution setups. Therefore, the spatial average of the input parameter is calculated over the whole case study area, and this value is set to every grid box. Resolution effects of these simulations  $RE_X^{\text{uniform}}$  are computed and the difference relative to the control simulations is calculated:

$$\Delta RE_X = RE_X^{\text{control}} - RE_X^{\text{uniform}} \quad (\text{A.2})$$

We calculate  $\Delta RE_X$  for every single input parameter individually to test their effects (supplementary material) and did not make parameter choices beforehand. To estimate if the differences between resolutions are statistically significant, two-tailed student's t-tests at 5% significance level are applied over spatial averages of 1980-2009 summer mean values and individual summer months's mean values. T-tests are adapted to account for autocorrelation (Lorenz et al., 2016; Zwiers & von Storch, 1995).

High-resolution input data was introduced for orography, soil and vegetation parameters (supplements). A soil parameter that is not common, but important in this context, is the Clapp and Hornberger parameter (CHP). It is employed to describe soil hydraulic properties. CHP is empirically estimated by suction wetness data and increases when moving from coarse to fine soil textures (Clapp & Hornberger, 1978). It determines the amount of supercooled water in the soil (Ekici et al., 2014). The vegetation distribution is based on Copernicus Sentinel-1 and -2 data from 2018 and 2019. The landcover retrieval scheme by (Bartsch et al., 2019) has been adapted including advanced pre-processing (similar as in (Bartsch et al., 2021)), re-calibration and grouping of classes at 10m nominal resolution.

## A.3 RESULTS

### A.3.1 RESOLUTION EFFECTS OF VEGETATION AND SOIL PARAMETERS

Resolution effects on fluxes and soil state variables are present in the control simulations (Table A.1). In the summer mean, ALD resolution effects are large and statistically significant. Resolution effects in other

	ALD [%]	Drainage [%]	Evaporation [%]
JJA $rRE_X^{\text{control}}$	20	0.8	5.5
June $rRE_X^{\text{control}}$	1.7	12	-3.8
July $rRE_X^{\text{control}}$	12	-7.1	<b>43</b>
August $rRE_X^{\text{control}}$	<b>43</b>	7.4	13
	GPP [%]	Soil temp. [°C]	Transp. [%]
JJA $rRE_X^{\text{control}}$	4.8	<b>0.34</b>	3.3
June $rRE_X^{\text{control}}$	-8.0	0.3	22
July $rRE_X^{\text{control}}$	13	<b>0.2</b>	21
August $rRE_X^{\text{control}}$	1.4	<b>0.5</b>	-7.6

Table A.1:  $rRE_X^{\text{control}}$  signifies the resolution effects between the two control simulations in 5 km and in 210 km resolution for the respective variables. They are calculated as the relative differences of the 5 km simulation relative to the 210 km simulation of 1980-2009 mean case study area averages [%] (Equ. A.1). Bold font indicates statistically significant differences between resolutions. Soil temperature difference refers to temperature in 19 cm depth [°C]. Transp. refers to transpiration, ALD to active layer depth and GPP to gross primary productivity.

variables are small, however soil temperature also shows statistically significant differences. In July, evaporation resolution effects  $RE_{\text{evap}}$  are large with 43% and statistically significant. In August, ALD resolution effects  $RE_{\text{ALD}}$  show statistical significant differences of 43%. Soil temperature differences are statistically significant in July and August. Transpiration, drainage and GPP do not exhibit statistically significant differences due to smaller differences and large interannual variability. Overall resolution effects are largest in July. Resolution effects of further variables such as soil ice and soil moisture, runoff, latent heat flux, sensible heat flux, soil heat conductivity and soil heat capacity are small (supplementary material).

Simulations with spatially uniform vegetation parameters show mostly small to negligible differences  $\Delta_{\text{RE}}$  for both the summer mean and July (Table A.2). In contrast, simulations with spatially uniform soil parameters reveal much larger differences  $\Delta_{\text{RE}}$ . This shows that soil heterogeneity is more important regarding resolution than vegetation properties. This result also holds for June and August (supplementary material). The sum of  $\Delta_{\text{RE}}$  with uniform vegetation parameters and  $\Delta_{\text{RE}}$  with uniform soil parameters do not equal the total resolution effects, since synergistic effects occur. An investigation of processes inducing the resolution effects is presented here for the variables ALD and evaporation, since they show very large and statistically signifi-

	ALD [%]	Drainage [%]	Evaporation [%]
JJA $\Delta rRE_X$ veg. param.	2.3	3.2	-0.5
JJA $\Delta rRE_X$ soil param.	20	-2.3	6.4
July $\Delta rRE_X$ veg. param.	2.2	0.9	6.1
July $\Delta rRE_X$ soil param.	12	-8.1	42
	GPP [%]	Soil temp. [°C]	Transp. [%]
JJA $\Delta rRE_X$ veg. param.	-1.6	0.03	-3.4
JJA $\Delta rRE_X$ soil param.	7	0.31	7.2
July $\Delta rRE_X$ veg. param.	-1.5	0.03	-3.1
July $\Delta rRE_X$ soil param.	15	0.19	24

Table A.2:  $\Delta rRE_X$  signifies the difference between resolution effects of simulations with uniform parameters and resolution effects of the control simulations for the respective variables [%] (Equ. A.2). Uniform parameters are represented in the lines and output variables in the columns. The 1980-2009 summer mean and July mean are shown (for June and August see ch. A.6.). Soil temperature difference refers to temperature in 19 cm depth [°C]. Transp. refers to transpiration, ALD to active layer depth and GPP to gross primary productivity. Veg. param. refers to vegetation parameters including the root depths and soil param. refers to soil parameters.

cant resolution effects in July (evaporation) resp. August (ALD). The remaining variables are discussed in the supplements.

### A.3.2 EFFECTS ON ACTIVE LAYER DEPTH

ALD shows substantial and statistically significant resolution effects of 20% in the summer mean and 43% in August (Table A.1). The resolution effects increase from June to August as the active layer depths deepens with the longer thawing period. In the 5km setup, the deepest ALDs occur in the southern mountain range (Fig. A.1). The soils in this area hold very little SOM. Clay soil regions, characterized by high CHP values, also exhibit slightly deeper ALDs than average. SOM and CHP are the main drivers of ALD resolution effects. When setting them to spatially uniform,  $\Delta RE_{ALD}$  amounts to 19% for SOM and to 15% for CHP in August (supplementary material). Setting both parameters uniform simultaneously gives  $\Delta RE_{ALD}$  equal to 40% in August.

Heterogeneous SOM induces resolution effects due to its impact on the soil heat conductivity and on soil moisture, which in turn influences heat capacity, heat conductivity and the soil ice content. The dry and saturated soil heat conductivities both depend on the ratio of soil organic and mineral fractions. Mineral soils have a higher

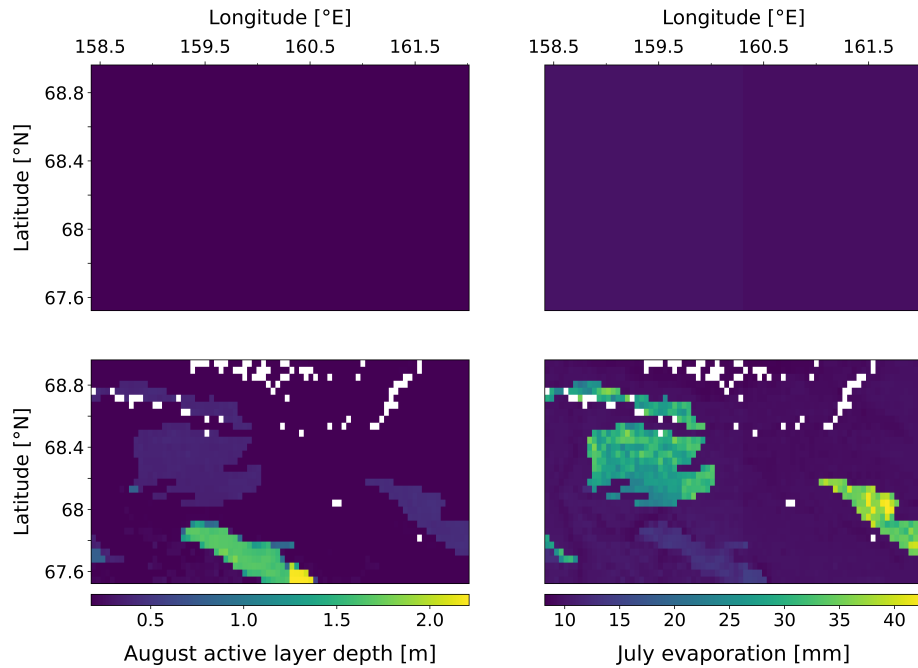


Figure A.1: 1980-2009 August mean active layer depth and July mean evaporation 210km (up) and 5km (down) resolution. White rectangles represent water bodies which are not modelled.

heat conductivity than organic soils due to two reasons. First, mineral particles such as sand, silt and clay have a higher heat conductivity than organic particles. Second, organic soils have a high porosity and thus a big pore volume. The air within the soil pores decrease the heat conductivity since air is a poor thermal conductor. Thus, soils with little SOM have a higher dry soil heat conductivity than soils with much SOM. Moreover, soil moisture plays a role since it affects the soil heat conductivity. Soils with high SOM characteristically store more absolute moisture than soils with little SOM, since the big pore volume gives much potential room for filling with water. However, due to the big potential space, in the model, these soils tend to have a lower soil saturation degree. In contrast, soils with small SOM usually show a higher saturation degree due to the model parametrisations. In the case study area, the soils in the mountain range have very low amounts of SOM and thus high saturation degrees. This reflects in deeper ALDs, because more saturated soils are better heat conductors than dry soils. In summer, the heat coming from above is well conducted to lower soil layers in the more saturated soils and leads to deeper ALDs. The heat conductivity of the first soil layer is thereby determining for the amount of energy transferred from the surface to the soil. The soil saturation degree  $sat$  is calculated as follows:

$$\text{sat} = \frac{\text{water}_{\text{soil}} + \text{ice}_{\text{soil}}}{\text{dsoil} \cdot \text{porosity}} \quad (\text{A.3})$$

with  $\text{water}_{\text{soil}}$  being the absolute water content of the soil layer,  $\text{ice}_{\text{soil}}$  the absolute ice content of the soil layer,  $\text{dsoil}$  the soil layer depth and  $\text{porosity}$  the volumetric porosity of the mixed mineral and organic soil. The total heat conductivity  $\lambda_{\text{tot}}$  of the respective soil layer is calculated as:

$$\lambda_{\text{tot}} = \lambda_{\text{sat}} \cdot \text{Ke} + \lambda_{\text{dry}} \cdot (1 - \text{Ke}) \quad (\text{A.4})$$

with  $\lambda_{\text{sat}}$  being the heat conductivity of saturated soil and  $\lambda_{\text{dry}}$  the heat conductivity of dry soil. The Kersten number equals  $\text{Ke} = \log_{10}(\text{sat}) + 1$  for  $\text{sat} > 0.1$  and  $\text{Ke} = 0$  for  $\text{sat} < 0.1$ .

Porosity decreases with decreasing SOM. A lower porosity leads to a higher saturation degree, because it is in the denominator of equation 1. A higher saturation degree causes a higher Kersten number and thus a higher total heat conductivity  $\lambda_{\text{tot}}$ , since the heat conductivity of saturated soils is much larger than the heat conductivity of dry soils due to water being a better heat conductor than air. Moreover, as explained above, both dry soil and saturated soil heat conductivities depend themselves on the ratio of mineral and organic soil fractions. Both increase with decreasing organic matter fractions. A higher total heat conductivity induces warmer soil temperatures and deeper ALDs. Therefore, low SOM is associated with deep ALDs. Notably, the ALD does not depend linearly on the SOM. SOM larger than 18% correspond to a mean ALD of 22cm with a maximum of 81cm, while SOM smaller than 14% are associated with ALDs of at least 80cm to a maximum of 221cm and a mean value of 158cm.

Resolution effects induced by CHP also act via soil moisture differences. High CHP values correspond to high amounts of supercooled water in the soils. Due to much supercooled water, less soil ice is present and less energy is required for phase changes in spring. Thus, a larger part of the available energy goes directly into soil temperature increase and induces deeper ALDs. Moreover, the year-round sum of soil moisture and soil ice within the first soil layer is largest where high CHP values are present. Thus, the numerator in equation 2 is large. The saturation degree is therefore higher than average and thus the heat conductivity is higher. Also the heat capacity is high due to the higher heat capacity of liquid water than of ice. A higher heat capacity increases the fraction of melting ice and contributes to deeper ALDs. In the 5km setup, the August ALD amounts to 42cm where CHP is high, while it amounts to only 24cm in the average soil.

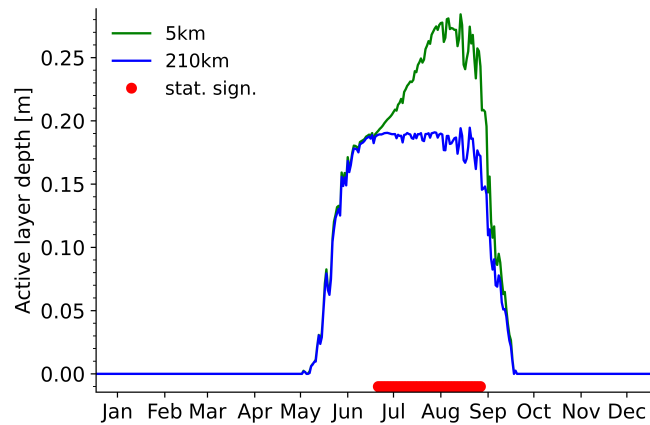


Figure A.2: Annual cycle of active layer depth averaged spatially and over the 1980-2009 period. Red marker indicates days with statistically significant differences between resolutions.

The annual cycle of ALD exhibits distinct behaviors in the two setups (Fig. A.2). The 210km simulation stops thawing at 19cm soil depth, which equals the second soil layer depth. This soil layer is considerably thicker than the first soil layer and thus holds more soil ice. All available energy goes into soil ice thawing, maintaining the temperature of the second soil layer at  $0^{\circ}\text{C}$  throughout the summer. In contrast, some grid cells in the 5km setup have more energy available and thaw beyond the second soil layer. On average, the soil thaws up until 28cm depth in August in the 5km setup. The key factor for the different behaviour in the two setups is the discrete treatment of the soil thermal processes, in which a soil layer of a given thickness is represented by a single set of variables, i.e. temperature, ice content etc. Thus, there is only one temperature per soil layer available which makes thawing of the respective layer binary and not gradual. The soil is characterized by a nonlinear vertical discretisation. Soil layers close to the surface are thinner than soil layers situated deeper in the soil column. Larger amounts of pore ice in thicker soil layers require more energy to thaw than ice in thinner soil layers so the zero curtain period lasts longer. Thus, the soil does not thaw linearly according to SOM and CHP, but the soil layer discretisation introduces nonlinearity.

The 1980-2009 yearly mean August ALD distributions show different medians (Fig. A.3). The western grid cells show a median of 34.0cm in 5km resolution and 18.6cm in 210km resolution and the eastern ones 22.5cm and 18.5cm respectively. The 5km western grid cells show the deepest ALDs, because they encompass the mountains with low SOM and large clay regions with much supercooled water. The 5km western grid cells also show the greatest interannual variability which is related to the mountains with low SOM. Areas with SOM smaller than 15% within 30cm soil depth show an ALD standard deviation

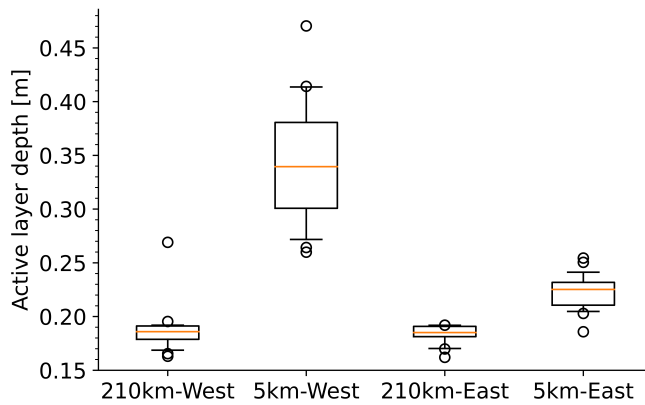


Figure A.3: Distributions of 1980-2009 August yearly mean active layer depth [m]. In the 5km setup, results are averaged within the 210km grid cell extent.

of 26.5 cm over time, while it is only 2.2 cm in regions with SOM larger than 15%. In contrast to the 5km setup, the 210km grid cells show little variability. More importantly, the 5th to 95th percentiles of the two 5km distributions are located entirely outside the 5th to 95th percentiles of the 210km distributions. This shows that resolution induces two substantially different distributions.

In summary, SOM and CHP induce spatial differences in ALD. The nonlinear vertical discretization of soil layers and the discrete treatment of soil thermal processes amplify these differences, so they do not average out over space anymore. This results in two significantly different distributions.

### A.3.3 EFFECTS ON EVAPORATION

Evaporation resolution effects are small when averaged over the whole summer (5.5%), but large and statistically significant in July (43%). In July, evaporation fluxes amount to 13.8mm in 5km and to 9.7mm in the 210km setup. Evaporation occurs from wet surfaces on vegetation and bare ground (skin evaporation), from the top soil layer (soil evaporation) and from snow. Snow evaporation is negligible in July. Skin evaporation comes to 8.9mm in both resolution setups. It thereby makes up the largest share of total evaporation, but it does not induce resolution effects since the amounts are equal in both setups. Skin evaporation is computed by multiplying the fraction of wet surfaces with potential evaporation. The fraction of wet surfaces depends heavily on precipitation, but also on the leaf area index and the maximum vegetated fraction of the grid box. The vegetation-dependence does

not induce resolution effects, since the differences in these vegetation parameters across the case study area are small. Precipitation is in low resolution and thus does not cause resolution effects. Potential evaporation depends on the vapour pressure deficit, temperature and wind speed. Since these forcing variables are also resolved in low resolution, they do not induce resolution effects in skin evaporation. Soil evaporation amounts to 4.8mm in the 5km setup and to only 0.7mm in the 210km setup. Thus, soil evaporation induces the resolution effects. Soil evaporation depends on the relative humidity  $h$  at the surface by

$$h = 0.5 \cdot \left(1 - \cos\left(\pi \cdot \frac{\theta}{\theta_{\text{cap}}}\right)\right) \quad (\text{A.5})$$

$\theta$  denotes the top layer soil moisture and  $\theta_{\text{cap}}$  the soil field capacity. The equation depicts a nonlinear dependency on the top layer soil moisture. Figure A.4 illustrates this relationship for July data. Evaporation increases nonlinearly with top layer soil moisture. The non-linearity induces the resolution effects. In comparison, in the 210km setup, the top layer soil moisture amounts to 0.013m and 0.012m in the two grid cells. The high soil moisture amounts are thus not represented in 210km, which is why soil evaporation in the 210km setup is significantly smaller than in the 5km setup.

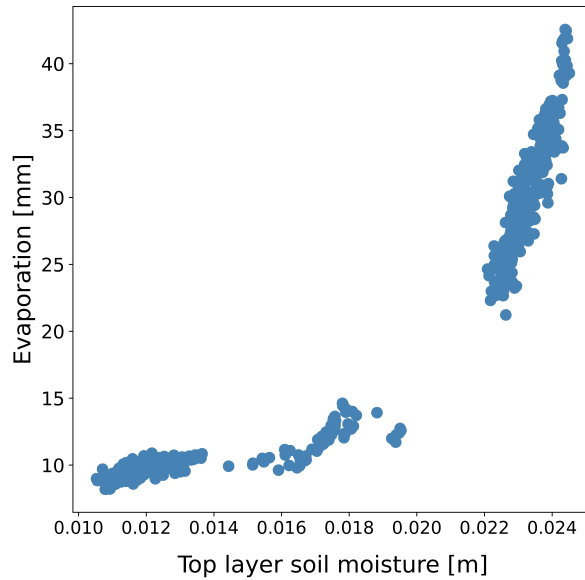


Figure A.4: Total evaporation in dependence of top layer soil moisture for 1980-2009 July mean.

Figure A.1 shows total July evaporation in the case study region. The areas with especially high evaporation fluxes are the clay soil

areas. They are characterized by a very high top layer soil moisture which sustains high evaporation fluxes. Clay soils hold high CHP values and thus have high amounts of supercooled water. Supercooled water is assumed to be immobile in the soil. However, as soon as it warms above  $0^{\circ}\text{C}$ , it is mobile and can move within the soil. Supercooled water is thus more quickly available for diffusion than soil ice, which needs to be thawed first. The water can diffuse from the moist thawing front in the second soil layer upwards to the top soil layer which is relatively drier. Moreover, CHP enters the equation to describe diffusion processes in the soil. High values increase the diffusion and provide more moisture supply. In simulations with uniform CHP values,  $\Delta\text{RE}_{\text{evap}}$  amounts to 42%, while it is less than 6.5% for all other parameters.

Evaporation resolution effects are smaller in June and August than in July. In June, total evaporation fluxes amount to 44mm in 5km and to 46mm in 210km setup. The fluxes are much larger than in July and August due to soils being very moist from prior snow melt. Since snow in winter is quite homogeneously distributed across the case study region due to low-resolution precipitation, also soil moisture and soil evaporation are relatively homogeneously distributed and resolution effects in June amount to only -3.8%. In August, the processes inducing resolution effects are similar to July, however resolution effects amount to only 13%. This is due to temperature limiting high evaporation fluxes in the clay areas. In July, 2m air temperature amounts to  $11.8^{\circ}\text{C}$ , while it is only  $8.9^{\circ}\text{C}$  in August. And also precipitation is smaller in August (36mm) than in July (40mm). Thus, also total evaporation fluxes are smaller in August than in July, with 9.7mm in the 5km and 8.6mm in the 210km setup.

#### A.4 DISCUSSION

We show that there are model resolution effects on fluxes and soil state in the Arctic. Uniform soil parameters show much larger reductions in resolution effects compared to control simulations than uniform vegetation parameters. This indicates that soil heterogeneity is the major player regarding resolution effects. Vegetation-induced resolution effects are minor in comparison. This is in alignment with a generally higher sensitivity of simulated water and energy fluxes to soil input parameters than vegetation parameters (Li et al., 2018). One factor for the smaller impact of vegetation are the setup of root depths in the model. They are not dependent on plant functional types, but distributed according to soil parameters (supplements). Moreover, we hypothesize that in simulations with coupled land and atmosphere components, vegetation would have a larger effect on resolution due to

feedbacks with the atmosphere. The albedo of trees and grasses is very different in winter, when snow is completely covering grasslands, but tree crowns stick out of the snow pack. Moreover, the differing roughness of trees and grasses influences the boundary layer turbulence and hence the land surface temperature. In the here conducted standalone simulations the land surface temperature is heavily dependent on the climate forcing and thus the impact of vegetation categories as defined for the model setup is small.

We further show that the resolution effects are induced by nonlinear characteristics of the model. The discrete treatment of soil thermal processes is most prominent and leads to resolution effects and differing behavior in ALD. We hypothesize that with a much finer vertical discretization of soil layers the resolution effects would decrease, because soil temperatures could change more continuously vertically. As shown for an inter-comparison of eight Arctic land surface models, the number of soil layers ranges from 3 to 30 for a depth of 2m to 47m (Andresen et al., 2020). The 18 layers utilized in this study are well within this range, however much more layers would be favourable to enable more gradual thawing.

We reveal that resolution effects due to SOM and CHP (determining the soil supercooled water amount) emerge to a large part due to impacts on the (relative) soil moisture distribution. This is in line with prior studies showing changes in modelled soil moisture with increasing resolution (Ji et al., 2017; Singh et al., 2015). This suggests that a good representation of (relative) soil moisture and more generally soil hydrology is important for high-resolution modelling. Furthermore, the sensitivity of model output to high-resolution soil input data indicates that high-quality soil data is required for future high-resolution land surface modelling. This is especially the case for SOM. However, in particular for Arctic and boreal regions, observations are scarce and soil parameter estimates are often based upon remotely sensed landcover as proxy or upon traditional generalized soil maps. Input data thus often contains large uncertainties. Differences between the soil carbon stock maps SoilGrids, HWSD, and NCSCD are especially large in boreal zones (Tifafi et al., 2018). Significant soil carbon data gaps are present i.a. in the High Arctic, in high-latitude mountain and Yedoma regions (Hugelius et al., 2014). Soil input data uncertainties are thus a potential source of error in high-resolution Arctic land surface modelling.

The generalisation of specific results from this study is limited by the use of only one land surface model and the coverage of only a small area. Different models may make different assumptions regarding the details of process representations such as the calculation of

the soil heat conductivity (Dai et al., 2019). This may lead to varying resolution effects between different land surface models. Experiments with a different remapping method and a different initialisation routine show quantitative variations in resolution effects compared to the control simulations (supplementary material). However, the processes inducing the resolution effects stay the same and are robust against different remapping techniques and initialisation approaches.

The spatial resolution of 5km is still coarse relative to the heterogeneous Arctic landscapes. Many land surface features and processes inducing lateral heterogeneity occur on smaller scales such as polygonal tundra landforms and thermokarst lakes. Even higher land surface model resolution resolving heterogeneities on scales of meters may produce even larger resolution effects. However, the parameterizations of lateral water fluxes in current land surface models do not allow resolutions finer than km-scale. Due to this limitation, we chose 5km resolution and show that even with this relatively coarse resolution, there are process-induced resolution effects.

#### A.5 CONCLUSION

We reveal model resolution effects on fluxes and soil state variables in the Arctic and show that these effects are primarily due to heterogeneous soil properties while vegetation characteristics play a minor role. Most effects are small in the summer mean, but larger within individual months. ALD presents the largest and statistically significant resolution effects of 20% in the summer mean and 43% in August. It shows a change in behavior between resolutions due to the discrete treatment of soil thermal processes amplifying impacts of soil parameter heterogeneity. July evaporation resolution effects are statistically significant and equal 43%. SOM and CHP cause great shares of the resolution effects, largely by inducing spatial differences in (relative) soil moisture. Good high-resolution input data for soil parameters are thus necessary for high-resolution simulations, but they are limited by scarcity of observations in the Arctic. We show that land surface model resolution matters, especially for variables affected by nonlinear model characteristics. In order to make precise projections of future Arctic hydrology and permafrost carbon fluxes, effects of model resolution need to be considered.

## A.6 SUPPLEMENTARY MATERIAL

### A.6.1 INPUT DATA

High-resolution input data was introduced for several parameters. Soil parameters include: Soil depth, soil organic matter content (SOM), soil texture-dependent parameters, soil moisture at initialisation and maximum root zone soil moisture. For soil depth to bedrock, we use a dataset in 250m resolution (Shangguan et al., 2017) which was generated using the SoilGrids system (Hengl et al., 2017). SOM is calculated as the quotient of soil organic carbon and a carbon biomass ratio of 0.5 and this divided by the density of organic material. Soil organic carbon data was acquired from the northern circumpolar soil carbon database in 0.012° resolution (Hugelius et al., 2013a; Hugelius et al., 2013b). The organic density was estimated to be 227 kg/m<sup>3</sup> for 0-30cm soil depth and 450 kg/m<sup>3</sup> for 30-300cm soil depth based on unpublished 2015 soil observational datasets (M. Göckede, pers. comm.).

Soil texture data was taken from the Harmonized World Soil Database in 30 arc-second resolution (FAO/IIASA/ISRIC/ISS-CAS/JRC, 2009). Literature values for soil texture-dependent parameters were assigned according to the respective soil texture. The soil texture-dependent parameter include the volumetric soil field capacity, the wilting point (Patterson, 1990), the pore size distribution index (Williams & Ahuja, 2003), the volumetric soil porosity, the saturated moisture potential, the saturated hydraulic conductivity, the heat capacity, the heat conductivity and the Clapp and Hornberger parameter (CHP) (Beringer et al., 2001).

Vegetation input parameters include the maximum vegetated fraction of the grid box, the cover fractions of each vegetation tile, i.e. grass, shrub and tree fraction, and the root depths. The first two parameters are based on Copernicus Sentinel-1 and -2 data (2018-2019). We use the three plant functional types “C<sub>3</sub> grass”, “deciduous shrubs” and “extratropical deciduous trees” in our model. Evergreen trees are neglected since they show a very scarce distribution in the case study area. Root depths are defined as the quotient of maximum root zone soil moisture and soil field capacity with soil depth as the upper bound. Maximum root zone soil moisture is based upon the Copernicus Sentinel derived landcover data and a climate model land surface parameter set (Stacke & Hagemann, 2013). The land-water distribution is based on ESA-CCI landcover data in 300m spatial resolution (ESA, 2017) and orography data was acquired from ETOPO1, a 1 arc-minute global relief model (Amante & Eakins, 2009). All parameters are transferred from the original resolution to 5km and 210km resolution using linear conservative remapping.

## A.6.2 OUTPUT

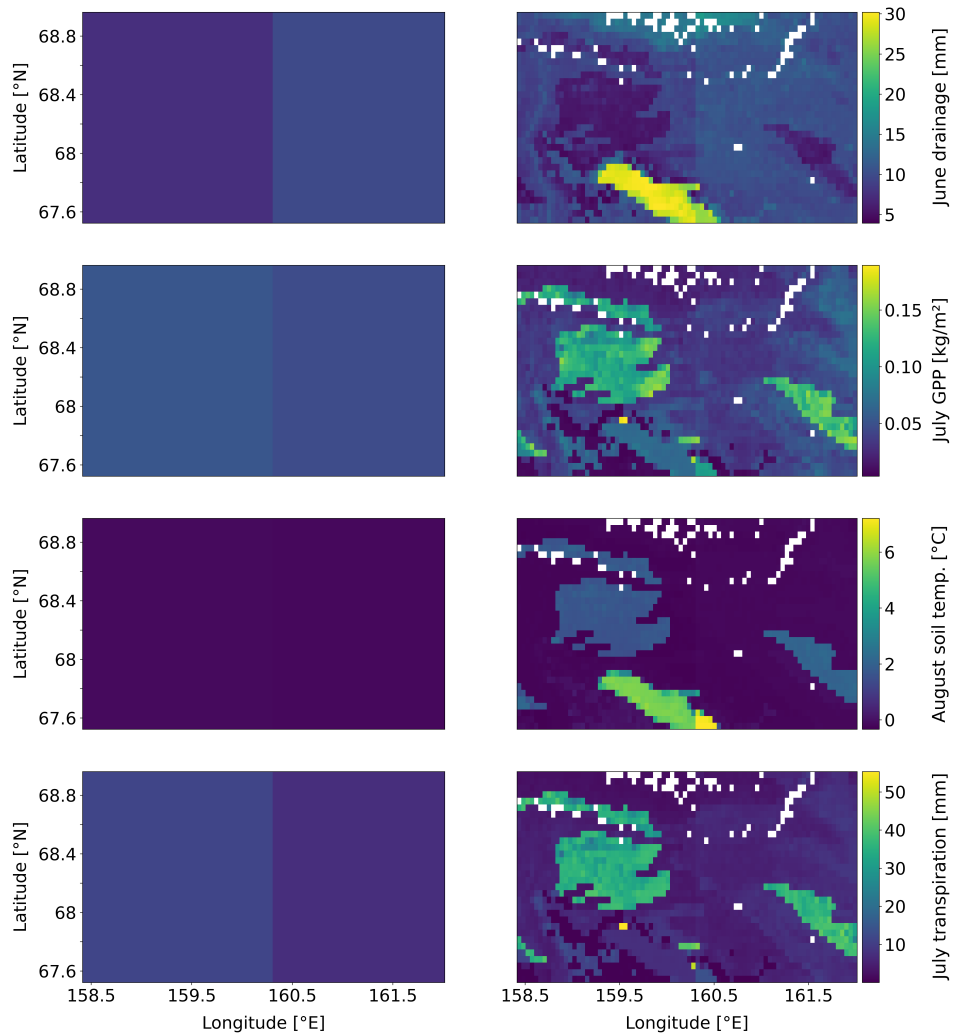


Figure A.5: Mean 1980-2009 June drainage, July gross primary productivity (GPP), August soil temperature in 19cm depth and July transpiration in 210km (left) and 5km resolution (right). The respective month with the largest resolution effects is shown.

## A.6.2.1 DRAINAGE

Drainage resolution effects are largest in June with 12% and the largest contributor is SOM.  $\Delta RE_{\text{drain}}$  for simulations with uniform SOM

amounts to 14% in June. Soils are only slightly thawed since summer just starts. However, in the mountains soils are already thawed a lot deeper than in the surrounding due to little SOM. Thus, drainage is also larger in the mountains in June since there is more water available for percolation and drainage (Fig. A.5). In contrast, ice and super-cooled water in frozen soils are immobile.

#### A.6.2.2 GPP

Gross primary productivity (GPP) resolution effects are largest in July with 13%. The processes inducing resolution effects on GPP are similar to transpiration processes, since plant productivity scales with plant transpiration (see section on transpiration). The 5km output maps for GPP show similar patterns as for transpiration (Fig. A.5). Fluxes are large in regions with high CHP values due to the high soil moisture amounts. SOM induced resolution effects are due to changes in relative soil moisture. Higher relative soil moisture in regions with little SOM produces higher plant productivity in those areas. Similar to transpiration, mineral soil field capacity induces resolution effects, since it also affects the relative soil moisture.

#### A.6.2.3 SOIL TEMPERATURE

Resolution effects on soil temperature are statistically significant in July and August and largest in August with 0.5°C, since soils are warmer in August than in June and July. The processes inducing resolution effects on soil temperature are similar to the ones for active layer depth (ALD). SOM changes the mixed soil mineral and organic heat conductivity and the soil saturation degree influencing the total soil heat conductivity. Regions with little SOM are associated with increased heat conductivity to lower soil layers and thus warmer soil temperatures. Also high CHP values induce high soil moisture amounts and thus better soil heat conductivity to lower layers and higher soil temperatures. Analogously to ALD, soil temperatures show nonlinear behavior due to the nonlinear vertical discretization of soil layers and the discrete treatment of soil thermal processes.

#### A.6.2.4 TRANSPIRATION

Transpiration resolution effects are largest in June with 22%, however this is due to the small transpiration flux in June. June transpiration amounts to 0.81mm in 5km and to 0.66mm in 210km. In July, resolution effects are almost as large with 21% and fluxes are substantially larger. They amount to 11.5mm in 5km and to 9.4mm in 210km. In

August, resolution effects are smaller with -7.6%. Thus, in the following we focus on the processes inducing July resolution effects:

The heterogeneous distribution of SOM induces a good share of the resolution effects.  $\Delta RE_{\text{tran}}$  amounts to -17%. Soils with high SOM characteristically store more absolute soil moisture than soils with little SOM due to a higher porosity. However, the relative soil moisture tends to be higher for soils with little SOM due to model parametrisations. The relative soil moisture  $\text{moist}_{\text{rel}}$  is calculated as:

$$\text{moist}_{\text{rel}} = \frac{\text{water}_{\text{soil}} - p_{\text{wilt}}}{\text{fieldcap} - p_{\text{wilt}}} \quad (\text{A.6})$$

with  $p_{\text{wilt}}$  being the wilting point and  $\text{fieldcap}$  the soil field capacity of the mixed mineral and organic soil.

The soil field capacity increases with increasing SOM. Soils with little SOM thus have a smaller soil field capacity and therefore a larger relative soil moisture. This leads to larger transpiration fluxes, since transpiration depends linearly on the relative soil moisture in the model. Figure A.5 shows transpiration fluxes which are only slightly higher in the mountains than in surrounding areas. The mountain soils contain little SOM and thus hold a high relative soil moisture. However, they also have very shallow soil depths of 10cm and a small porosity with little SOM. Both leads to them quickly drying out in summer. Thus, the soils cannot provide substantially more water for transpiration than surrounding soils and are only slightly visible in figure A.1.

Transpiration values are especially high in clay areas which hold high CHP values and thus high amounts of supercooled water (Fig. A.1).  $\Delta RE_{\text{tran}}$  of simulations with uniform CHP amount to 33%, thus CHP induces the largest share of transpiration resolution effects. In the model, supercooled water is available for plants as soon as it is warmed above 0°C in summer. Thus, supercooled water is available earlier than water from melted soil ice. This effect increases the transpiration fluxes in clay areas. Overall, clay soils hold high amounts of absolute soil moisture. High soil moisture increases the numerator in the equation above and thus also the relative soil moisture and transpiration. Additionally, mineral soil field capacity has a small effect on transpiration resolution effects, since the mixed mineral and organic soil field capacity enters the equation above.

#### A.6.2.5 FURTHER OUTPUT VARIABLES

Resolution effects for runoff, latent and sensible heat flux, heat capacity, heat conductivity, near-surface soil ice and near-surface soil

	Heat cap. [%]	Heat cond. [%]	LHF [%]	Runoff [%]
JJA $RE_X^{\text{control}}$	-0.7	<b>-4.0</b>	4.8	-3.3
June $RE_X^{\text{control}}$	0.6	<b>-3.9</b>	-3.4	-3.4
July $RE_X^{\text{control}}$	<b>0.8</b>	<b>-5.3</b>	<b>32</b>	<b>-4.0</b>
August $RE_X^{\text{control}}$	<b>-3.2</b>	-2.5	-0.6	-4.5

	SHF [%]	Soil ice [%]	Soil moisture [%]
JJA $RE_X^{\text{control}}$	-0.1	<b>-6.4</b>	<b>-4.6</b>
June $RE_X^{\text{control}}$	3.5	<b>-5.8</b>	<b>-5.2</b>
July $RE_X^{\text{control}}$	-5.2	<b>-6.6</b>	<b>-4.0</b>
August $RE_X^{\text{control}}$	2.3	<b>-6.9</b>	<b>-4.6</b>

Table A.3:  $RE_X^{\text{control}}$  signify the resolution effects between the two control simulations in 5km and in 210km resolution for the respective variables. They are calculated as the differences of the 5km simulation relative to the 210km simulation of 1980-2009 mean case study area averages [%] (Equ. A.1). Bold font indicates statistically significant differences between resolutions. LHF refers to latent heat flux, SHF to sensible heat flux, Heat cond. to heat conductivity in 19cm depth and Heat cap. to heat capacity in 19cm depth. Runoff denotes surface runoff. Soil ice and soil moisture indicate near-surface conditions (up to a depth of 3m).

moisture were examined and are shown in table A.3. They all amount to values below 10% in all months and are thus small. Latent heat flux is an exception here and shows larger values in July. Latent heat flux translates to the heat included in the sum of evaporation and transpiration. The resolution effects are thus induced by the same processes as evaporation and transpiration resolution effects.

#### A.6.2.6 SOIL AND VEGETATION PARAMETERS IN COMPARISON

Table A.4 shows simulations with spatially uniform vegetation and soil parameters for the months of June and August. In the main body, we show for the summer mean and July that soil parameters are more important regarding resolution than vegetation parameters. This holds also for June and August.  $\Delta RE_X$  is in most cases larger for soil parameters than for vegetation parameters.

#### A.6.3 SOIL MOISTURE INITIALIZATION

The soil moisture initialisation plays a role for resolution effects, because it determines the amount of water available in the soil at the simulation start. Excess water can drain away in the first simulation days. However, since soil ice starts freezing right away, a higher amount of

	ALD [%]	Drainage [%]	Evaporation [%]
June $\Delta RE_X$ veg. param.	0.18	3.9	-1.5
June $\Delta RE_X$ soil param.	1.5	6.8	-2.2
August $\Delta RE_X$ veg. param.	4.01	6.6	-3.0
August $\Delta RE_X$ soil param.	42	1.9	12
	GPP [%]	Soil temp. [°C]	Transp. [%]
June $\Delta RE_X$ veg. param.	-15	0.03	-17
June $\Delta RE_X$ soil param.	4.3	0.27	33
August $\Delta RE_X$ veg. param.	0.18	0.04	-2.7
August $\Delta RE_X$ soil param.	2.2	0.48	-3.8

Table A.4:  $\Delta rRE_X$  signifies the difference between resolution effects of simulations with uniform parameters and resolution effects of the control simulations for the respective variables [%] (Equ. A.2). Uniform parameters are represented in the lines and output variables in the columns. The 1980-2009 June and August mean are shown. Soil temperature difference refers to temperature in 19 cm depth [°C]. Transp. refers to transpiration, ALD to active layer depth and GPP to gross primary productivity. Veg. param. refers to vegetation parameters including the root depths and soil param. refers to soil parameters.

soil water at simulation start leads to a higher soil ice content in the long term. We initialized the soil moisture at 200% of soil field capacity in the 5km version, thus with a lot of excess water and then remapped this to 210km. This enables the model to find its own equilibrium state for soil moisture in both resolution versions, because there is enough water available. However, with initialisation at 200%, there is more soil ice present than with less initial soil moisture. We tested soil moisture initialisation at 95% of soil field capacity, thus with less initial soil water. This approach works very well for the 5km version, but does not fit very well to the 210km version due to not fitting soil depths and soil field capacity. This mismatch leads to substantially larger resolution effects for multiple variables with the 95% approach as shown in table A.5. For example, transpiration exhibits resolution effects of -18% here, but only 3% in the 200% approach. An exception here are ALD and soil temperature, whose resolution effects are slightly larger with the 95% approach than with 200%. ALD resolution effects amount to 18% with the 95% approach and to 20% with the 200% approach. This is due to more soil ice in the 200% approach, because there are higher soil moisture amounts at initialisation. More soil ice within one soil layer leads to longer thawing timescales for that layer. However, the nonlinear behavior observable in the ALD annual cycle is similar for both initialization approaches. We decided to use an initialization at 200% of soil field capacity to stay on the conservative side, since the resolution effects are predominantly smaller with this approach.

	ALD [%]	Drainage [%]	Evaporation [%]
$RE_X^{SM-95\%}$	<b>18</b>	7	7
	GPP [%]	Soil temp. [°C]	Transp. [%]
$RE_X^{SM-95\%}$	-10	0.25	-18

Table A.5:  $RE_X^{SM-95\%}$  signifies the resolution effects between the simulations in 5km and in 210km resolution with soil moisture initialization at 95% of soil field capacity. The resolution effects are calculated as the differences of the 5km simulation relative to the 210km simulation of 1980-2009 summer mean case study area averages [%] (Equ. A.1). Bold font indicates statistically significant differences between resolutions. Soil temperature difference refers to temperature at 19cm depth and is calculated as absolute difference. Transp. refers to transpiration, GPP to gross primary productivity, ALD to active layer depth and LHF to latent heat flux.

#### A.6.4 REMAPPING WITH MEDIAN

	ALD [%]	Drainage [%]	Evaporation [%]
$RE_X^{SOM-median}$	<b>21</b>	-5.8	6.1
	GPP [%]	Soil temp. [°C]	Transp. [%]
$RE_X^{SOM-median}$	23	<b>0.36</b>	32

Table A.6:  $RE_X^{SOM-median}$  signifies the resolution effects between the simulations in 5km and in 210km resolution with median remapping for soil organic matter content. The resolution effects are calculated as the differences of the 5km simulation relative to the 210km simulation of 1980-2009 summer mean case study area averages [%] (Equ. A.1). Bold font indicates statistically significant differences between resolutions. Soil temperature difference refers to temperature at 19cm depth and is calculated as absolute difference. Transp. refers to transpiration, GPP to gross primary productivity, ALD to active layer depth and LHF to latent heat flux.

In order to test the robustness of results, we experimented with a different remapping technique to transfer the input data from 5km to 210km resolution (A.6). Instead of computing the conservative average, we calculated the median of the 5km grid cells within the corresponding 210km grid box. We chose to do this solely for SOM, since this is the most important parameter and thereby we can examine the individual effect of median remapping of this single parameter. The 5km input stays the same as in the control simulations. The 210km SOM with median remapping is slightly larger than in the control simulations. The resolution effects for ALD however stay similar as in the control simulations. The areas with little SOM in the 5km setup

are crucial in this regard, as these are the areas where there is a large enough soil heat conductivity and thus enough energy present to thaw the soil further than the second soil layer. The slightly higher SOM in the 210km setup with median remapping still supplies enough energy for thawing until the second soil layer, but not any further. Thus, resolution effects stay the same. Evaporation resolution effects are also similar in magnitude compared to the control simulations, however transpiration resolution effects are substantially larger with median remapping than in the control simulations. In the control simulations, transpiration resolution effects are small. With median remapping, the larger SOM causes smaller transpiration fluxes in 210km and thus the difference of 5km fluxes relative to 210km fluxes becomes large. To sum up, using a different remapping technique results in partly different numbers, however the processes and parameters inducing the resolution effects stay the same.

#### A.6.5 EFFECT OF INDIVIDUAL INPUT PARAMETERS

Tables A.7 and A.8 show resolution effects of individual input parameters. Resolution effects induced by SOM and CHP induce the largest  $\Delta rRE_X$  and were discussed above in detail. All other input parameters induce small resolution effects in comparison.

<b>JJA</b>	ALD [%]	Drainage [%]	Evaporation [%]
$\Delta rRE_X$ SOM	9.8	5.7	-0.34
$\Delta rRE_X$ CHP	5.5	-4.7	7.8
$\Delta rRE_X$ elevation and oro std	0.07	0.32	-0.29
$\Delta rRE_X$ soil depth	-1.0	0.89	-0.17
$\Delta rRE_X$ field cap	-3.1	-1.3	0.34
$\Delta rRE_X$ soil porosity	0.9	1.7	0.5
$\Delta rRE_X$ hydraulic cond	-0.11	0.37	-0.31
$\Delta rRE_X$ sat moist pot	1.0	-0.74	0.91
$\Delta rRE_X$ max root moist	0	0	0
$\Delta rRE_X$ wilting point	-0.03	-0.14	0.01
$\Delta rRE_X$ pore size distr	-0.01	-0.04	0.01
$\Delta rRE_X$ min heat cap	0	0	0
$\Delta rRE_X$ min heat cond	-0.82	-0.45	0.04
<b>July</b>			
$\Delta rRE_X$ SOM	7.7	1.4	3.9
$\Delta rRE_X$ CHP	-0.7	-8.2	4.2
$\Delta rRE_X$ elevation and oro std	0.14	-0.03	-0.39
$\Delta rRE_X$ soil depth	-0.35	2.9	-0.18
$\Delta rRE_X$ field cap	-3.5	-0.61	-0.57
$\Delta rRE_X$ soil porosity	1.3	1.03	4.7
$\Delta rRE_X$ hydraulic cond	0.16	0.23	-1.9
$\Delta rRE_X$ sat moist pot	0.92	-0.24	6.3
$\Delta rRE_X$ max root moist	0	0	0
$\Delta rRE_X$ wilting point	-0.02	-0.1	-0.2
$\Delta rRE_X$ pore size distr	-0.01	-0.04	-0.03
$\Delta rRE_X$ min heat cap	0	0	0
$\Delta rRE_X$ min heat cond	-0.83	-0.26	-1.7

Table A.7:  $\Delta rRE_X$  signifies the difference between resolution effects of simulations with uniform parameters and resolution effects of the control simulations for the respective variables [%] (Equ. A.2). Uniform parameters are represented in the lines and output variables in the columns. The 1980-2009 summer mean and July mean are shown. ALD refers to active layer depth. Max root moist refers to maximum root zone soil moisture, oro std to orographic standard deviation, field cap to soil field capacity, hydraulic cond to hydraulic conductivity, sat moist pot to saturated moisture potential, pore size distr to pore size distribution index, min heat cap to mineral heat capacity and min heat cond to mineral heat conductivity.

<b>JJA</b>	GPP [%]	Soil temp. [°C]	Transp. [%]
$\Delta rRE_X$ SOM	-9.1	0.09	-15
$\Delta rRE_X$ CHP	9.5	0.18	15
$\Delta rRE_X$ elevation and oro std	0.41	0	0.1
$\Delta rRE_X$ soil depth	-5.8	-0.01	-3.4
$\Delta rRE_X$ field cap	9.5	-0.01	9.5
$\Delta rRE_X$ soil porosity	-4.7	0	-6.9
$\Delta rRE_X$ hydraulic cond	-0.97	-0.01	-1.5
$\Delta rRE_X$ sat moist pot	3.4	0.02	2.6
$\Delta rRE_X$ max root moist	0	0	0
$\Delta rRE_X$ wilting point	0.04	0	0.15
$\Delta rRE_X$ pore size distr	-0.02	0	0.01
$\Delta rRE_X$ min heat cap	0	0	0
$\Delta rRE_X$ min heat cond	-0.19	0.01	0.07
<b>July</b>			
$\Delta rRE_X$ SOM	-10.2	0.07	-16.9
$\Delta rRE_X$ CHP	18	0.06	33
$\Delta rRE_X$ elevation and oro std	0.43	0	0.17
$\Delta rRE_X$ soil depth	-7.3	-0.01	-4.9
$\Delta rRE_X$ field cap	8.9	-0.04	10
$\Delta rRE_X$ soil porosity	-4.5	0.01	-7.4
$\Delta rRE_X$ hydraulic cond	-1.4	0	-2.6
$\Delta rRE_X$ sat moist pot	4.0	0.02	2.9
$\Delta rRE_X$ max root moist	0	0	0
$\Delta rRE_X$ wilting point	-0.02	0	0.1
$\Delta rRE_X$ pore size distr	-0.02	0	0.04
$\Delta rRE_X$ min heat cap	0	0	0
$\Delta rRE_X$ min heat cond	-0.28	-0.01	0.28

Table A.8:  $\Delta rRE_X$  signifies the difference between resolution effects of simulations with uniform parameters and resolution effects of the control simulations for the respective variables [%] (Equ. A.2). Uniform parameters are represented in the lines and output variables in the columns. The 1980-2009 summer mean and July mean are shown. Soil temperature difference refers to temperature in 19 cm depth [°C]. Transp. refers to transpiration and GPP to gross primary productivity. Max root moist refers to maximum root zone soil moisture, oro std to orographic standard deviation, field cap to soil field capacity, hydraulic cond to hydraulic conductivity, sat moist pot to saturated moisture potential, pore size distr to pore size distribution index, min heat cap to mineral heat capacity and min heat cond to mineral heat conductivity.



# B

## HIGH-RESOLUTION FORCING STRONGLY CHANGES EVAPORATION IN LAND SURFACE MODEL APPLIED TO ARCTIC CONDITION

---

The work in this appendix is a manuscript in preparation to be published:

**Schickhoff M.**, de Vrese P., and Brovkin V. "High-resolution forcing strongly changes evaporation in land surface model applied to Arctic condition". Manuscript in preparation.

### AUTHOR CONTRIBUTIONS

MS, PdV and VB designed the study. MS conducted the simulations and carried out the analysis. MS, PdV and VB contributed to the writing.



# High-resolution forcing strongly changes evaporation in land surface model applied to Arctic condition

**Meike Schickhoff<sup>1</sup>, Philipp de Vrese<sup>1</sup> and Victor Brovkin<sup>1,2</sup>**

<sup>1</sup> Max Planck Institute for Meteorology, Bundesstrasse 53, 20146 Hamburg, Germany

<sup>2</sup> Center for Earth System Research and Sustainability, University of Hamburg, Bundesstrasse 55, 20146 Hamburg, Germany

## ABSTRACT

The impact as well as potential limitations of using high-resolution forcing data on modelled terrestrial processes in the Arctic have never been systematically investigated. Here, we run the state-of-the-art land surface model JSBACH<sub>3</sub> with forcing-data on a 5km resolution for a case study in eastern Siberia and compare the results to a low-resolution setup on a 210km-scale. The differences in forcing resolution mainly impact the hydrology and we find a 21% reduction in summer evaporation relative to the low-resolution setup, which is statistically significant in July. The effect is especially large in the lowlands that make up large parts of the study domain, suggesting that the reduction in evaporation in simulations with high-resolution forcing does not necessarily constitute an improvement of the simulated moisture fluxes. In the model, the precipitated water in the highlands that does not evaporate locally drains from the soil as groundwater flow without passing the adjacent lowlands. In reality, however, a fraction of the surface- and subsurface runoff would provide an additional source for evaporation in the lowlands. Thus, the resolution effects are possibly the result of missing lateral connections between grid cells, suggesting that these need to be included in land surface models even for resolutions of several kilometers.

## B.1 INTRODUCTION

The recent growth in computational resources offers new opportunities for advances in land-surface modelling. Increasing the horizontal resolution allows for a better representation of surface heterogeneity and small-scale interactions with the atmosphere. This is especially important for the high latitudes, as the Arctic warms at least twice as quick as the global average and the land areas are characterized by a diverse small-scale landscape heterogeneity (Biskaborn et al., 2019; Rantanen et al., 2022; van Cleve et al., 1983; Viereck, 1992). Land-surface-model-only, so-called offline, simulations depend on the quality of the model itself and of the boundary conditions, as well as on a realistic representation of the climate forcing (Balsamo et al., 2015). The availability of high-resolution climate-forcing data recently improved as general circulation models increased their resolution. So-called storm-resolving models enable the explicit representation of deep convection as they run on scales of 10km or less (Hohenegger et al., 2020; Satoh et al., 2008). Orographic and convective precipitation, precipitation extremes and blocking events are more realistically represented in high-resolution simulations (Hohenegger et al., 2023; Prein et al., 2015). Also, wind extremes are better resolved (Iles et al., 2020) as well as the distribution of temperature in mountainous regions (Prein et al., 2013), while net shortwave radiation improves due to better representation of clouds (Hohenegger et al., 2020). Specifically for the Arctic, higher resolutions show more realistic representations of partitioning between rain and snow as well as of snow melt (Liu et al., 2017; Rasmussen et al., 2014; Wang et al., 2018).

The availability of these forcing variables in high quality offers large potential to improve land-surface-only simulations. The spatial distribution of precipitation affects water and carbon fluxes, especially in dry areas. The partitioning of rain and snow impacts the timing and division between runoff, drainage and evaporation. The proximity to the Arctic Ocean can induce high wind speeds, which may affect water fluxes by fast exchange of moist and dry air. The occurrence of clouds impacts photosynthesis. And, due to the Arctic being an energy-limited region, temperature plays an important role in nearly all land processes.

Although high-resolution climate-forcing data has recently become available and promises realism, its impact on the simulation of Arctic terrestrial processes as well as potential limitations have not yet been systematically studied. This is however crucial in order to direct future endeavors in high-resolution land modelling. Here, we investigate resolution effects due to a high-resolution climate forcing by running the land surface model JSBACH<sub>3</sub> for a case-study region in

Siberia. We compare simulations with a forcing resolution of 5km and a 210km resolution of the boundary conditions with simulations with both forcing and boundary data in a 210km horizontal resolution.

## B.2 DATA AND METHODS

The case-study area is located around Chersky in eastern Siberia within the continuous permafrost zone and encompasses the region from 158.4°-162°E and 67.5°-69°N. The area is characterized mainly by lowlands, however a mountain range is located in the South. For a more detailed description of the case study area, see A.2.

We use the land surface model JSBACH<sub>3</sub> in the model version 3.2 (Reick et al., 2021), which is part of the global Earth System Model MPI-ESM version 1.2 (Giorgetta et al., 2013). We include permafrost soil physics as well as a vertical soil organic-matter scheme that extends over the first three meters of the soil column (de Vrese et al., 2021). The soil column is composed of 18 soil layers of differing thicknesses, of which 11 layers are situated within the uppermost three meters. The model depth amounts to 40m encompassing soil as well as bedrock layers. The temporal resolution of the model simulations is 30 minutes. The horizontal resolution differs between the two setups (Tab. B.1). The first setup runs on 1.88° which equates to 210x77km in the case study area and is called "210km" in the following. The whole case-study region encompasses only two grid cells in 210km. The second setup is called "5km" and runs on 0.045°, which corresponds to 5x2km, and results in 2560 grid cells within the case-study region. For the 5km setup, the boundary conditions including soil, vegetation and orography only include the information at the 210km resolution while the forcing data is spatially resolved in 5km. This setup allows us to only investigate forcing effect and not effects due to the resolution of the boundary conditions.

Model setup	Model resolution [km]	Boundary conditions [km]	Climate forcing [km]
5 km setup	5	210	5
210 km setup	210	210	210 (upscaled from 5)

Table B.1: Model setups for 5 km and 210 km simulations.

The climate forcing data stems from a 5-year global simulation in 5km horizontal resolution of the model ICON-Sapphire (Hohenegger et al., 2023). The five years were used as cyclic forcing over a period of 85 years: 80 years of spin-up are followed by 5 years of analysis period. To compare with simulations based on a low-resolution forcing, the forcing data was remapped conservatively to 210km resolution.

Forcing variables include temperature and humidity at the lowest atmospheric layer, precipitation, 10m wind speed as well as downwelling net shortwave and longwave radiation. CO<sub>2</sub> concentration is held constant at the 2020 global mean of 413.2ppm.

We calculate relative resolution effects of variable  $X$  ( $rRE_X$ ) as

$$rRE_X = \frac{(X_{5km} - X_{210km}) \cdot 100}{|X_{210km}|} \quad (B.1)$$

, with relative differences allowing for a better comparison between different variables. For comparisons of statistical distributions, we use the absolute units and calculate resolution effects as  $aRE_X = X_{5km} - X_{210km}$ . In addition to the resolution effects for simulations with all forcing variables in 5km resolution ( $rRE_X^{control}$ ), we estimate the impact of a individual forcing variables on the resolution effects, using idealized simulations. These simulations were conducted with single forcing variables set to spatially uniform values: The average over the whole field is calculated for the respective variable, and this average is used to force every grid box. After the simulation, resolution effects  $rRE_X^{uniform}$  are calculated and the difference relative to the resolution effects of the control simulations is estimated:

$$\Delta rRE_X = rRE_X^{control} - rRE_X^{uniform} \quad (B.2)$$

Except otherwise stated, results refer to the mean over the (bo-real) summer period of June, July and August. The summer period is chosen since water and carbon fluxes, active layer depths and soil temperatures are largest in summer. To test for statistically significant differences between resolutions, two-tailed student's t-tests at 5% significance level over all days of a summer month times five years of forcing data are used. Tests over summer mean values are not meaningful since only five years of forcing data are available. T-tests are modified to account for autocorrelation ???. To calculate spatial correlations, Spearman rank-order correlations are used. To obtain a better understanding of the causes of the resolution effects, we divide the 5km grid cells into highlands and lowlands. Here, lowlands are defined as grid cells with less than 300m of altitude and highlands as grid cells above this threshold (Jones et al., 2022; Paltan et al., 2015), with the latter comprising about 7% of all grid cells in the 5km setup.

	ALD [%]	Drainage [%]	Evaporation [%]
JJA $rRE_X^{\text{control}}$	-0.4	8.9	-21
	GPP [%]	LHF [%]	Runoff [%]
JJA $rRE_X^{\text{control}}$	-3.7	-7.3	5.4
	SHF [%]	Soil temp. [°C]	Transpiration [%]
JJA $rRE_X^{\text{control}}$	3.4	-0.05	-1.1

Table B.2:  $rRE_X^{\text{control}}$  signifies the resolution effects between the two control simulations in 5 km and in 210 km resolution for the respective variables in this table. They are calculated as the relative differences between the 5 km simulation and the 210 km simulation of summer mean values averaged over the case study area [%] (Equ. B.1). Soil temperature difference refers to the temperature in 19cm depth [°C]. GPP refers to gross primary productivity, ALD to active layer depth, LHF to latent heat flux and SHF refers to sensible heat flux.

### B.3 RESULTS

#### B.3.1 RESOLUTION EFFECTS

Table A.1 shows summer resolution effects as relative differences between the simulation with a 5km resolution and a 210km resolution, the former with high resolution forcing but low resolution boundary conditions. With -21%, evaporation shows the largest relative resolution effects, with  $\Delta rRE_{\text{evap}}$  corresponding to -8mm over the summer months. Drainage exhibits  $rRE_{\text{drain}}$  of 9%, while the latent heat flux, which is the heat included in the sum of evaporation and transpiration, shows resolution effects,  $rRE_{\text{LHF}}$ , of -7%. All other variables exhibit smaller effects, which suggests that changes in resolution mainly affect the simulated surface- and subsurface hydrology. Thus, in the following, we focus on how the resolution of the climate forcing affects the simulated water fluxes.

In the model, the change in the soil water and ice content,  $\Delta_{\text{soil}}$ , is calculated as  $\Delta_{\text{soil}} = P - E - T - D - R$ . Here, P is precipitation (as an input parameter the respective domain average does not change between resolution setups, i.e. 180mm in summer), E is evaporation, T is transpiration, D is drainage and R is surface runoff. Figure B.1 depicts the absolute water fluxes in 5km and in 210km summed up over the summer months, showing that large resolution effects on the terrestrial water budget are limited to the simulated drainage- and evaporation rates. For simulations with uniform precipitation, the evaporation resolution effect,  $\Delta rRE_{\text{evap}}$ , amounts to -22%, while it is around  $\pm 1\%$  for simulations with other forcing variables set uniform (supplementary material). This shows that the spatial distribution of

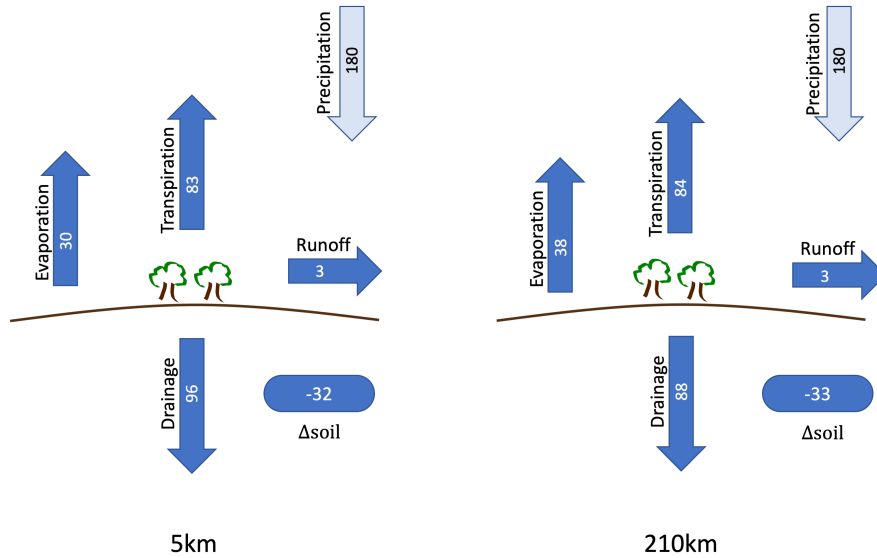


Figure B.1: Water budget in the 5km setup (left) and in the 210km setup (right) for JJA [mm].  $\Delta_{\text{soil}}$  is the change in the soil water and ice content. Drainage refers to all below ground fluxes, while runoff refers exclusively to surface runoff. Precipitation is an input parameter and does not change between resolutions.

precipitation is the major driver of  $RE_{\text{evap}}$ . Similarly, the resolution effects in the drainage fluxes are also caused by the spatial distribution of precipitation. The latter is mainly related to the orography within the study domain (see below), and for simulations with uniform precipitation,  $\Delta rRE_{\text{drain}}$  amounts to 8%. In the context of the terrestrial water budget the positive resolution effects of drainage (+8mm) balance out the negative resolution effects of evaporation (-8mm).

Evaporation resolution effects are statistically significant in July and with -27% (-4.8mm) they are larger in July than in June (-20%, -1.0mm) and August (-15%, -2.3mm). The effects are largest in July partly since evaporation rates are highest, as a result of high precipitation rates in connection with high temperatures. Precipitation in July (79mm) is slightly smaller than in August (81mm), but temperatures are warmer in July (12°C) than in August (9°C), indicating that temperature does play a role, however minor in comparison to precipitation. In June, temperatures are high (14°C), but precipitation amounts are very low (21mm), so absolute evaporation fluxes are also lower in June than in July and August.

In order to explain the negative evaporation resolution effects, i.e. why the spatial distribution of precipitation and temperatures causes smaller evaporation fluxes in the 5km than in 210km setup, we analyse the resolution effects accounting for the elevation of the high-resolution grid cells, applying a division into high- and lowland

regions.

### B.3.2 HIGHLANDS AND LOWLANDS

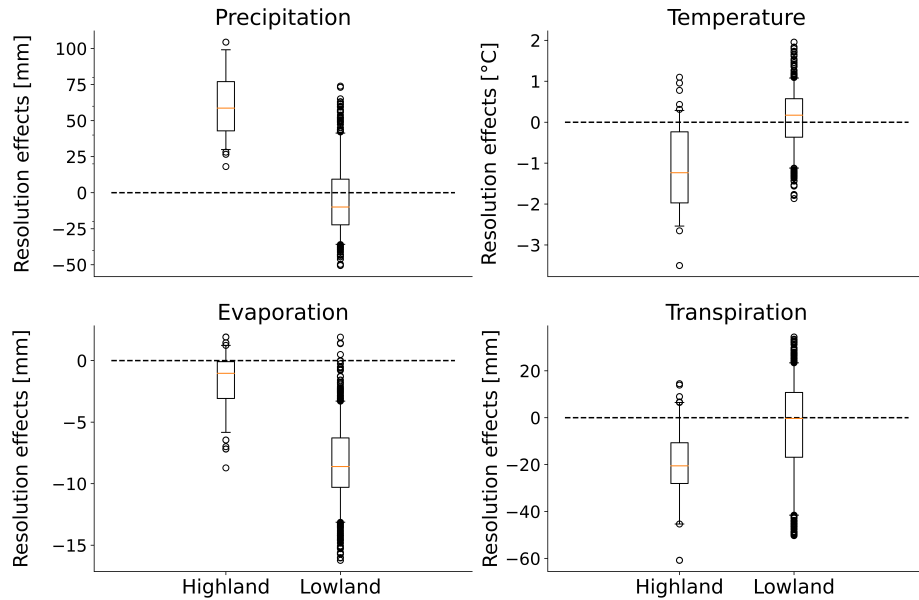


Figure B.2: Boxplots show resolution effects of precipitation (upper left), air temperature at lowest atmospheric layer (upper right), evaporation (lower left) and transpiration (lower right). Resolution effects are calculated as the difference of simulations in 5 km relative to 210 km setups (Equ. B.2) for JJA for every grid cell on the 5 km grid. Grid cells in the 5km setup are differentiated in highland (elevation  $\geq 300$  a.s.l.) and lowland locations. Lowlands encompass the vast majority of the case study area. Resolution effects for temperature and precipitation balance out over the case study area as they are input parameters.

In the 5km setup, summer evaporation fluxes are highest in the South of the domain around the mountain range. This is where precipitation rates are highest due to orographic precipitation processes (Fig. B.3). High precipitation rates provide a large water reservoir from which evapotranspiration occurs and the distributions of resolution effects is substantially different between high- and lowland grid cells (Fig. B.2; note that for precipitation and 2m temperature, the differences in resolution balance out over the whole case study area as they are input parameters). For precipitation, resolution differences are larger in the highlands than in the lowlands, because (i) precipitation fluxes in the highlands are much larger than in the lowlands,

and (ii) lowlands and highlands are not equal in area. In contrast, temperatures are lower in the highlands than in the lowlands since temperatures decrease with altitude.

The distribution of evaporation resolution effects is determined by the distribution of precipitation and temperatures, resulting in negative effects in both the high- and the lowlands (Fig. B.2). The median of highland effects amounts to  $-1\text{mm}$ , while the median of lowlands effects is  $-9\text{mm}$ . The 5th percentile of highland evaporation resolution effects is larger than the upper quartile of the lowland evaporation data, while the 95th percentile of lowland evaporation resolution effects is smaller than the lower quartile of highland evaporation effects. This shows that the distribution of evaporation resolution effects is substantially different in the highlands compared to the lowlands. High precipitation amounts in the highlands induce higher evaporation fluxes than in the lowlands (Fig. B.3), but the fluxes are still lower than those in the  $210\text{km}$  simulation. This is because temperatures in the highlands are lower than in the  $210\text{km}$  setup (which does not differentiate between highlands and lowlands) and cold temperatures limit the available energy and, thus, the highland evaporation flux. In the lowlands, resolution effects are larger and more negative than in the highlands. They are the result of lowland precipitation being smaller than the rates in the  $210\text{km}$  setup – or in other words, in  $5\text{km}$  these regions are more water-limited than the domain average simulated in  $210\text{km}$ . Since the lowlands encompass the far larger area than the highlands, total evaporation resolution effects are also large and negative.

Surprisingly our simulations do not show the same strong precipitation dependency for transpiration, with the temperature distribution playing a much more important role. Transpiration in the highlands is much smaller than in the lowlands and, with predominantly lower temperatures in the highlands than in  $210\text{km}$ , transpiration resolution effects are largely negative. Here, the median of highland transpiration resolution effects is substantially larger than the respective value for evaporation, amounting to  $-21\text{mm}$ . In the lowlands, the effects due to higher temperatures almost perfectly balance the effects due to lower precipitation rates so that the resolution effects in transpiration amount to merely  $-0.3\text{mm}$ . Due to the much smaller highland area in the model domain, this results in  $-1\text{mm}$  ( $-1\%$ ) in spatially averaged resolution effects. The different dependencies of evaporation and transpiration are also evident in the spatial correlations: The correlation coefficient of evaporation and precipitation is  $0.89$ , while it is only  $0.39$  for evaporation and temperature. In contrast, the coefficient of transpiration and temperature amounts to  $0.84$ , while it is only  $0.35$

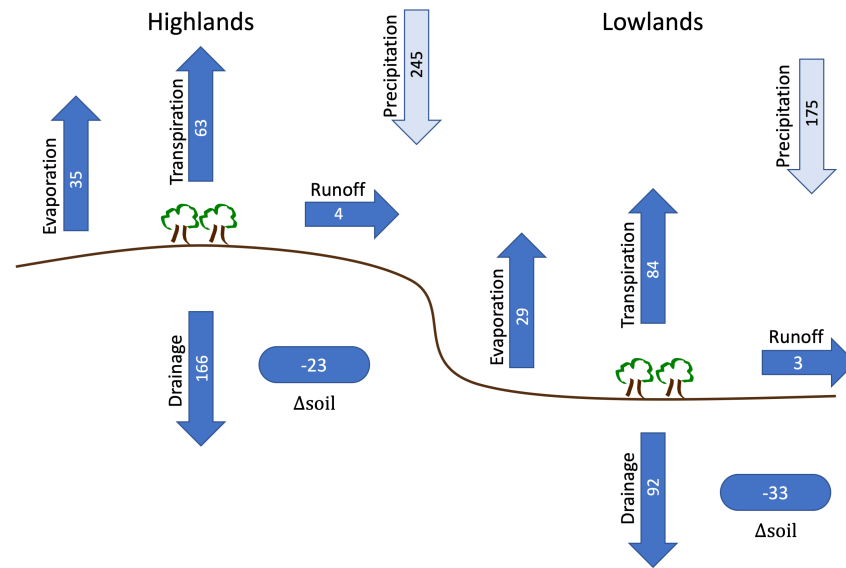


Figure B.3: Water budget in the highlands (left) and in the lowlands (right) for JJA in the 5km setup [mm].  $\Delta_{\text{soil}}$  is the change in the soil water and ice content. Drainage includes subsurface runoff and runoff only depicts surface runoff. Precipitation is an input parameter.

for transpiration and precipitation.

Drainage shows much larger fluxes in the highlands (166mm) than the lowlands (92mm) due to greater precipitation fluxes. However, resolution effects are still slightly positive in the lowlands. The surplus of drainage relative to the 210km setup in the lowlands balances the negative evaporation resolution effects in terms of the terrestrial water balance.

### B.3.3 EVAPORATION AND TRANSPIRATION IN JSBACH

In JSBACH, evaporation occurs from snow (snow evaporation, negligible during summer), from wet surfaces on vegetation and on bare ground (skin evaporation) and from the top soil layer (soil evaporation). Skin evaporation makes up the largest share of evaporation with 84% in 5km and 88% in 210km of total evaporation. It uses the water from the skin reservoir which includes only the very thin film of water on top of the vegetation and bare ground. Soil evaporation amounts to 15% resp. 11% and utilizes the water from the top soil layer which includes the upper 6.5cm of the soil column. Thus, evaporation is very dependent on regular precipitation as both the skin reservoir and the top soil layer quickly dry out due to the small water reservoir. At the same time, the very large precipitation rates in the highlands in 5km may not lead to an additional increase in evaporation (Fig.

B.4) because the latter is limited by the available energy and vapour-pressure deficit. Furthermore, the skin reservoir and the top soil layer only offer a limited reservoir to store water during heavy precipitation events further contributing to the non-linear evaporation-precipitation relationship. Here, events with individual grid cells receiving more than 20mm/day of precipitation during the summer month occur only three times in the low resolution, but 14245 times in the high resolution simulation. Due to this non-linear dependency, precipitation is a bigger limitation for evaporation in 5km than temperature.

In contrast, transpiration uses water from the entire thawed part of the rootzone which on average amounts to 29cm over the JJA period. Thus, transpiration depends upon a much larger water reservoir, that can store also the fluxes during more extreme precipitation events, and is not as dependent on constant (moderate) rainfall as evaporation. Due to this buffer and the Arctic being a temperature-limited region, transpiration reacts more sensitively to temperature than to precipitation, with resolution effects largely balancing out across the study domain.

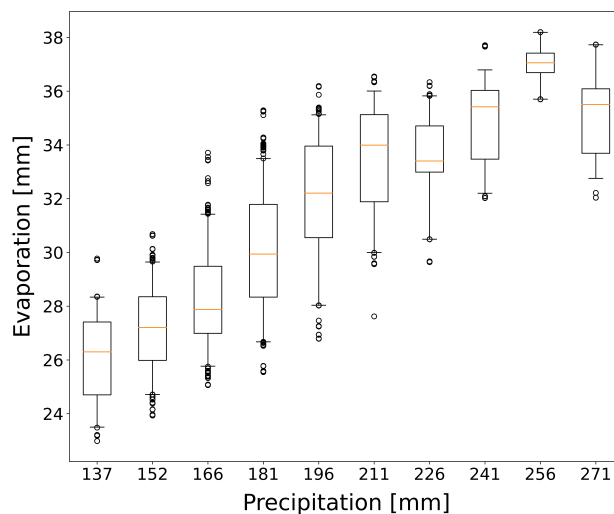


Figure B.4: The boxplots show the dependence of evaporation on precipitation for JJA in the 5km setup.

#### B.4 DISCUSSION

Comparing simulations with high- and low-resolution forcing, we found large negative resolution effects in evaporation fluxes. They are statistically significant for July. Drainage and latent heat flux show smaller resolution effects. This sensitivity of the hydrology is in line with prior findings that show a larger effect of forcing resolution for

hydrological variables than for vegetation variables (Albergel et al., 2018). This may increase the importance of resolution also for the Arctic carbon budget as the hydrology impacts carbon dioxide and methane fluxes (Albuhaisi et al., 2023; Miner et al., 2022). We further show that evaporation resolution effects are negative overall and larger in the lowlands than in the highlands, i.e. evaporation fluxes are smaller in the lowlands than in the highlands, which is caused by higher precipitation amounts in the highlands.

The fact that the evaporation flux is smaller in the lowlands than in the highlands in 5km, suggest that the representation of the hydrological cycle is not necessarily improved by the high-resolution forcing. In reality, a large portion of the precipitated water in the highlands is expected to runoff through the lowlands towards the Kolyma river, while the model has no lateral connection between grid cells. As a result, neither surface- nor subsurface runoff is routed from the high- to the lowlands and all water that exceeds the atmospheric moisture demand plus the water-holding capacity of the soil contributes to the river discharge without affecting the state of the lowland soils. Additionally, slopes in the highlands increase the surface and subsurface runoff and impede large amounts of ponding water as well as high soil moisture amounts which both fuel evaporation. In contrast, the lowlands are often characterized by (seasonally) standing water and saturated soils which makes evaporation usually larger in the lowlands than in the highlands, contrary to our modelling results. In the model, however, the representation of subsurface runoff is independent of the local slope. Drainage includes subsurface runoff in the model and the high drainage fluxes in the highlands would in reality contribute to subsurface runoff to the lowlands. Thus, the result that overall evaporation is significantly smaller in the 5km setup than in the 210km setup does not suggest improved modelling outcomes due to the high-resolution forcing. In contrast, it highlights the shortcomings of our particular model and the necessity to account for the lateral water transport between grid cells in land surface models, in general, if these are to be used for high resolution simulations. This is consistent with studies by the hydrological community which call for the implementation of lateral water transport in high-resolution land surface models (Clark et al., 2015; Ji et al., 2017; Maxwell & Condon, 2016).

As of now, land surface models including JSBACH3 do not commonly incorporate lateral water fluxes between grid cells. Often, runoff and drainage is coupled to a river routing scheme and eventually transported to the oceans to calculate the freshwater input into the sea ((Hagemann et al., 2020; Riddick et al., 2018)). This however usually does not involve water getting transported from highlands to lowlands. Other approaches introduce lateral water fluxes on sub-grid

scale to better represent sub-grid processes in low-resolution models (Clark et al., 2015; Fan et al., 2019; Nitzbon et al., 2020a). Sub-grid topography-induced lateral water fluxes improve evapotranspiration estimates along highland-lowland gradients in coarse-resolution Earth system models (Rouholahnejad Freund & Kirchner, 2017; Swenson et al., 2019). This approach includes however only flow within one grid cell, not between grid cells. Concerning high-resolution models, this study indicates that lateral water exchange between grid cells is likely a crucial prerequisite for km-scale simulations and should be accounted for.

Having the largest resolution effects in evaporation stands in contrast to our findings based on simulations with high-resolution soil, vegetation and elevation parameters, but low-resolution forcing (called "parameter-simulations" hereafter, see appendix A). When comparing the simulations with a 210km setup, they found the largest resolution effects in active layer depth. A high-resolution forcing (called "forcing-simulations" hereafter) thus affects evaporation as a hydrological and surface variable most, while parameter-simulations affect more active layer depth as a soil state and subsurface variable. The reason why forcing-simulations do not affect active layer depths much becomes evident when looking at the processes inducing active layer depth resolution effects in parameter-simulations. Spatially heterogeneous soil parameters induce different soil saturation degrees and different dry soil heat conductivities which together return different wet soil heat conductivities (Appendix A). The top soil layer is thereby crucial since it decides how much of the incoming heat from the surface in summer is conducted to lower soil layers. The histograms of wet top soil layer heat conductivities in the 5km setup are shown in figure B.5. The distributions are very different. While the forcing-simulations distribution ranges only from 1.27 to 1.35 W/m/K, the range of parameter-simulations extends from 1.02 to 2.40 W/m/K. The very different top soil layer heat conductivities of the parameter-simulations get nonlinearly translated by the soil layer discretization into very different active layer depths and thereby induce large resolution effects (Appendix A). The forcing-simulation exhibits very similar top soil layer heat conductivities in the 5km grid cells due to soil parameters being resolved in 210km. This results in similar active layer depths in both resolution setups and negligible resolution effects.

## B.5 CONCLUSION

We show that a high-resolution forcing affects the modelled hydrology and induces large resolution effects in evaporation, when compared with a low-resolution setup. The resolution effects are statistically sig-

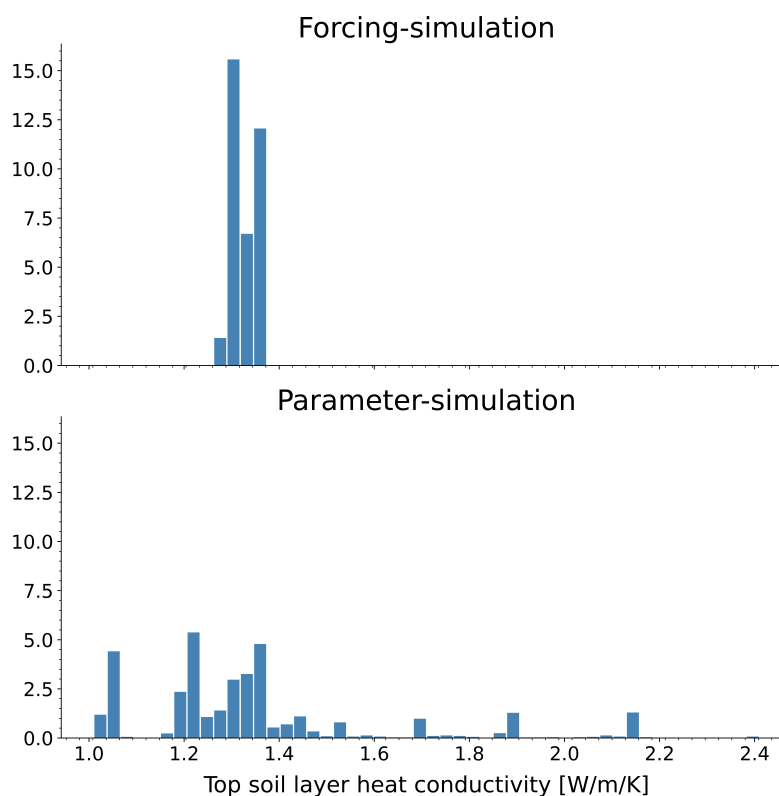


Figure B.5: The histograms show the probability density distributions of summer top soil layer heat conductivities of all grid cells in the 5km setup for forcing-simulations (left) and parameter-simulations (right). The bin width amounts to 0.028 W/m/K.

nificant in July and are especially large and negative in the lowlands. The large lowland effects are presumably due to missing lateral water fluxes in the model to connect highlands and lowlands. Precipitated water in the mountains evaporates and drains away locally, instead of being transported to the lowlands to evaporate there. Thus, in order to obtain improved modelling results on km-scale resolutions, it is likely not sufficient to only use a high-resolution forcing. Lateral water exchange processes between grid cells presumably need to be accounted for in future high-resolution land surface models.

## BIBLIOGRAPHY

---

- Aas, K. S., Martin, L., Nitzbon, J., Langer, M., Boike, J., Lee, H., Berntsen, T. K., & Westermann, S. (2019). Thaw processes in ice-rich permafrost landscapes represented with laterally coupled tiles in a land surface model. *Cryosphere*, 13(2), 591–609. <https://doi.org/10.5194/tc-13-591-2019>
- Albergel, C., Dutra, E., Munier, S., Calvet, J. C., Munoz-Sabater, J., De Rosnay, P., & Balsamo, G. (2018). ERA-5 and ERA-Interim driven ISBA land surface model simulations: Which one performs better? *Hydrology and Earth System Sciences*, 22(6), 3515–3532. <https://doi.org/10.5194/hess-22-3515-2018>
- Albuhaisi, Y., Velde, Y. V. D., & Houweling, S. (2023). The importance of spatial resolution in the modeling of methane emissions from natural wetlands. *Remote Sensing*, 15(11), 2840. <https://doi.org/https://doi.org/10.3390/rs15112840>
- Amante, C., & Eakins, B. W. (2009). *ETOPO1 arc-minute global relief model : procedures, data sources and analysis*. NOAA National Centers for Environmental Information.
- Andresen, C. G., Lawrence, D. M., Wilson, C. J., David McGuire, A., Koven, C., Schaefer, K., Jafarov, E., Peng, S., Chen, X., Gouttevin, I., Burke, E., Chadburn, S., Ji, D., Chen, G., Hayes, D., & Zhang, W. (2020). Soil moisture and hydrology projections of the permafrost region-a model intercomparison. *Cryosphere*, 14(2), 445–459. <https://doi.org/10.5194/tc-14-445-2020>
- Balsamo, G., Albergel, C., Beljaars, A., Boussetta, S., Brun, E., Cloke, H., Dee, D., Dutra, E., Munoz-Sabater, J., Pappenberger, F., De Rosnay, P., Stockdale, T., & Vitart, F. (2015). ERA-Interim/Land: A global land surface reanalysis data set. *Hydrology and Earth System Sciences*, 19(1), 389–407. <https://doi.org/10.5194/hess-19-389-2015>
- Bartsch, A., Leibman, M., Strozzi, T., Khomutov, A., Widhalm, B., Babkina, E., Mullanurov, D., Ermokhina, K., Kroisleitner, C., & Bergstedt, H. (2019). Seasonal progression of ground displacement identified with satellite radar interferometry and the impact of unusually warm conditions on permafrost at the Yamal Peninsula in 2016. *Remote Sensing*, 11(16), 1–25. <https://doi.org/10.3390/rs11161865>
- Bartsch, A., Pointner, G., Nitze, I., Efimova, A., Jakober, D., Ley, S., Högström, E., Grosse, G., & Schweitzer, P. (2021). Expanding infrastructure and growing anthropogenic impacts along Arctic coasts. *Environmental Research Letters*, 16(11). <https://doi.org/10.1088/1748-9326/ac3176>
- Beer, C. (2016). Permafrost sub-grid heterogeneity of soil properties key for 3-D soil processes and future climate projections. *Frontiers in Earth Science*, 4(81). <https://doi.org/10.3389/feart.2016.00081>
- Beringer, J., Lynch, A. H., Chapin, F. S., Mack, M., & Bonan, G. B. (2001). The representation of arctic soils in the land surface model: The importance of

- mosses. *Journal of Climate*, 14(15), 3324–3335. [https://doi.org/https://doi.org/10.1175/1520-0442\(2001\)014<3324:TROASI>2.0.CO;2](https://doi.org/https://doi.org/10.1175/1520-0442(2001)014<3324:TROASI>2.0.CO;2)
- Biskaborn, B. K., Smith, S. L., Noetzli, J., Matthes, H., Vieira, G., Streletskiy, D. A., Schoeneich, P., Romanovsky, V. E., Lewkowicz, A. G., Abramov, A., Allard, M., Boike, J., Cable, W. L., Christiansen, H. H., Delaloye, R., Diekmann, B., Drozdov, D., Etzelmüller, B., Grosse, G., Guglielmin, M., Ingeman-Nielsen, T., Isaksen, K., Ishikawa, M., Johansson, M., Johannsson, H., Joo, A., Kaverin, D., Kholodov, A., Konstantinov, P., Kröger, T., Lambiel, C., Lanckman, J. P., Luo, D., Malkova, G., Meiklejohn, I., Moskalenko, N., Oliva, M., Phillips, M., Ramos, M., Sannel, A. B. K., Sergeev, D., Seybold, C., Skryabin, P., Vasiliev, A., Wu, Q., Yoshikawa, K., Zheleznyak, M., & Lantuit, H. (2019). Permafrost is warming at a global scale. *Nature Communications*, 10(1), 1–11. <https://doi.org/10.1038/s41467-018-08240-4>
- Blyth, E. M., Arora, V. K., Clark, D. B., Dadson, S. J., De Kauwe, M. G., Lawrence, D. M., Melton, J. R., Pongratz, J., Turton, R. H., Yoshimura, K., & Yuan, H. (2021). Advances in Land Surface Modelling. *Current Climate Change Reports*, 7, 45–71. <https://doi.org/https://doi.org/10.1007/s40641-021-00171-5>
- Bring, A., Fedorova, I., Dibike, Y., Hinzman, L., Mård, J., Mernild, S. H., Prowse, T., Semenova, O., Stuefer, S. L., & Woo, M. K. (2016). Arctic terrestrial hydrology: A synthesis of processes, regional effects, and research challenges. *Journal of Geophysical Research: Biogeosciences*, 121(3), 621–649. <https://doi.org/10.1002/2015JG003131>
- Burke, E. J., Zhang, Y., & Krinner, G. (2020). Evaluating permafrost physics in the Coupled Model Intercomparison Project 6 (CMIP6) models and their sensitivity to climate change. *The Cryosphere*, 14(9), 3155–3174. <https://doi.org/10.5194/tc-14-3155-2020>
- Cai, L., Lee, H., Schanke Aas, K., & Westermann, S. (2020). Projecting circum-Arctic excess-ground-ice melt with a sub-grid representation in the Community Land Model. *Cryosphere*, 14(12), 4611–4626. <https://doi.org/10.5194/tc-14-4611-2020>
- Chen, F., Liu, C., Dudhia, J., & Chen, M. (2014). A sensitivity study of high-resolution regional climate simulations to three land surface models over the western United States. *Journal of Geophysical Research: Atmospheres*, 119, 7271–7291. <https://doi.org/10.1002/2014JD021891>.Received
- Cheng, Y., Musselman, K. N., Swenson, S., Lawrence, D., Hamman, J., Dagon, K., Kennedy, D., & Newman, A. J. (2023). Moving Land Models Toward More Actionable Science: A Novel Application of the Community Terrestrial Systems Model Across Alaska and the Yukon River Basin. *Water Resources Research*, 59(1). <https://doi.org/10.1029/2022wro32204>
- Clapp, R. B., & Hornberger, G. M. (1978). Empirical Equations for Some Soil Hydraulic Properties. *Water Resources Research*, 14(4). <https://doi.org/https://doi.org/10.1029/WR014i004p00601>
- Clark, M. P., Fan, Y., Lawrence, D. M., Adam, J. C., Bolster, D., Gochis, D. J., Hooper, R. P., Kumar, M., Leung, L. R., Mackay, D. S., & Maxwell, R. M. (2015). Improving the representation of hydrological processes in Earth System

- Models. *Water Resources Research*, 51, 5929–5956. <https://doi.org/10.1002/2015WR017096>. Received
- Dai, Y., Wei, N., Yuan, H., Zhang, S., Shangguan, W., Liu, S., Lu, X., & Xin, Y. (2019). Evaluation of Soil Thermal Conductivity Schemes for Use in Land Surface Modeling. *Journal of Advances in Modeling Earth Systems*, 11, 3454–3473. <https://doi.org/10.1029/2019MS001723>
- de Vrese, P., & Brovkin, V. (2021). Timescales of the permafrost carbon cycle and legacy effects of temperature overshoot scenarios. *Nature Communications*, 12(1), 1–13. <https://doi.org/10.1038/s41467-021-23010-5>
- de Vrese, P., Stacke, T., Kleinen, T., & Brovkin, V. (2021). Diverging responses of high-latitude CO<sub>2</sub> and CH<sub>4</sub> emissions in idealized climate change scenarios. *The Cryosphere*, 15, 1097–1130. <https://doi.org/10.5194/tc-2020-164>
- Dirmeyer, P. A., Gao, X., Zhao, M., Guo, Z., Oki, T., & Hanasaki, N. (2006). GSWP-2: Multimodel analysis and implications for our perception of the land surface. *Bulletin of the American Meteorological Society*, 87(10), 1381–1397. <https://doi.org/10.1175/BAMS-87-10-1381>
- Dobiński, W. (2020). Permafrost active layer. *Earth-Science Reviews*, 208(103301). <https://doi.org/10.1016/j.earscirev.2020.103301>
- Edwards, P. N. (2011). History of climate modeling. *Wiley Interdisciplinary Reviews: Climate Change*, 2(1), 128–139. <https://doi.org/10.1002/wcc.95>
- Ekici, A., Beer, C., Hagemann, S., Boike, J., Langer, M., & Hauck, C. (2014). Simulating high-latitude permafrost regions by the JSBACH terrestrial ecosystem model. *Geoscientific Model Development*, 7(2), 631–647. <https://doi.org/10.5194/gmd-7-631-2014>
- ESA. (2017). *Land Cover CCI Product User Guide Version 2* (tech. rep.).
- European Commission Joint Research Centre. (2003). *Global Land Cover 2000 database* (tech. rep.).
- Fan, Y., Clark, M., Lawrence, D. M., Swenson, S., Band, L. E., Brantley, S. L., Brooks, P. D., Dietrich, W. E., Flores, A., Grant, G., Kirchner, J. W., Mackay, D. S., McDonnell, J. J., Milly, P. C., Sullivan, P. L., Tague, C., Ajami, H., Chaney, N., Hartmann, A., Hazenberg, P., McNamara, J., Pelletier, J., Perket, J., Rouholahnejad-Freund, E., Wagener, T., Zeng, X., Beighley, E., Buzan, J., Huang, M., Livneh, B., Mohanty, B. P., Nijssen, B., Safeeq, M., Shen, C., van Verseveld, W., Volk, J., & Yamazaki, D. (2019). Hillslope Hydrology in Global Change Research and Earth System Modeling. *Water Resources Research*, 55, 1737–1772. <https://doi.org/10.1029/2018WR023903>
- FAO/IIASA/ISRIC/ISS-CAS/JRC. (2009). *Harmonized World Soil Database (version 1.1)*. FAO, Rome, Italy; IIASA, Laxenburg, Austria.
- Fisher, R. A., & Koven, C. D. (2020). Perspectives on the Future of Land Surface Models and the Challenges of Representing Complex Terrestrial Systems. *Journal of Advances in Modeling Earth Systems*, 12(4). <https://doi.org/10.1029/2018MS001453>
- Giorgetta, M. A., Jungclaus, J., Reick, C. H., Legutke, S., Bader, J., Böttinger, M., Brovkin, V., Crueger, T., Esch, M., Fieg, K., Glushak, K., Gayler, V., Haak, H., Hollweg, H.-D., Ilyina, T., Kinne, S., Kornblueh, L., Matei, D., Mauritsen, T., Mikolajewicz, U., Mueller, W., Notz, D., Pithan, F., Raddatz, T., Rast,

- S., Redler, R., Roeckner, E., Schmidt, H., Schnur, R., Segschneider, J., Six, K. D., Stockhause, M., Timmreck, C., Wegner, J., Widmann, H., Wieners, K.-H., Claussen, M., Marotzke, J., & Stevens, B. (2013). Climate and carbon cycle changes from 1850 to 2100 in MPI-ESM simulations for the Coupled Model Intercomparison Project phase 5. *Journal of Advances in Modeling Earth Systems*, 5(3), 572–597. <https://doi.org/10.1002/jame.20038>
- Guo, D., & Wang, H. (2017). Simulated Historical (1901–2010) Changes in the Permafrost Extent and Active Layer Thickness in the Northern Hemisphere. *Journal of Geophysical Research: Atmospheres*, 122(22), 12, 285–12, 295. <https://doi.org/10.1002/2017JD027691>
- Gurney, S. D. (1998). Aspects of the genesis and geomorphology of pingos: perennial permafrost mounds. *Progress in Physical Geography*, 22(3), 307–324. <https://doi.org/10.1191/030913398667794933>
- Hagemann, S., Stacke, T., & Ho-Hagemann, H. T. (2020). High Resolution Discharge Simulations Over Europe and the Baltic Sea Catchment. *Frontiers in Earth Science*, 8(February), 1–19. <https://doi.org/10.3389/feart.2020.00012>
- Hartley, A. J., MacBean, N., Georgievski, G., & Bontemps, S. (2017). Uncertainty in plant functional type distributions and its impact on land surface models. *Remote Sensing of Environment*, 203(July), 71–89. <https://doi.org/10.1016/j.rse.2017.07.037>
- Heijmans, M. M. P. D., Magnússon, R. Í., Lara, M. J., Frost, G. V., Myers-Smith, I. H., van Huissteden, J., Jorgenson, M. T., Fedorov, A. N., Epstein, H. E., Lawrence, D. M., & Limpens, J. (2022). Tundra vegetation change and impacts on permafrost. *Nature Reviews Earth & Environment*, 3(1), 68–84. <https://doi.org/10.1038/s43017-021-00233-0>
- Hengl, T., De Jesus, J. M., Heuvelink, G. B., Gonzalez, M. R., Kilibarda, M., Blagotić, A., Shangquan, W., Wright, M. N., Geng, X., Bauer-Marschallinger, B., Guevara, M. A., Vargas, R., MacMillan, R. A., Batjes, N. H., Leenaars, J. G., Ribeiro, E., Wheeler, I., Mantel, S., & Kempen, B. (2017). SoilGrids250m: Global gridded soil information based on machine learning. *PLoS ONE*, 12(2), 1–40. <https://doi.org/10.1371/journal.pone.0169748>
- Hohenegger, C., Brockhaus, P., & Schär, C. (2008). Towards climate simulations at cloud-resolving scales. *Meteorologische Zeitschrift*, 17(4), 383–394. <https://doi.org/10.1127/0941-2948/2008/0303>
- Hohenegger, C., Korn, P., Linardakis, L., Redler, R., Schnur, R., Adamidis, P., Bao, J., Bastin, S., Behraves, M., Bergemann, M., Biercamp, J., Bockelmann, H., Brokopf, R., Brüggemann, N., Casaroli, L., Chegini, F., Datseris, G., Esch, M., George, G., Giorgetta, M., Gutjahr, O., Haak, H., Hanke, M., Ilyina, T., Jahns, T., Jungclaus, J., Kern, M., Klocke, D., Kluft, L., Kölling, T., Kornblueh, L., Kosukhin, S., Kroll, C., Lee, J., Mauritsen, T., Mehlmann, C., Mieslinger, T., Naumann, A. K., Paccini, L., Peinado, A., Praturi, D. S., Putrasahan, D., Rast, S., Riddick, T., Roeber, N., Schmidt, H., Schulzweida, U., Schütte, F., Segura, H., Shevchenko, R., Singh, V., Specht, M., Stephan, C. C., Von Storch, J. S., Vogel, R., Wengel, C., Winkler, M., Ziemann, F., Marotzke, J., & Stevens, B. (2023). ICON-Sapphire: Simulating the components of the Earth system and

- their interactions at kilometer and subkilometer scales. *Geoscientific Model Development*, 16, 779–811. <https://doi.org/10.5194/gmd-16-779-2023>
- Hohenegger, C., Kornbluh, L., Klocke, D., Becker, T., Cioni, G., Engels, J. F., Schulzweida, U., & Stevens, B. (2020). Climate statistics in global simulations of the atmosphere, from 80 to 2.5 km grid spacing. *Journal of the Meteorological Society of Japan*, 98(1), 73–91. <https://doi.org/10.2151/jmsj.2020-005>
- Hugelius, G., Bockheim, J. G., Camill, P., Elberling, B., Grosse, G., Harden, J. W., Johnson, K., Jorgenson, T., Koven, C. D., Kuhry, P., Michaelson, G., Mishra, U., Palmtag, J., O'Donnell, J., Schirrmeister, L., Schuur, E. A., Sheng, Y., Smith, L. C., Strauss, J., & Yu, Z. (2013a). A new data set for estimating organic carbon storage to 3 m depth in soils of the northern circumpolar permafrost region. *Earth System Science Data*, 5(2), 393–402. <https://doi.org/10.5194/essd-5-393-2013>
- Hugelius, G., Strauss, J., Zubrzycki, S., Harden, J. W., Schuur, E. A., Ping, C. L., Schirrmeister, L., Grosse, G., Michaelson, G. J., Koven, C. D., O'Donnell, J. A., Elberling, B., Mishra, U., Camill, P., Yu, Z., Palmtag, J., & Kuhry, P. (2014). Estimated stocks of circumpolar permafrost carbon with quantified uncertainty ranges and identified data gaps. *Biogeosciences*, 11(23), 6573–6593. <https://doi.org/10.5194/bg-11-6573-2014>
- Hugelius, G., Tarnocai, C., Broll, G., Canadell, J. G., Kuhry, P., & Swanson, D. K. (2013b). The northern circumpolar soil carbon database: Spatially distributed datasets of soil coverage and soil carbon storage in the northern permafrost regions. *Earth System Science Data*, 5(1), 3–13. <https://doi.org/10.5194/essd-5-3-2013>
- Iles, C. E., Vautard, R., Strachan, J., Joussaume, S., Eggen, B. R., & Hewitt, C. D. (2020). The benefits of increasing resolution in global and regional climate simulations for European climate extremes. *Geoscientific Model Development*, 13(11), 5583–5607. <https://doi.org/10.5194/gmd-13-5583-2020>
- IPCC. (2013). *Climate Change 2013: The Physical Science Basis. Contribution of Working Group 1 to the Fifth Assessment Report of the Intergovernmental Panel on Climate Change* (T. Stocker, D. Qin, G.-K. Plattner, M. Tignor, S. Allen, J. Boschung, A. Nauels, Y. Xia, V. Bex, & P. Midgley, Eds.). Cambridge University Press.
- Ji, P., Yuan, X., & Liang, X. Z. (2017). Do Lateral Flows Matter for the Hyperresolution Land Surface Modeling? *Journal of Geophysical Research: Atmospheres*, 122(22), 12, 077–12, 092. <https://doi.org/10.1002/2017JD027366>
- Jones, B. M., Grosse, G., Arp, C. D., Jones, M. C., Walter Anthony, K. M., & Romanovsky, V. E. (2011). Modern thermokarst lake dynamics in the continuous permafrost zone, northern Seward Peninsula, Alaska. *Journal of Geophysical Research: Biogeosciences*, 116(3), 1–13. <https://doi.org/10.1029/2011JG001666>
- Jones, B. M., Grosse, G., Farquharson, L. M., Roy-Léveillé, P., Veremeeva, A., Kanevskiy, M. Z., Gaglioti, B. V., Breen, A. L., Parsekian, A. D., Ulrich, M., & Hinkel, K. M. (2022). Lake and drained lake basin systems in lowland permafrost regions. *Nature Reviews Earth and Environment*, 3(1), 85–98. <https://doi.org/10.1038/s43017-021-00238-9>

- Juutinen, S., Aurela, M., Tuovinen, J. P., Ivakhov, V., Linkosalmi, M., Räsänen, A., Virtanen, T., Mikola, J., Nyman, J., Vähä, E., Loskutova, M., Makshtas, A., & Laurila, T. (2022). Variation in CO<sub>2</sub> and CH<sub>4</sub> fluxes among land cover types in heterogeneous Arctic tundra in northeastern Siberia. *Biogeosciences*, *19*(13), 3151–3167. <https://doi.org/10.5194/bg-19-3151-2022>
- Kleinen, T., & Brovkin, V. (2018). Pathway-dependent fate of permafrost region carbon. *Environmental Research Letters*, *13*(9), 94001. <https://doi.org/10.1088/1748-9326/aad824>
- Korn, P., Brüggemann, N., Jungclaus, J. H., Lorenz, S. J., Gutjahr, O., Haak, H., Linardakis, L., Mehlmann, C., Mikolajewicz, U., Notz, D., Putrasahan, D. A., Singh, V., von Storch, J. S., Zhu, X., & Marotzke, J. (2022). ICON-O: The Ocean Component of the ICON Earth System Model—Global Simulation Characteristics and Local Telescoping Capability. *Journal of Advances in Modeling Earth Systems*, *14*(10), 1–29. <https://doi.org/10.1029/2021MS002952>
- Kou, D., Virtanen, T., Treat, C. C., Tuovinen, J. P., Räsänen, A., Juutinen, S., Mikola, J., Aurela, M., Heiskanen, L., Heikkilä, M., Weckström, J., Juselius, T., Piilo, S. R., Deng, J., Zhang, Y., Chaudhary, N., Huang, C., Väiliranta, M., Biasi, C., Liu, X., Guo, M., Zhuang, Q., Korhola, A., & Shurpali, N. J. (2022). Peatland Heterogeneity Impacts on Regional Carbon Flux and Its Radiative Effect Within a Boreal Landscape. *Journal of Geophysical Research: Biogeosciences*, *127*(9). <https://doi.org/10.1029/2021JG006774>
- Koven, C. D., Schuur, E. A., Schädel, C., Bohn, T. J., Burke, E. J., Chen, G., Chen, X., Ciais, P., Grosse, G., Harden, J. W., Hayes, D. J., Hugelius, G., Jafarov, E. E., Krinner, G., Kuhry, P., Lawrence, D. M., MacDougall, A. H., Marchenko, S. S., McGuire, A. D., Natali, S. M., Nicolsky, D. J., Olefeldt, D., Peng, S., Romanovsky, V. E., Schaefer, K. M., Strauss, J., Treat, C. C., & Turetsky, M. (2015). A simplified, data-constrained approach to estimate the permafrost carbon-climate feedback. *Philosophical Transactions of the Royal Society A: Mathematical, Physical and Engineering Sciences*, *373*(2054). <https://doi.org/10.1098/rsta.2014.0423>
- Koven, C. D., Riley, W. J., & Stern, A. (2013). Analysis of permafrost thermal dynamics and response to climate change in the CMIP5 earth system models. *Journal of Climate*, *26*(6), 1877–1900. <https://doi.org/10.1175/JCLI-D-12-00228.1>
- Lal, R. (2009). Challenges and opportunities in soil organic matter research. *European Journal of Soil Science*, *60*(2), 158–169. <https://doi.org/10.1111/j.1365-2389.2008.01114.x>
- Lara, M. J., McGuire, A. D., Euskirchen, E. S., Genet, H., Yi, S., Rutter, R., Iversen, C., Sloan, V., & Wullschleger, S. D. (2020). Local-scale Arctic tundra heterogeneity affects regional-scale carbon dynamics. *Nature Communications*, *11*(4925). <https://doi.org/10.1038/s41467-020-18768-z>
- Lawrence, D. M., & Slater, A. G. (2008). Incorporating organic soil into a global climate model. *Climate Dynamics*, *30*(2-3), 145–160. <https://doi.org/10.1007/s00382-007-0278-1>

- Lehmann, J., & Kleber, M. (2015). The contentious nature of soil organic matter. *Nature*, 528(7580), 60–68. <https://doi.org/10.1038/nature16069>
- Li, J., Chen, F., Zhang, G., Barlage, M., Gan, Y., Xin, Y., & Wang, C. (2018). Impacts of Land Cover and Soil Texture Uncertainty on Land Model Simulations Over the Central Tibetan Plateau. *Journal of Advances in Modeling Earth Systems*, 10(9), 2121–2146. <https://doi.org/10.1029/2018MS001377>
- Li, W., Yan, D., Weng, B., & Zhu, L. (2023). Research progress on hydrological effects of permafrost degradation in the Northern Hemisphere. *Geoderma*, 438(December 2022), 116629. <https://doi.org/10.1016/j.geoderma.2023.116629>
- Lindgren, A., Hugelius, G., & Kuhry, P. (2018). Extensive loss of past permafrost carbon but a net accumulation into present-day soils. *Nature*, 560(7717), 219–222. <https://doi.org/10.1038/s41586-018-0371-0>
- Liu, C., Ikeda, K., Rasmussen, R., Barlage, M., Newman, A. J., Prein, A. F., Chen, F., Chen, L., Clark, M., Dai, A., Dudhia, J., Eidhammer, T., Gochis, D., Gutmann, E., Kurkute, S., Li, Y., Thompson, G., & Yates, D. (2017). Continental-scale convection-permitting modeling of the current and future climate of North America. *Climate Dynamics*, 49(1-2), 71–95. <https://doi.org/10.1007/s00382-016-3327-9>
- Lorenz, R., Pitman, A. J., & Sisson, S. A. (2016). Does Amazonian deforestation cause global effects; Can we be sure? *Journal of Geophysical Research*, 121(10), 5567–5584. <https://doi.org/10.1002/2015JD024357>
- Mackay, J. (1983). Downward water movement into frozen ground, western arctic coast, Canada. *Canadian Journal of Earth Sciences*, 20(1), 120–134. <https://doi.org/10.1139/e83-012>
- Maxwell, R. M., & Condon, L. E. (2016). Connections between groundwater flow and transpiration partitioning. *Science*, 353(6297), 377–380. <https://doi.org/10.1126/science.aaf7891>
- Mccarty, J. L., Aalto, J., Paunu, V. V., Arnold, S. R., Eckhardt, S., Klimont, Z., Fain, J. J., Evangeliou, N., Venäläinen, A., Tchebakova, N. M., Parfenova, E. I., Kupiainen, K., Soja, A. J., Huang, L., & Wilson, S. (2021). Reviews and syntheses: Arctic fire regimes and emissions in the 21st century. *Biogeosciences*, 18(18), 5053–5083. <https://doi.org/10.5194/bg-18-5053-2021>
- McGuire, A. D., Lawrence, D. M., Koven, C., Clein, J. S., Burke, E., Chen, G., Jafarov, E., MacDougall, A. H., Marchenko, S., Nicolsky, D., Peng, S., Rinke, A., Ciais, P., Gouttevin, I., Hayes, D. J., Ji, D., Krinner, G., Moore, J. C., Romanovsky, V., Schädel, C., Schaefer, K., Schuur, E. A., & Zhuang, Q. (2018). Dependence of the evolution of carbon dynamics in the northern permafrost region on the trajectory of climate change. *Proceedings of the National Academy of Sciences of the United States of America*, 115(15), 3882–3887. <https://doi.org/10.1073/pnas.1719903115>
- Meredith, M., Sommerkorn, M., Cassotta, S., Derksen, C., Ekaykin, A., Hollowed, A., Kofinas, G., Mackintosh, A., Melbourne-Thomas, J., Muelbert, M., Ottersen, G., Pritchard, H., & Schuur, E. (2019). Polar regions. In H.-O. Pörtner, D. Roberts, V. Masson-Delmotte, P. Zhai, M. Tignor, E. Poloczanska, K. Mintenbeck, A. Alegría, M. Nicolai, A. Okem, J. Petzold, B. Rama, & N.

- Weyer (Eds.), *Ipc special report on the ocean and cryosphere in a changing climate* (pp. 203–320). Cambridge University Press. <https://doi.org/10.1017/cbo9780511975301.013>
- Miner, K. R., Turetsky, M. R., Malina, E., Bartsch, A., Tamminen, J., McGuire, A. D., Fix, A., Sweeney, C., Elder, C. D., & Miller, C. E. (2022). Permafrost carbon emissions in a changing Arctic. *Nature Reviews Earth & Environment*, 3(1), 55–67. <https://doi.org/10.1038/s43017-021-00230-3>
- Montesano, P. M., Neigh, C. S., MacAnder, M., Feng, M., & Noojipady, P. (2020). The bioclimatic extent and pattern of the cold edge of the boreal forest: The circumpolar taiga-tundra ecotone. *Environmental Research Letters*, 15(10). <https://doi.org/10.1088/1748-9326/abb2c7>
- Natali, S. M., Holdren, J. P., Rogers, B. M., Treharne, R., Duffy, P. B., Pomerance, R., & MacDonald, E. (2021). Permafrost carbon feedbacks threaten global climate goals. *Proceedings of the National Academy of Sciences of the United States of America*, 118(21), 1–3. <https://doi.org/10.1073/pnas.2100163118>
- Nitzbon, J., Langer, M., Martin, L. C. P., Westermann, S., Von, T. S., & Boike, J. (2020a). Effects of multi-scale heterogeneity on the simulated evolution of ice-rich permafrost lowlands under a warming climate. *The Cryosphere*, (June), 1–29. <https://doi.org/https://doi.org/10.5194/tc-15-1399-2021>
- Nitzbon, J., Westermann, S., Langer, M., Martin, L. C., Strauss, J., Laboor, S., & Boike, J. (2020b). Fast response of cold ice-rich permafrost in northeast Siberia to a warming climate. *Nature Communications*, 11(1), 1–11. <https://doi.org/10.1038/s41467-020-15725-8>
- Niu, G. Y., & Yang, Z. L. (2006). Effects of frozen soil on snowmelt runoff and soil water storage at a continental scale. *Journal of Hydrometeorology*, 7(5), 937–952. <https://doi.org/10.1175/JHM538.1>
- Paltan, H., Dash, J., & Edwards, M. (2015). A refined mapping of Arctic lakes using Landsat imagery. *International Journal of Remote Sensing*, 36(23), 5970–5982. <https://doi.org/10.1080/01431161.2015.1110263>
- Patterson, K. A. (1990). *Global distributions of total and total-avaiable soil water-holding capacities* (Msc. Thesi). University of Delaware.
- Ping, C. L., Jastrow, J. D., Jorgenson, M. T., Michaelson, G. J., & Shur, Y. L. (2015). Permafrost soils and carbon cycling. *Soil*, 1(1), 147–171. <https://doi.org/10.5194/soil-1-147-2015>
- Prein, A. F., Gobiet, A., Suklitsch, M., Truhetz, H., Awan, N. K., Keuler, K., & Georgievski, G. (2013). Added value of convection permitting seasonal simulations. *Climate Dynamics*, 41(9-10), 2655–2677. <https://doi.org/10.1007/s00382-013-1744-6>
- Prein, A. F., Langhans, W., Fosser, G., Ferrone, A., Ban, N., Goergen, K., Keller, M., Tölle, M., Gutjahr, O., Feser, F., Brisson, E., Kollet, S., Schmidli, J., Van Lipzig, N. P., & Leung, R. (2015). A review on regional convection-permitting climate modeling: Demonstrations, prospects, and challenges. *Reviews of Geophysics*, 53(2), 323–361. <https://doi.org/10.1002/2014RG000475>
- Rantanen, M., Karpechko, A. Y., Lipponen, A., Nordling, K., Hyvärinen, O., Ruosteenoja, K., Vihma, T., & Laaksonen, A. (2022). The Arctic has warmed

- nearly four times faster than the globe since 1979. *Communications Earth and Environment*, 3(1), 1–10. <https://doi.org/10.1038/s43247-022-00498-3>
- Rasmussen, R., Ikeda, K., Liu, C., Gochis, D., Clark, M., Dai, A., Gutmann, E., Dudhia, J., Chen, F., Barlage, M., Yates, D., & Zhang, G. (2014). Climate change impacts on the water balance of the Colorado headwaters: High-resolution regional climate model simulations. *Journal of Hydrometeorology*, 15(3), 1091–1116. <https://doi.org/10.1175/JHM-D-13-0118.1>
- Reick, C. H., Gayler, V., Goll, D., Hagemann, S., Heidkamp, M., & et al. Nabel, J. E. M. S. (2021). JSBACH 3 - The land component of the MPI Earth System Model: Documentation of version 3.2. *Berichte zur Erdsystemforschung*.
- Riddick, T., Brovkin, V., Hagemann, S., & Mikolajewicz, U. (2018). Dynamic hydrological discharge modelling for coupled climate model simulations of the last glacial cycle: The MPI-DynamicHD model version 3.0. *Geoscientific Model Development*, 11(10), 4291–4316. <https://doi.org/10.5194/gmd-11-4291-2018>
- Romanovsky, V. E., & Osterkamp, T. E. (2000). Effects of unfrozen water on heat and mass transport processes in the active layer and permafrost. *Permafrost and Periglacial Processes*, 11(3), 219–239. [https://doi.org/10.1002/1099-1530\(200007/09\)11:3<219::AID-PPP352>3.0.CO;2-7](https://doi.org/10.1002/1099-1530(200007/09)11:3<219::AID-PPP352>3.0.CO;2-7)
- Rouf, T., Maggioni, V., Mei, Y., & Houser, P. (2021). Towards hyper-resolution land-surface modeling of surface and root zone soil moisture. *Journal of Hydrology*, 594, 125945. <https://doi.org/10.1016/j.jhydrol.2020.125945>
- Rouholahnejad Freund, E., & Kirchner, J. W. (2017). A Budyko framework for estimating how spatial heterogeneity and lateral moisture redistribution affect average evapotranspiration rates as seen from the atmosphere. *Hydrology and Earth System Sciences*, 21(1), 217–233. <https://doi.org/10.5194/hess-21-217-2017>
- Satoh, M., Matsuno, T., Tomita, H., Miura, H., Nasuno, T., & Iga, S. (2008). Nonhydrostatic icosahedral atmospheric model (NICAM) for global cloud resolving simulations. *Journal of Computational Physics*, 227(7), 3486–3514. <https://doi.org/10.1016/j.jcp.2007.02.006>
- Satoh, M., Tomita, H., Yashiro, H., Miura, H., Kodama, C., Seiki, T., Noda, A. T., Yamada, Y., Goto, D., Sawada, M., Miyoshi, T., Niwa, Y., Hara, M., Ohno, T., Ichi Iga, S., Arakawa, T., Inoue, T., & Kubokawa, H. (2014). The Nonhydrostatic Icosahedral Atmospheric Model: description and development. *Progress in Earth and Planetary Science*, 1(1). <https://doi.org/10.1186/s40645-014-0018-1>
- Schuur, E. A. G., McGuire, A. D., Schädel, C., Grosse, G., Harden, J. W., Hayes, D. J., Hugelius, G., Koven, C. D., Kuhry, P., & Lawrence, D. M. (2015). Climate change and the permafrost carbon feedback. *Nature*, 520(7546), 171–179. <https://doi.org/https://doi.org/10.1038/nature14338>
- Serreze, M. C., & Barry, R. G. (2011). Processes and impacts of Arctic amplification: A research synthesis. *Global and Planetary Change*, 77(1-2), 85–96. <https://doi.org/10.1016/j.gloplacha.2011.03.004>
- Shangguan, W., Hengl, T., Mendes de Jesus, J., Yuan, H., & Dai, Y. (2017). Mapping the global depth to bedrock for land surface modeling. *Journal of Advances in Modeling Earth Systems*, 9, 65–88. <https://doi.org/10.1002/2016MS000625>

- Siewert, M. B., Lantuit, H., Richter, A., & Hugelius, G. (2021). Permafrost Causes Unique Fine-Scale Spatial Variability Across Tundra Soils. *Global Biogeochemical Cycles*, 35(3), 1–19. <https://doi.org/10.1029/2020GB006659>
- Singh, R., Reager, J., Miller, N., & Famiglietti, J. (2015). Toward hyper-resolution land-surface modeling: The effects of fine-scale topography and soil texture on CLM4.0 simulations over the Southwestern U.S. *Water Resources Research*, 51(4), 2648–2667. <https://doi.org/10.1111/j.1752-1688.1969.tb04897.x>
- Smith, N. D., Burke, E. J., Aas, K. S., Althuisen, I. H. J., Boike, J., Christiansen, C. T., Etzelmüller, B., Friborg, T., Lee, H., Rumbold, H., Turton, R. H., Westermann, S., & Chadburn, S. E. (2022a). Explicitly modelling microtopography in permafrost landscapes in a land surface model. *Geoscientific Model Development*, 15, 3603–3639. <https://doi.org/https://doi.org/10.5194/gmd-15-3603-2022>
- Smith, S. L., O'Neill, H. B., Isaksen, K., Noetzli, J., & Romanovsky, V. E. (2022b). The changing thermal state of permafrost. *Nature Reviews Earth and Environment*, 3(1), 10–23. <https://doi.org/10.1038/s43017-021-00240-1>
- Solomon, S., Qin, D., Manning, M., Chen, Z., Marquis, M., Averyt, K., Tignor, M., & Miller, H.-L. (2007). *Contribution of Working Group 1 to the Fourth Assessment Report of the Intergovernmental Panel on Climate Change*. Cambridge University Press.
- Specht, N. F., Claussen, M., & Kleinen, T. (2022). Simulated range of mid-Holocene precipitation changes from extended lakes and wetlands over North Africa. *Climate of the Past*, 18(5), 1035–1046. <https://doi.org/10.5194/cp-18-1035-2022>
- Stacke, T., & Hagemann, S. (2013). *Generation of new rooting depths for the LSP3 dataset* (tech. rep.).
- Stevens, B., Acquistapace, C., Hansen, A., Heinze, R., Klinger, C., Klocke, D., Harald, R., Schubotz, W., Windmiller, J., Adamidis, P., Arka, I., Barlakas, V., Biercamp, J., Brueck, M., Brune, S., Buehler, S. A., Burkhardt, U., Guido, C., Costa-Surós, M., Crewell, S., Crüger, T., Deneke, H., Friedrichs, P., Henken, C. C., Hohenegger, C., Jacob, M., Jakub, F., Kalthoff, N., Köhler, M., van Laar, T. W., Li, P., Ulrich, L., Macke, A., Madenach, N., Mayer, B., Nam, C., Naumann, A. K., Peters, K., Poll, S., Quaas, J., Röber, N., Nicolas, R., Scheck, L., Vera, S., Schnitt, S., Seifert, A., Senf, F., Shapkaliyevski, M., Simmer, C., Singh, S., Sourdeval, O., Spickermann, D., Strandgren, J., Tessiot, O., Vercauteren, N., Vial, J., Voigt, A., & Zängl, G. (2020). The Added Value of Large-Eddy and Storm-Resolving Models for Simulating Clouds and Precipitation. *Journal of the Meteorological Society of Japan. Ser. II*, 98(January). <https://doi.org/10.2151/jmsj.2020-021>
- Swenson, S. C., Clark, M., Fan, Y., Lawrence, D. M., & Perket, J. (2019). Representing Intrahillslope Lateral Subsurface Flow in the Community Land Model. *Journal of Advances in Modeling Earth Systems*, 11(12), 4044–4065. <https://doi.org/10.1029/2019MS001833>
- Tarnocai, C., Canadell, J. G., Schuur, E. A., Kuhry, P., Mazhitova, G., & Zimov, S. (2009). Soil organic carbon pools in the northern circumpolar permafrost

- region. *Global Biogeochemical Cycles*, 23(2), 1–11. <https://doi.org/10.1029/2008GB003327>
- Tifafi, M., Guenet, B., & Hatté, C. (2018). Large Differences in Global and Regional Total Soil Carbon Stock Estimates Based on SoilGrids, HWSD, and NCSCD: Intercomparison and Evaluation Based on Field Data From USA, England, Wales, and France. *Global Biogeochemical Cycles*, 32(1), 42–56. <https://doi.org/10.1002/2017GB005678>
- Tong, B., Gao, Z., Horton, R., Li, Y., & Wang, L. (2016). An empirical model for estimating soil thermal conductivity from soil water content and porosity. *Journal of Hydrometeorology*, 17(2), 601–613. <https://doi.org/10.1175/JHM-D-15-0119.1>
- Torre Jorgenson, M., Harden, J., Kanevskiy, M., O'Donnell, J., Wickland, K., Ewing, S., Manies, K., Zhuang, Q., Shur, Y., Striegl, R., & Koch, J. (2013). Reorganization of vegetation, hydrology and soil carbon after permafrost degradation across heterogeneous boreal landscapes. *Environmental Research Letters*, 8(3). <https://doi.org/10.1088/1748-9326/8/3/035017>
- Treat, C. C., Marushchak, M. E., Voigt, C., Zhang, Y., Tan, Z., Zhuang, Q., Virtanen, T. A., Räsänen, A., Biasi, C., Hugelius, G., Kaverin, D., Miller, P. A., Stendel, M., Romanovsky, V., Rivkin, F., Martikainen, P. J., & Shurpali, N. J. (2018). Tundra landscape heterogeneity, not interannual variability, controls the decadal regional carbon balance in the Western Russian Arctic. *Global Change Biology*, 24(11), 5188–5204. <https://doi.org/10.1111/gcb.14421>
- Turetsky, M. R., Jones, M., Walter Anthony, K., Olefeldt, D., Schuur, E. A., Koven, C., Mcguire, A. D., & Grosse, G. (2019). Permafrost collapse is accelerating carbon release. *Nature*, 569, 32–24. <https://doi.org/https://doi.org/10.1038/d41586-019-01313-4>
- van Cleve, K., Dyrness, C. T., Viereck, L. A., Fox, J., Chapin, F. S., & Oechel, W. (1983). Taiga Ecosystems in Interior Alaska. *BioScience*, 33(1), 39–44. <https://doi.org/10.2307/1309243>
- Veremeeva, A., & Gubin, S. (2009). Modern Tundra Landscapes of the Kolyma Lowland and their Evolution in the Holocene. *Permafrost and Periglacial Processes*, 20, 399–406. <https://doi.org/https://doi.org/10.1002/ppp.674>
- Viereck, L. (1992). *The Alaska vegetation classification* (Vol. 286). US Department of Agriculture, Forest Service, Pacific Northwest Research Station.
- Walvoord, M. A., & Kurylyk, B. L. (2016). Hydrologic Impacts of Thawing Permafrost—A Review. *Vadose Zone Journal*, 15(6), 1–20. <https://doi.org/10.2136/vzj2016.01.0010>
- Wang, Y., Geerts, B., & Liu, C. (2018). A 30-year convection-permitting regional climate simulation over the interior western United States. Part I: Validation. *International Journal of Climatology*, 38(9), 3684–3704. <https://doi.org/10.1002/joc.5527>
- Williams, R., & Ahuja, L. (2003). Scaling and estimating the soil water characteristic using a one-parameter model. In Y. Pachepsky, D. E. Radcliffe, & H. Magdi Selim (Eds.), *Scaling methods in soil physics* (pp. 35–48). CRC Press.

- Zimov, S. A., Schuur, E. A. G., & Chapin III, F. S. (2006). Permafrost and the global carbon budget. *Science*, *312*(5780), 1612–1613. <https://doi.org/10.1126/science.1128908>
- Zwiers, F. W., & von Storch, H. (1995). Taking Serial Correlation into Account in Tests of the Mean. *Journal of Climate*, *8*, 336–351. [https://doi.org/10.1175/1520-0442\(1995\)008<0336:TSCIAI>2.0.CO;2](https://doi.org/10.1175/1520-0442(1995)008<0336:TSCIAI>2.0.CO;2)

EIDESSTATTLICHE VERSICHERUNG

*DECLARATION ON OATH*

---

Hiermit erkläre ich an Eides statt, dass ich die vorliegende Dissertationsschrift selbst verfasst und keine anderen als die angegebenen Quellen und Hilfsmittel benutzt habe.

*I hereby declare upon oath that I have written the present dissertation independently and have not used further resources and aids than those stated.*

*Hamburg, den 27. November 2023*

---

Meike Schickhoff

## Hinweis / Reference

Die gesamten Veröffentlichungen in der Publikationsreihe des MPI-M  
„Berichte zur Erdsystemforschung / Reports on Earth System Science“,  
ISSN 1614-1199

sind über die Internetseiten des Max-Planck-Instituts für Meteorologie erhältlich:  
**<https://mpimet.mpg.de/forschung/publikationen>**

*All the publications in the series of the MPI -M  
„Berichte zur Erdsystemforschung / Reports on Earth System Science“,  
ISSN 1614-1199*

*are available on the website of the Max Planck Institute for Meteorology:  
**<https://mpimet.mpg.de/en/research/publications>***

